Outline

The development of supramolecular chemistry started forty years ago, moving from the simple studies of recognition towards self-organisation. Lehn, considered the father of this field, says: "Beyond molecular chemistry, supramolecular chemistry aims at constructing highly complex, functional chemical system from components held together by intermolecular forces"[1]. Its high potentiality relies on the enormous number of applications. Indeed changing the functional groups and the exploited interaction, these systems can be reinvested in: molecular recognition[2], catalysis[3], polymerization[4], nanomaterials, supramolecular devices[5]. Such systems are by definition dynamic, because of the lability of non-covalent interactions and this property leads to responsive systems, which can "feel" an external stimuli. This area is in continuous evolution, as is demonstrated by the restless increasing of the appeared publications.

Moving within the supramolecular area, this PhD thesis develops four main themes. The study of formation of supramolecular architectures by use of different building blocks is reported. In chapter 1 metal-salophen complexes, which are largely exploited in supramolecular chemistry, will be introduced. These ligands are Shiff bases which can coordinate different metals, tuning in this way the properties of the complex. In the first chapter their potentiality to behave as building blocks for the generation of supramolecular architectutes is explored.

The family of bis-urea derived molecules represents another example of building blocks frequently used in supramolecular chemistry. These molecules are self organised through hydrogen bonds in supramolecular polymeric tubular gels, and guest molecules can be hosted within the tubes[6]. The functionalisation of the basic structure of urea derived aompounds and the studies of their properties are described in chapter 2.

Metal-salophen derivatives can have interesting application in the field of material chemistry. Macrocyclic structures incorporating such units have been used to generate interpenetrated systems like pseudo-rotaxanes[7] and [2]rotaxanes. The force that keeps together the two units of the system is an acid-base Lewis interaction. These structures can

[1] J.-M. Lehn, *Chem. Soc. Rev.*, **2007**, 36, 151-160.
[2] D. Fiedler, D. H. Leung, R. G. Bergman, K. N. Raymond, *Acc. Chem. Res.*, **2005**, *38* (4), 349-358.
[3] T.-M. Yao, **Z.-F.** Ye**, L.** Wang**, J.-Y.** Gu**, S.-D.** Yao**, X.-F.** Shi**,** *Spectrochim. Acta: Part A*, **2002**, *58*, 3033-3038.
[4] L. Brunsveld, B. J. B. Folmer, E. W. Meijer, R. P. Sijbesma, *Chem. Rev.*, **2001**, *101*, 4071-4098.
[5] O.-K. Kim, J. Melinger, S.-J. Chung, M. Pepitone, *Org. Lett.*, **2008**, *10* , 1625-1628.
[6] B. Isare, M. Linares, R. Lazzaroni, L. Bouteiller, *J. Phys. Chem. B* **2009,** *113,* 3360–3364.
[7] Dalla Cort, L. Mandolini, C. Pasquini, L. Schiaffino, *Org. Biomol. Chem*., **2006**, *4*, 4543-4546.

work as molecular machines, giving response to an external stimuli. In chapter 3 different approaches to the synthesis of such systems are described.

For the construction of [2]-rotaxane systems a series of three new macrocycles of different dimension were synthesized. Chapter 4 deals with preliminary experiments focused on their potential behaviour as ion-pair receptors.

Chapter 1

New metal-salophen complexes to build up supramolecular architectures in solution and in solid state

1.1 Introduction

a. Self-assembling

Inspired by biological systems and by how nature uses self assembly processes, supramolecular chemistry finds interesting applications in the design of materials, which are obtained through self-assembly of small building blocks[8,9].

In the literature a large number of building blocks have been already reported, each of them being characterised by the presence of functional groups able to achieve direct organization through the formation of non-covalent interactions. All these molecules are designed to interact in a predictable way to give clever materials[10]. Usually the resulting systems are classified depending on the exploited interaction.

Coordinative motifs have been frequently used to construct various types of supramolecular structures. To this purpose metal-porphyrins complexes represent an important class of building blocks and several strategies to assemble porphyrins into higher ordered structures have been developed so far. In these structures two different binding sites can be envisioned:

- the metal center, which is coordinated by the planar ligand and possesses one or two free apical sites,
- functional groups incorporated in the ligand skeleton, which can give interactions with guests or with the metal center itself.

These features suggest the design of self-assembled systems such the one reported in figure 1.1. In this example the complex bears a morpholine moiety, which is responsible for the binding organisation around the zinc atom.

[8] J.-M. Lehn, *Supramolecular Chemistry*, VCH Press, New York, **1995**.
[9] J.-M. Lehn, *PNAS*, **2002**, *99*,4763-4768.
[10] S. I. Stupp, V. LeBonheur, K. Walker, L. S. Li, K. E. Huggins, M. Keser, A. Amstutz, *Science*, **1997**, *276*, 384-389.

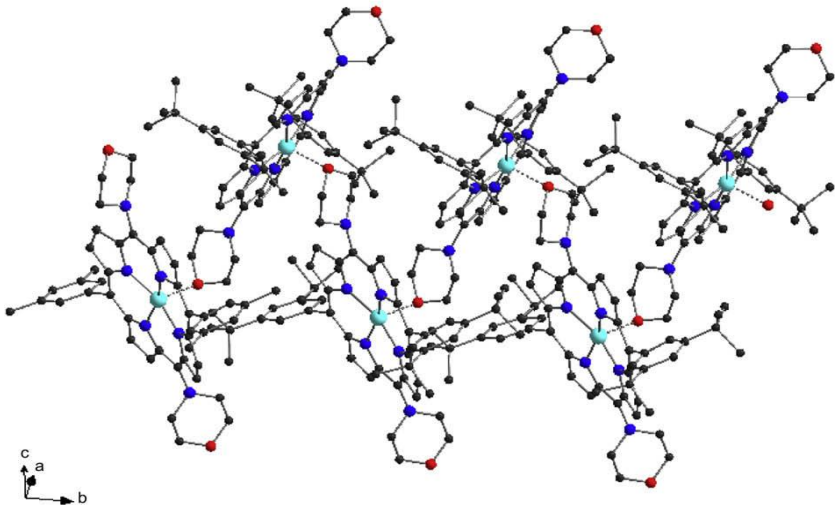

Figure 1.1 Porphyrinoid network assembled by Zn–O ligations. Colour coding: carbon-black, nitrogen-blue, hydrogen-red and zinc-cyan. Hydrogen atoms were omitted for clarity[11].

In figure 1.2 a porphyrin derivative is employed in the construction of different MOFs (metal-organic frameworks), depending on the nature of the complexed metal. Using the free-ligand dipyridyl porphyrin, an highly porous Zn(porphyrin)-based material incorporating a tetratopic carboxylate strut can be easily synthesized (top right of fig. 1.2). On the other hand the Mn(porphyrin) yields only a 2D material, in which the Mn in the porphyrin center acts as a structural node and the tetratopic carboxylate strut is not included (bottom right of fig.1.2) [12].

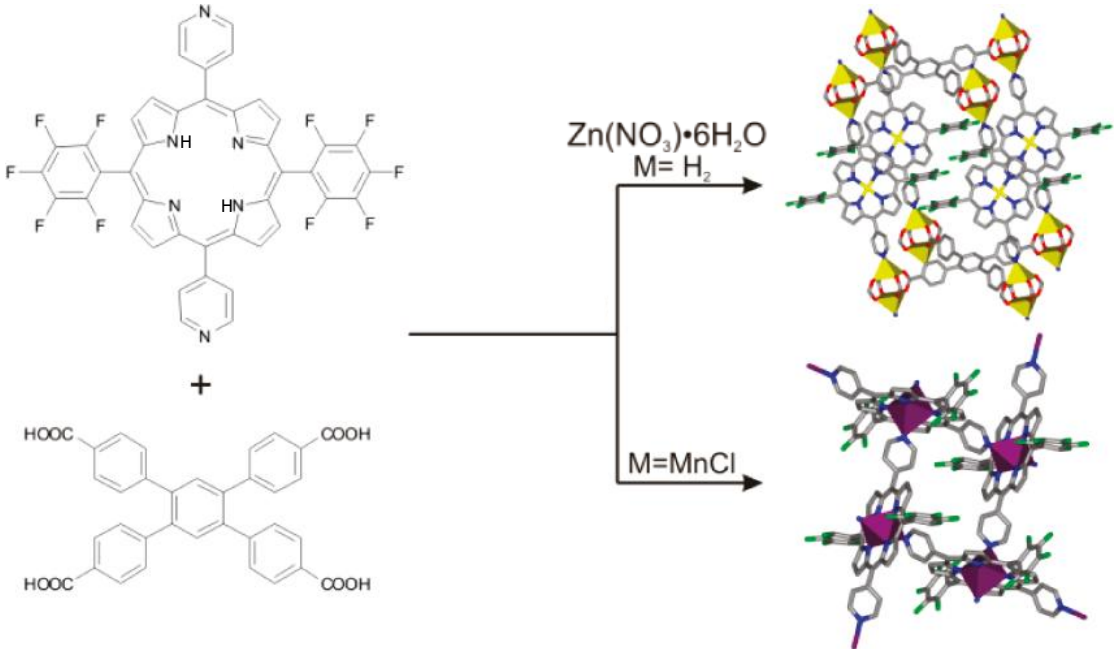

Figure 1.2 Structures of the porphyrin complex, of the tetratopic carboxylate and of the aggregates.

[11] M. C. Balaban, C. Chappaz-Gillot, G. Canard, O. Fuhr, C. Roussel, T. S. Balaban, *Tetrahedron*, **2009**, *65,* 3733-3739.
[12] O. K. Farha, A. M. Shultz, A. A. Sarjeant, S. T. Nguyen, J. T. Hupp, *J. Am. Chem. Soc.*, **2011**, *133*, 5652-5655.

As pointed out in the previous examples, often the pyridine-M^{II}-porphyrin motif is exploited, because it allows a good control over the stoichiometry and orientation of the self-assembly reaction and Zinc results to be a good acceptor unit commonly used for this purpose[13,14].

But porphyrin complexes have a big disadvantage, their synthesis is usually characterised by very low yield. An alternative to them are metal salophen complexes, which have an easy synthesis and large possibilities of functionalisation. Salophen ligands are planar tetradentate Schiff bases, which can coordinate different metals in various oxidation state tuning their properties. They can be easily obtained by the condensation of two equivalents of **sal**ycilaldehyde and one of ***o*-phen**ylendiamine (scheme 1.1). The name salophen derives from this.

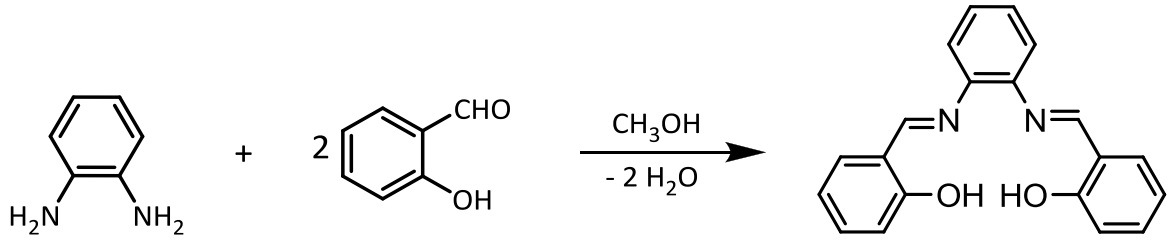

Scheme 1.1 Synthesis of a salophen ligand. IUPAC name N,N'-*o*-phenylenebis(salicyldimine).

The synthesis can be also performed in the presence of the metal salt, which works as a template and leads directly to the formation of the metal complex. Changing the metal, the geometry of the coordinative sites will also change. For example Zinc has a tetragonal bipyramidal coordination geometry. The four binding sites on the equatorial position are occupied by the donating atoms of the ligand, and this leaves two apical sites free to coordinate different guests. Different situation is that of the Uranyl dication (UO_2), which has a pentagonal bipyramidal geometry. In this case besides the four sites coordinated by the ligand, and the two apical position already occupied by the oxygen atoms, there is a fifth equatorial position that remains free to bind a potential guest (figure 1.3).

[13] S. J. Wezemberg, G.A. Metselaar, E. C. Escudero-Adàn, J. Benet-Buchholz, A. W. Kleij, *Inorg. Chim. Acta*, **2009**, *362*, 1053-1057.
[14] I.-W. Hwang, T. Kamada, T. K. Ahn, D. M. Ko, T. Nakamura, A. Tsuda, A. Osuka, D. Kim, *J. Am. Chem. Soc*., **2004**, *49*, 16187-16198.

Figure 1.3 Coordination geometry of Zn^{2+} and UO_2^{2+} cations.

All the four units that form the complex can be modified to tune its properties: the metal, the diamine or the two salycilaldhyde. For this reason salophen complexes can be easily build in a modular way. In analogy to Zn-porphyrin complexes, Zn-salophen ones present high affinity for molecules such as pyridine.

For example Kleij et al.[15] prepared a new generation of catalysts with an interesting three dimensional geometry, generated by the presence of tripyridylphosphine, with the three pyridine nitrogens complexed by the zinc of three zinc-salophen complexes, as reported in figure 1.4.

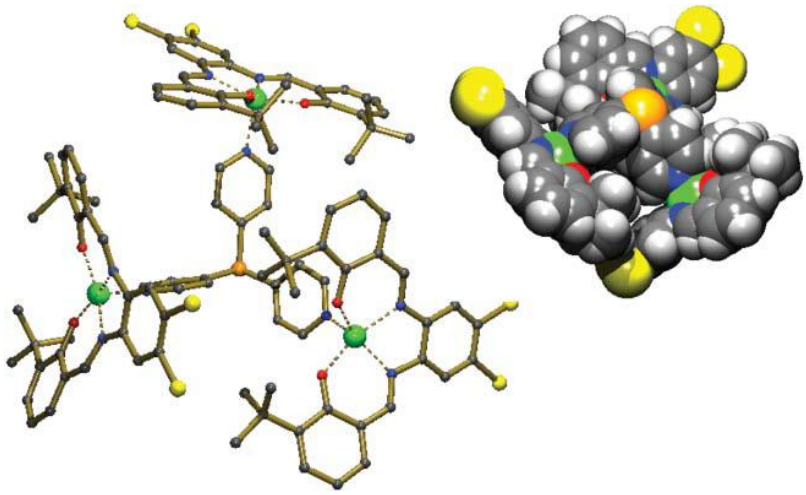

Figure 1.4 Structure of the aggregate obtained from to the axial interaction between tripyridilphosphine and the Zinc centre of the complexes.

Another important application is the construction of metal-salophen frameworks having porous properties. The formation of well defined boxes was investigated by Wezemberg et al.[16] using 4-4'bipyridine as a guest (figure 1.5).

[15] A. W. Kleij, M. Lutz, A. L. Spek, P. W. N. M. Van Leeuwen, J. N. H. Reek, *Chem. Commun.,* **2005**, 3661-3663.
[16] S. J. Wezemberg, A. W. Kleij, *Angew. Chem. Int. Ed.*, **2008**, *47*, 2354-2364.

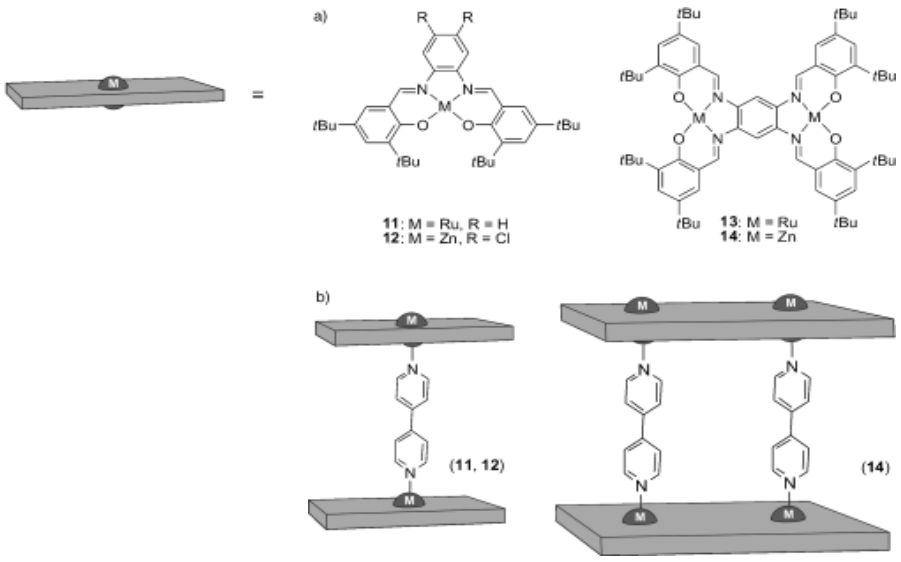

Figure 1.5 a) Mono- and bis-salophenic building blocks. b) Aggregates formed with 4,4'-bipyridine.

So the introduction of both the components of the N_{pyr}-Zn^{II} motif on the same molecule can be a good approach to obtain self-organised nanostructures also in the case of metal salophen complexes[17,18].

b. Aim of the research

Following this idea we designed a number of salophen complexes (**5**, **7**, **9**) containing in their skeleton a nitrogen donor atom. The purpose was to obtain self-assembled structures through the coordination between the ligand of one complex and the metal of a second one.

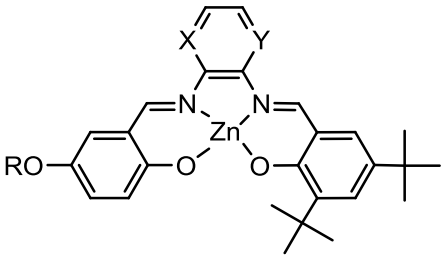

5a X = C, Y = N, R = *n*-$C_{10}H_{21}$
5b X = C, Y = N, R = *n*-$C_{16}H_{33}$
7a X = N, Y = C, R = *n*-$C_{10}H_{21}$
7b X = N, Y = C, R = *n*-$C_{16}H_{33}$

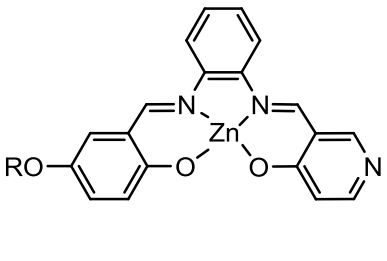

9a R = *n*-$C_{10}H_{21}$
9b R = *n*-$C_{16}H_{33}$

[17] S. J. Wezemberg, E. C. Escudero-Adàn, J. Benet-Buchholz, A. W. Kleij, *Inorg. Chem.*, **2008**, *47*, 2925-2927.
[18] A. W. Kleij, Mark Kuil, D. M. Tooke, A. L. Spek, J. N. H. Reek, *Inorg. Chem.*, **2007**, *46*, 5829-5831.

The *t*-butyl and the long alkyl chain substituents were introduced to increase the solubility of the complexes. It is also known that long aliphatic chain can contribute to the organisation in solid state, as reported for analogous structures[19,20] in figure 1.6.

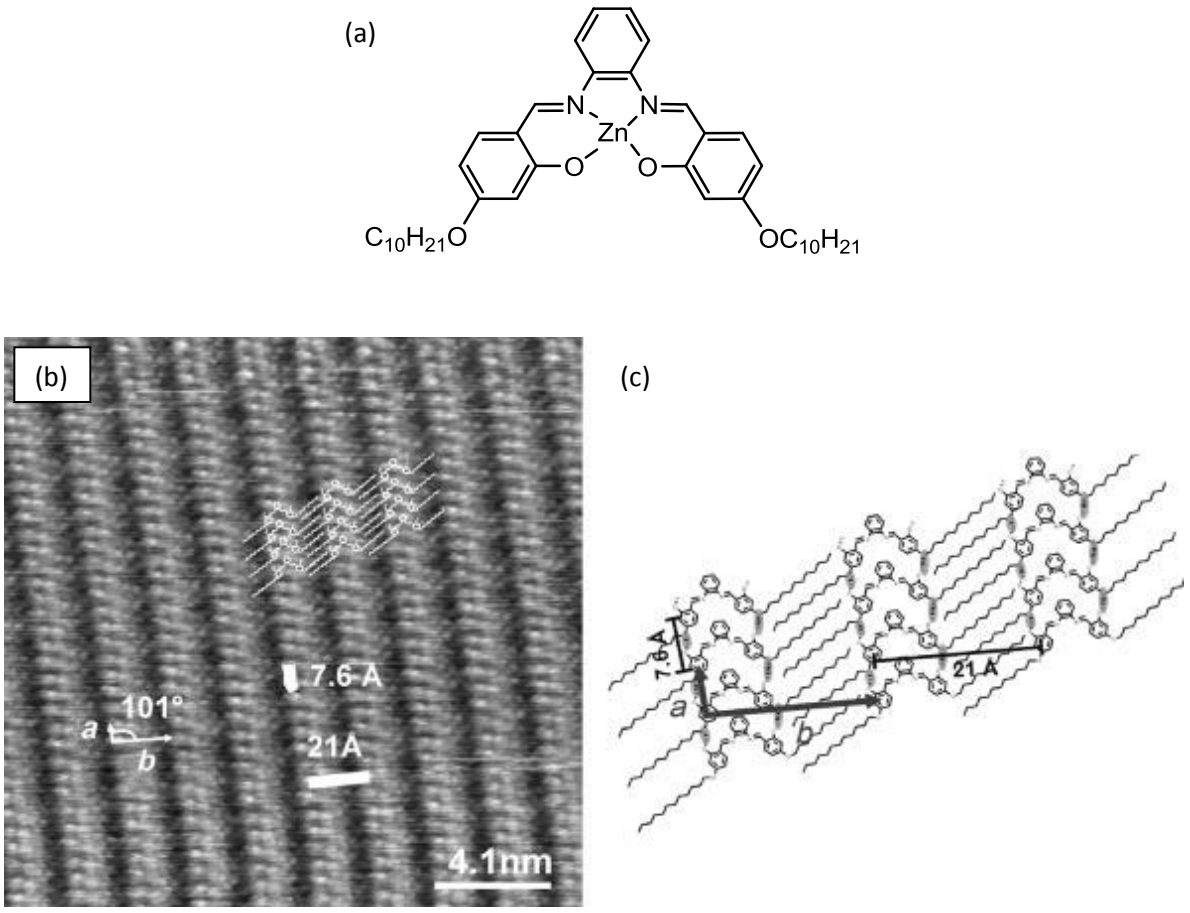

Figura 1.6 Structure of the zinc-salophen derivative (a). The STM image (b) and the proposed molecular model (c) for *N*,*N*_-(*o*-phenylene)bis(4-decyloxysalicylideneimine) organisation on HOPG.

[19] J. A. A. W. Elemans, S. J. Wezenberg, M. J. J. Coenen, E. C. Escudero-Adàn, J. Benet-Buchholz, D. den Boer, S. Speller, A. W. Kleij, S. De Feyter, *Chem. Commun.*, **2010**, *46*, 2548-2550.

[20] M. T. Räisänen, F. Mögele, S. Feodorow, B. Rieger, U. Ziener, M. Leskelä, T. Repo, *Eur. J. Inorg. Chem.* **2007**, 4028-4034.

1.2 Results and discussion

A common way to functionalise salophen ligands is the introduction of substituents on the single components that form the ligand, i.e. on the salicylaldehyde ring or on the *o*-phenilenediamine moiety.

a. Synthesis of Zn-salophen complexes using 2,3-diaminopyridine

The best protocol to synthesize the salicylaldehydes with alkoxy chain substituents **3a** and **3b** was found to be: 1) the O-alkylation of 4-(benzyloxy)phenol with the alkyl bromide of the desired length[21]; 2) the hydrogenolysis of benzyl groups with H_2 and Pd^0 as catalyst and 3) the ortho formylation with *p*-formaldehyde[22].

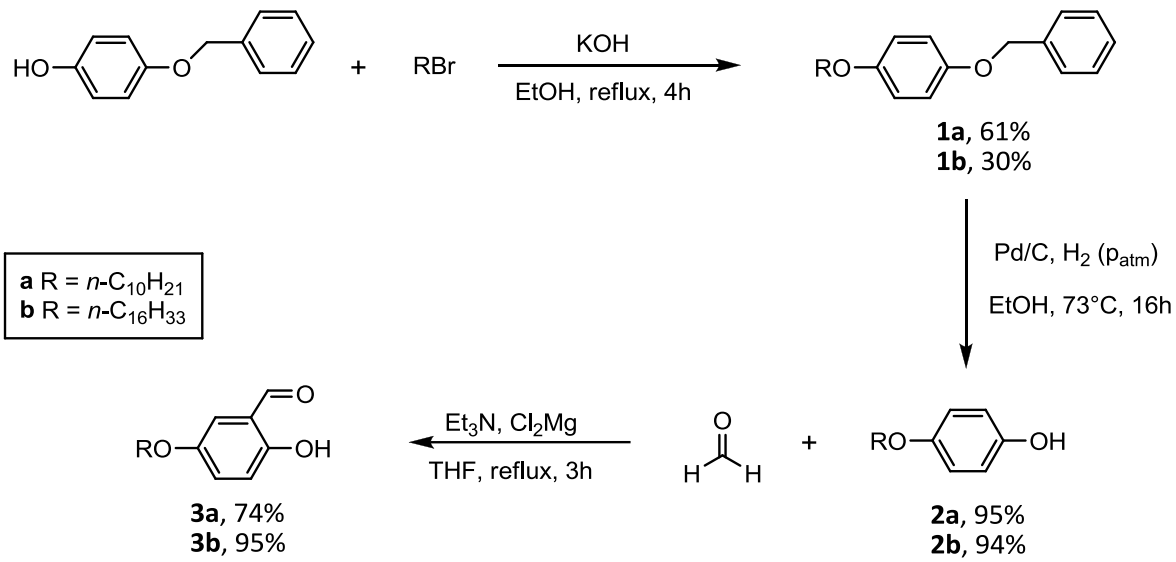

Scheme 1.2

The classical approach to the formation of non symmetrical substituted salophens can be a statistical synthesis, whose limitation is the yield (50% maximum) deriving from the statistical combination of the components. Instead, after the purification of the salicylaldehydes **3**, these ones were reacted with 2,3-diaminopyridine to give the corresponding monoimines **4a**

[21] M. E. Neubert, S. J. Laskos, L J. Maurer, L. T. Carlino, J. P. Ferrato, *Mol. Cryst. Liq. Cryst.*, **1978**, *44*, 197-210.
[22] E. Verner, B. A. Katz, J. R. Spencer, D. Allen, J. Hataye, W. Hruzewicz, H. C. Hui, A. Kolesnikov, Y. Li, C. Luong, A. Martelli, K. Radika, R. Rai, M. She, W. Shrader, P. A. Sprengeler, S. Trapp, J. Wang, W. B. Young, R. L. Mackman, *J. Med. Chem.*, **2001**, *44*, 2753-2767.

and **4b**. Thanks to the different reactivity of the two NH_2 these reactions provides exclusively one of the two possible products[23].

Such selectivity makes the synthesis of non symmetrically substituted salophen quite straightforward. It is sufficient to mix the reactants in methanol at room temperature in the presence of the metal salt, to obtain the corresponding complexes, that can be easily isolated by filtration, without any further purification.

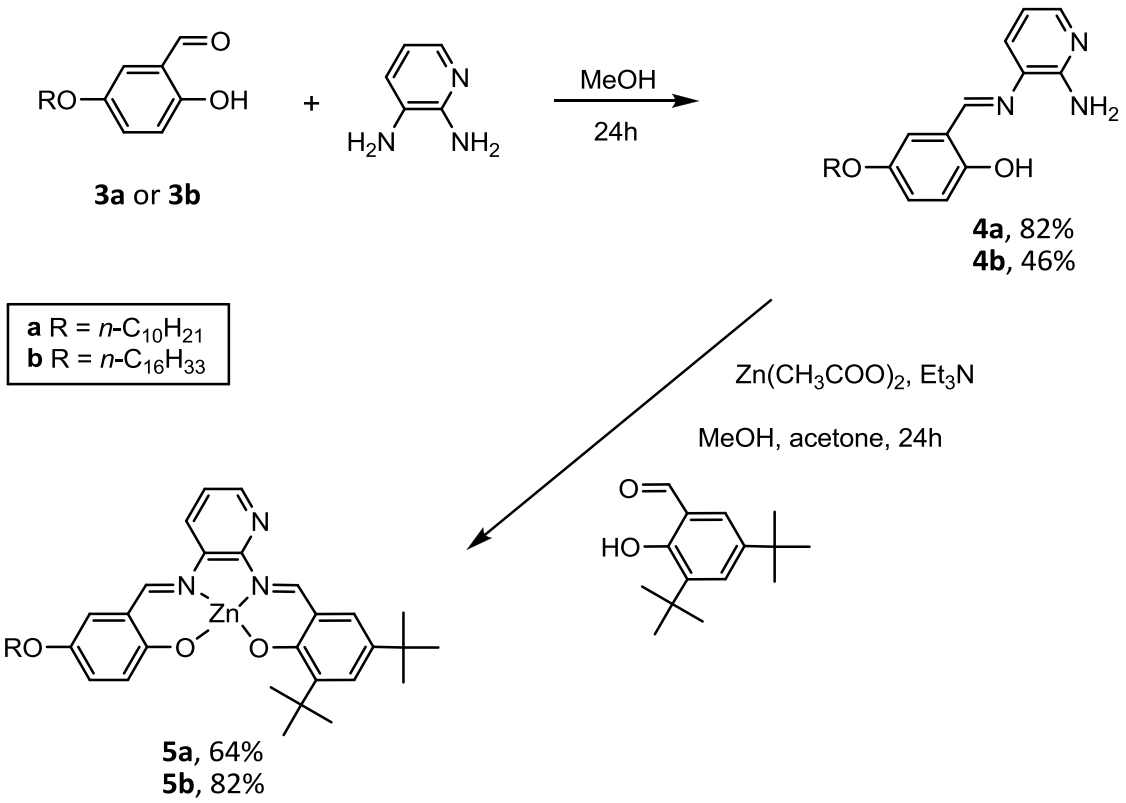

Scheme 1.3

In a similar way the complexes **7a** and **7b** were synthesized.

[23] A. W. Kleij, D. M. Tooke, A. L. Spek, J. N. H. Reek, *Eur. J. Inorg. Chem.*, **2005**, 4626-4634.

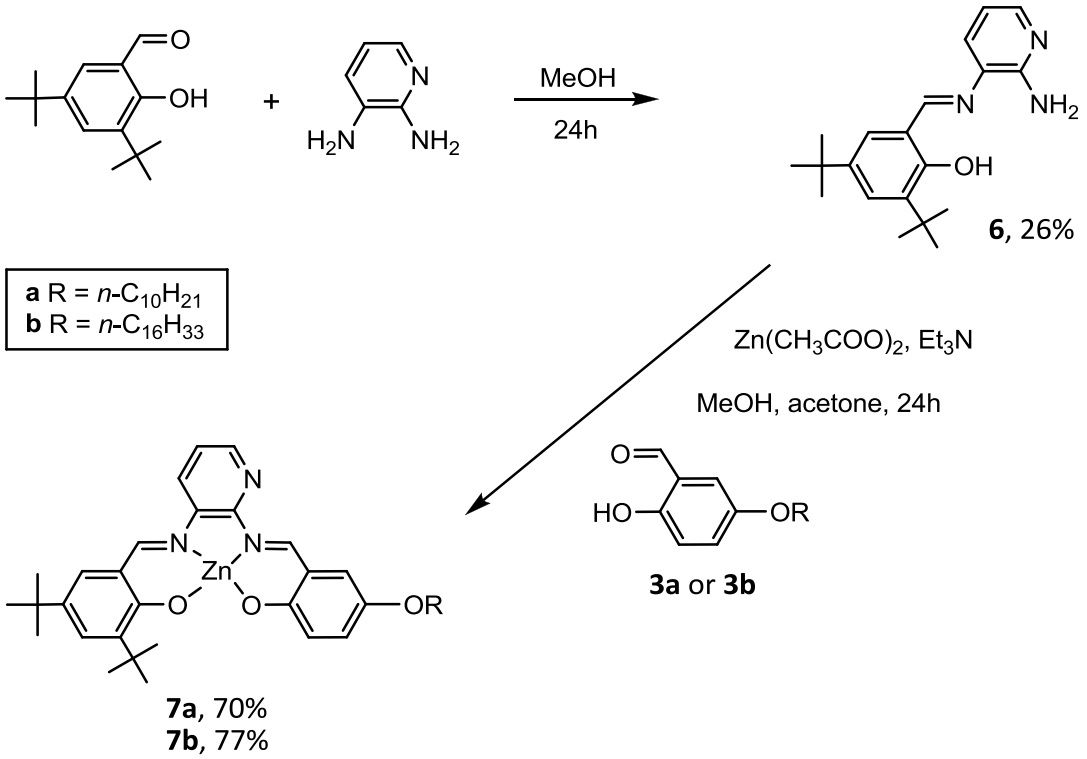

Scheme 1.4

b. Characterisation

All the complexes were characterised by NMR spectroscopy and mass spectrometry. The ^{1}H-NMR spectra in chloroform resulted to be not well resolved pointing out the formation of aggregates. (figure 1.7, top).

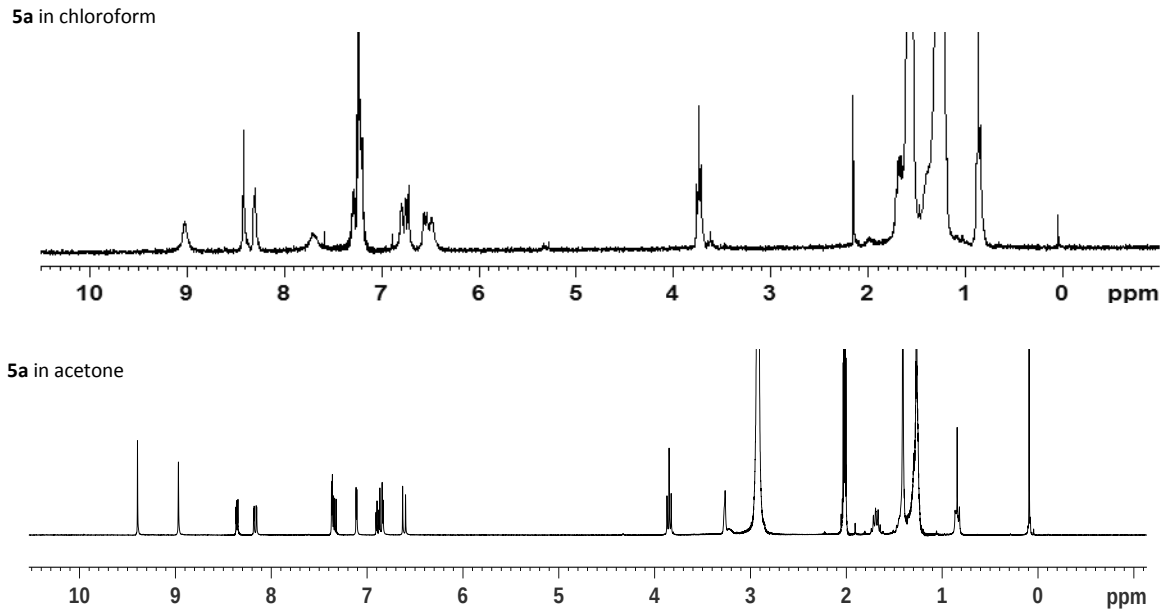

Figure 1.7 ^{1}H-NMR spectra of complex **5a** in different solvents.

A perfectly resolved spectrum was instead obtained in acetone (figure 1.7 bottom). The polar solvent breaks the aggregates and gives access to the resolved spectrum of the monomeric Zn-salophen complex.

There are at least two different intermolecular binding modes through which aggregation can take place. One is that reported in figure 1.8, that implies the formation of a μ_2-O-bridging complex, already reported in similar cases[24,25]. The other might be obtained thanks to the interaction of the pyridine nitrogen of one complex with the metal center of another complex.

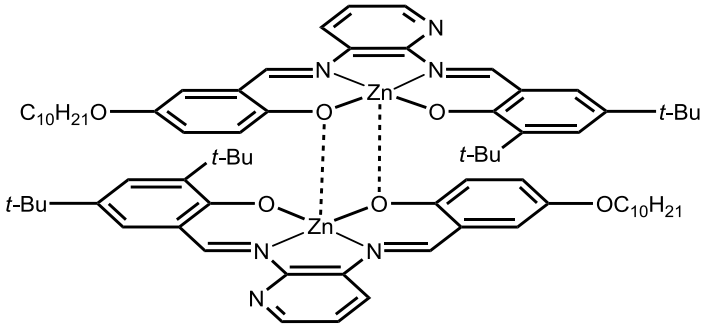

Figure 1.8 Molecular structure of the dimeric aggregate of complex **5a.**

c. X-ray diffraction

One of the possibilities to establish the nature of such interaction is by X-ray diffraction. The X-ray diffraction from a single crystal grown from acetone has confirmed the first hypothesis. In figure 1.9 the crystal structure of complex **5a** is reported. Probably the hindrance around the pyridinic Nitrogen makes this site less available with respect to the oxygen.

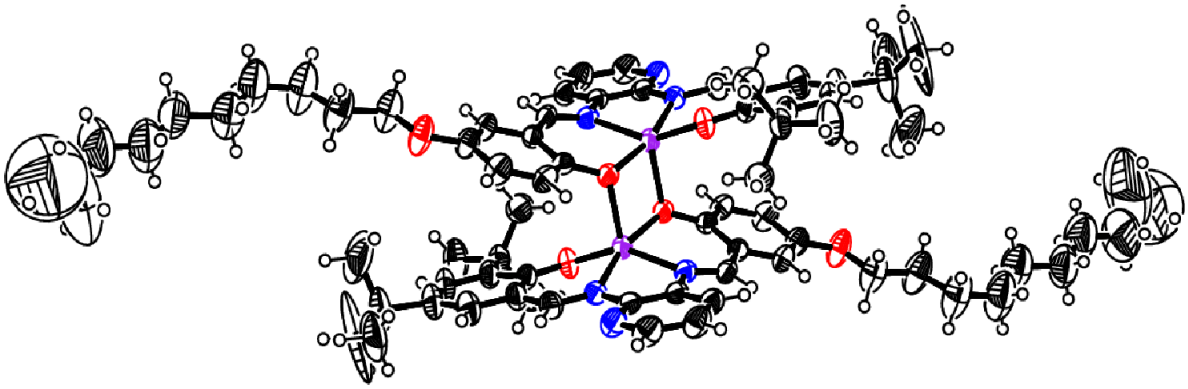

Figure 1.9 X-Ray structure of the dimeric aggregate of complex **5a**.

[24]A. W. Kleij, M. Kuil, M. Lutz, D. M. Tooke, A. L. Spek, P. C. J. Kamer, P. W. N. M. van Leeuwen , J. N. H. Reek, *Inorg. Chim. Acta* , **2006**, *359*, 1807-1814.
[25]A. Dalla Cort, L. Mandolini, C. Pasquini, K. Rissanen, L. Russo, L. Schiaffino, *New J. Chem.*, **2007**, *31*, 1633-1638.

The crystals of the complex **5a** were also observed at the Scanning Electron Microscope (SEM), and they resulted to have a parallelepiped shape (figure 1.10).

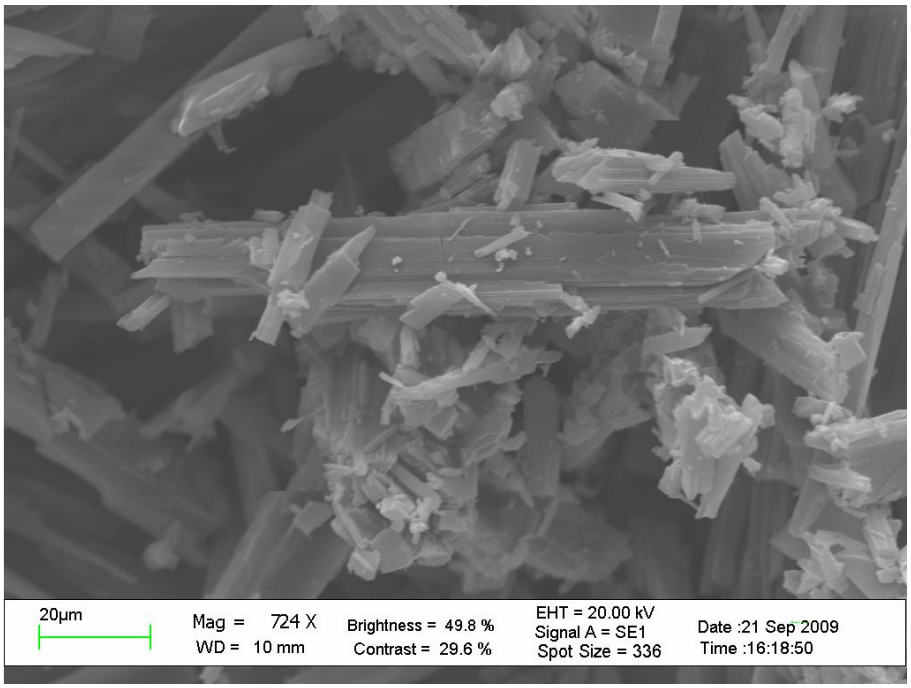

Figure 1.10 SEM photograph of complex **5a**.

Single crystal obtained from acetone and pyridine revealed the formation of a monomeric units as reported in figure 1.11. In this case the pyridine, a strong donor, competes effectively with the oxygen and the μ_2-O-bridging dimeric complexes are not formed.

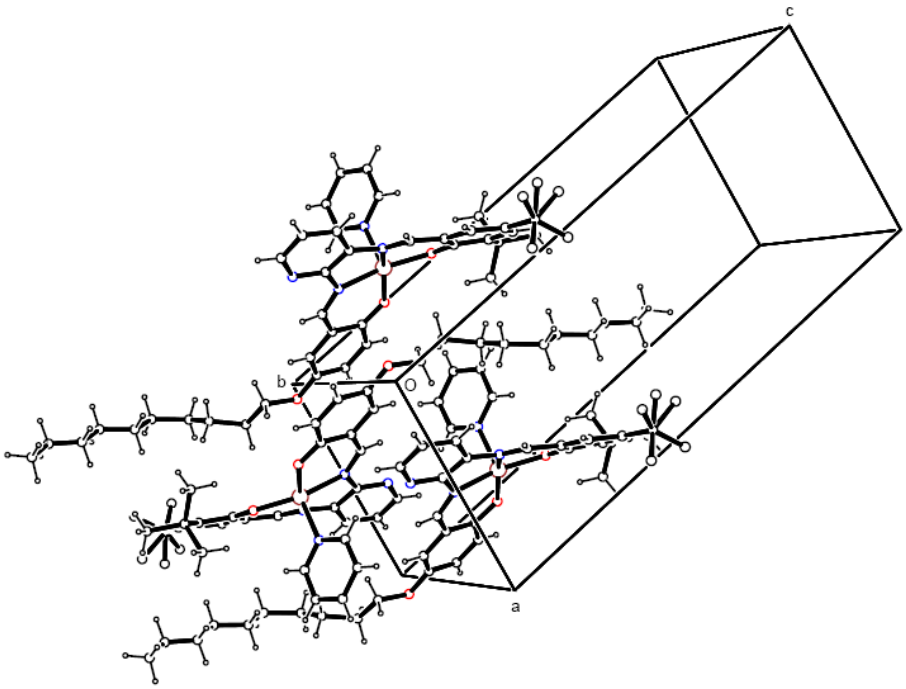

Figure 1.11 Ortep drawing of the half unit cell of the complex **5b**-pyridine.

^{1}H-NMR experiments confirmed this behaviour also in solution. The addition of few drops of deuterated pyridine to a solution of **5a** in $CDCl_3$ leads to a well-resolved spectrum (figure 1.12).

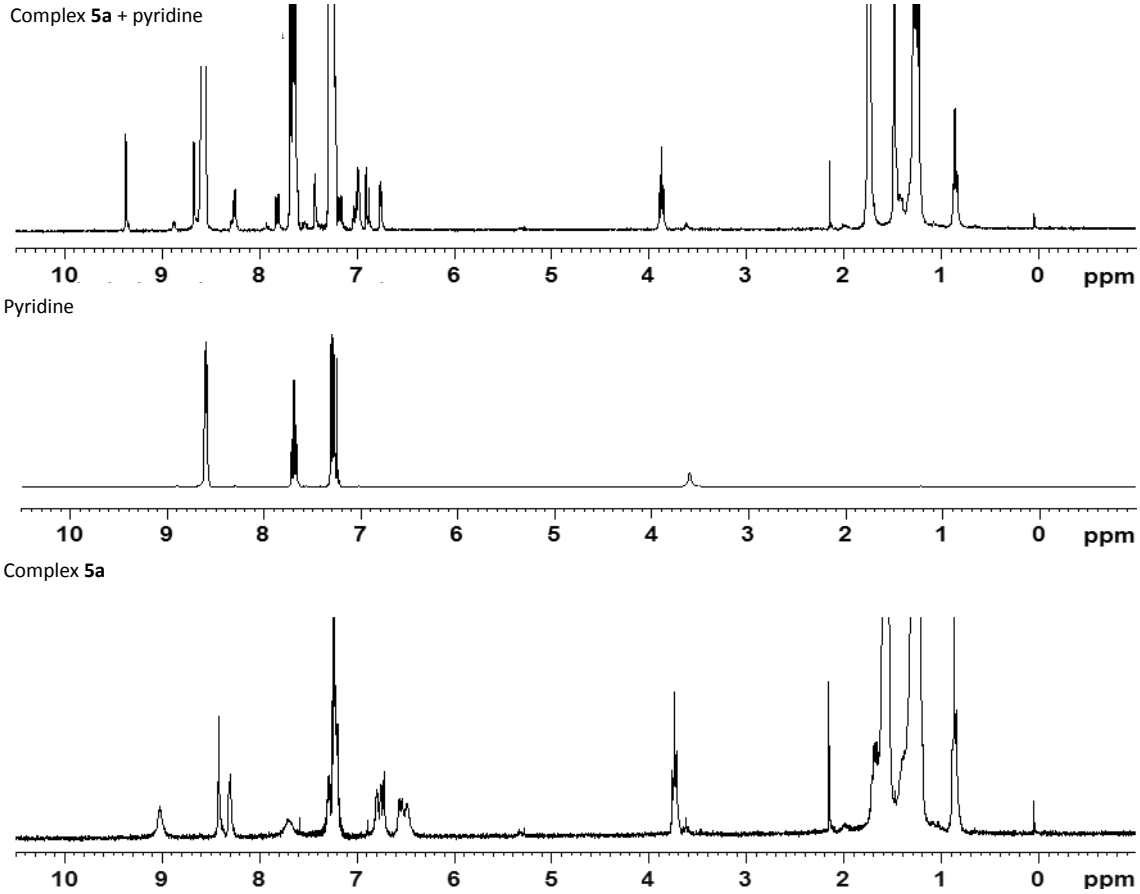

Figure 1.12 Starting from below, ^{1}H-NMR spectra: of complex **5a** in chloroform, of pyridine in chloroform, of both complex **5a** and pyridine in chloroform.

UV-Vis titrations, carried out by adding increasing amount of pyridine to a chloroform solution of complex **5a**, lead to evaluate a binding constant of 12500± 500 M^{-1}. The trend of one of the UV-Vis titrations is showed in figure 1.13.

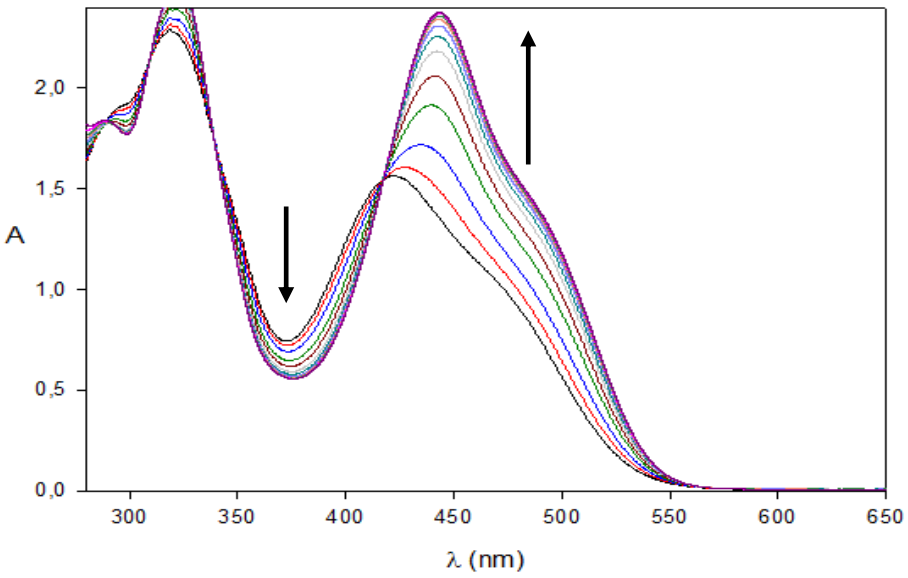

Figure 1.13 UV-Vis titration of complex **5a** with a solution of pyridine [2.9 e^{-3} M] in chloroform. The value of the constant results to be K_{pyr} = 12500 ± 500 M^{-1}.

To exploit the potentialities of the strong interaction that occurs between the Nitrogen atom of pyridine and the Zinc, we tried to obtain crystals from a solution containing complex **5b** and 4,4'-bipyridine, a ditopic guest that in principle can coordinate two Zn-salophen complexes at the same time. The crystal structure showed in figure 1.14 reveals the presence of micropores.

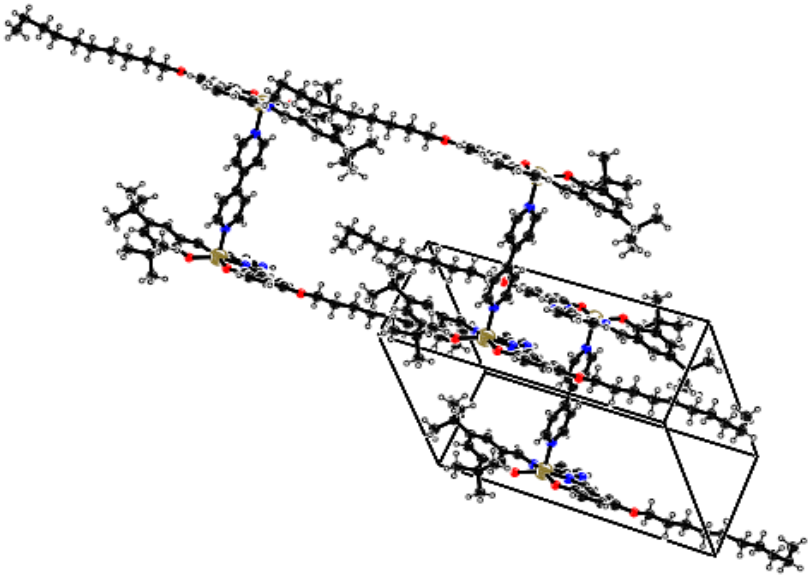

Figure 1.14 Ortep drawing of the half unit cell of the complex **5b**-4,4'-bipyridine.

Similar porous structures were obtained for crystals grown from DMF solutions (figure 1.15 and 1.16).

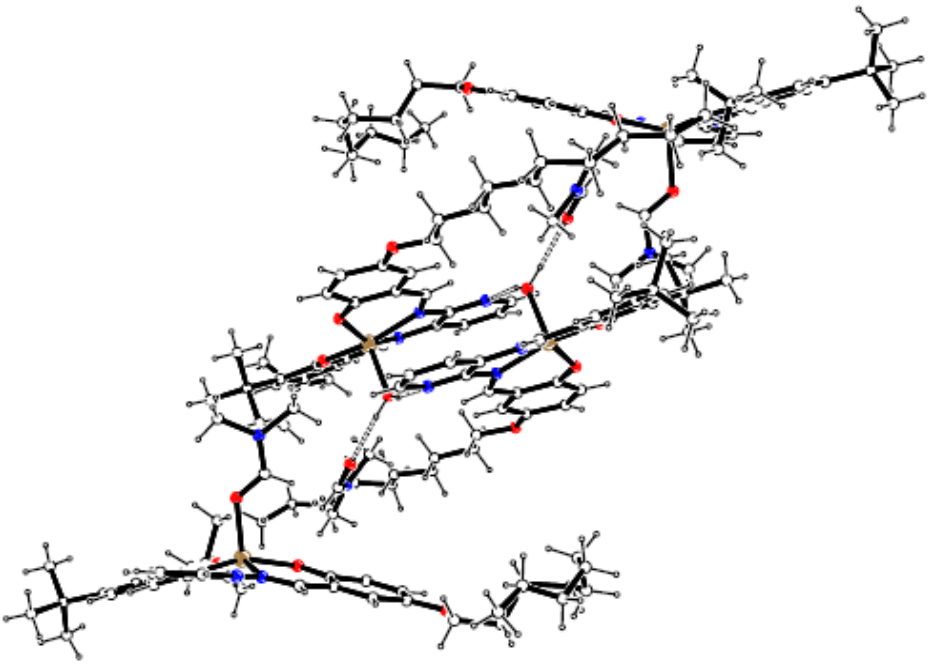

Figure 1.15 Ortep drawing of the half unit cell of the complex **5b**-H_2O-DMF.

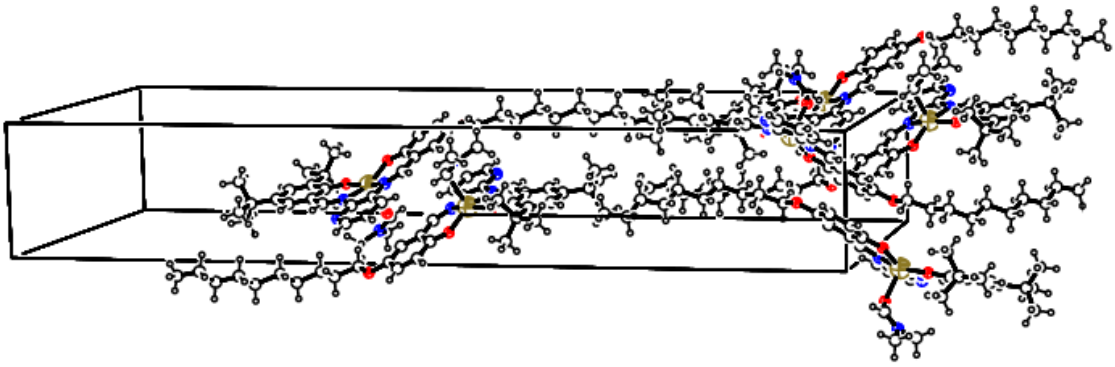

Figure 1.16 Ortep drawing of the half unit cell of the complex **5a**-DMF.

d. Synthesis of Zn-salophen complexe 9

Another approach to pyridine derivatized zinc salophen complexes was also pursued. It comprises the synthesis of 4-hydrossi-nicotinaldehyde to be used instead of salicylaldehyde. This was prepared according scheme 1.5.

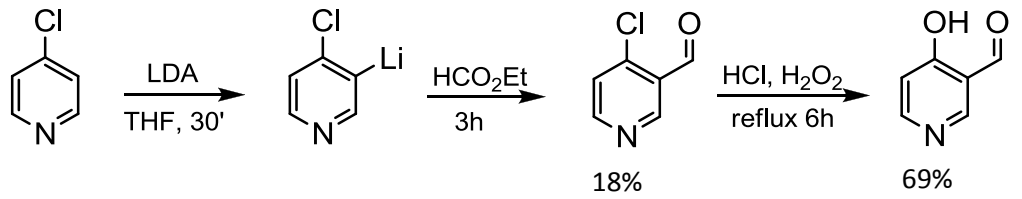

Scheme 1.5

This one was reacted with *o*-phenilenediamine to give the monoamine **8**, that was obtained in 18% yield. Compound **3a** was then reacted with **8** according to the usual procedure in the presence of zinc acetate (scheme 1.6).

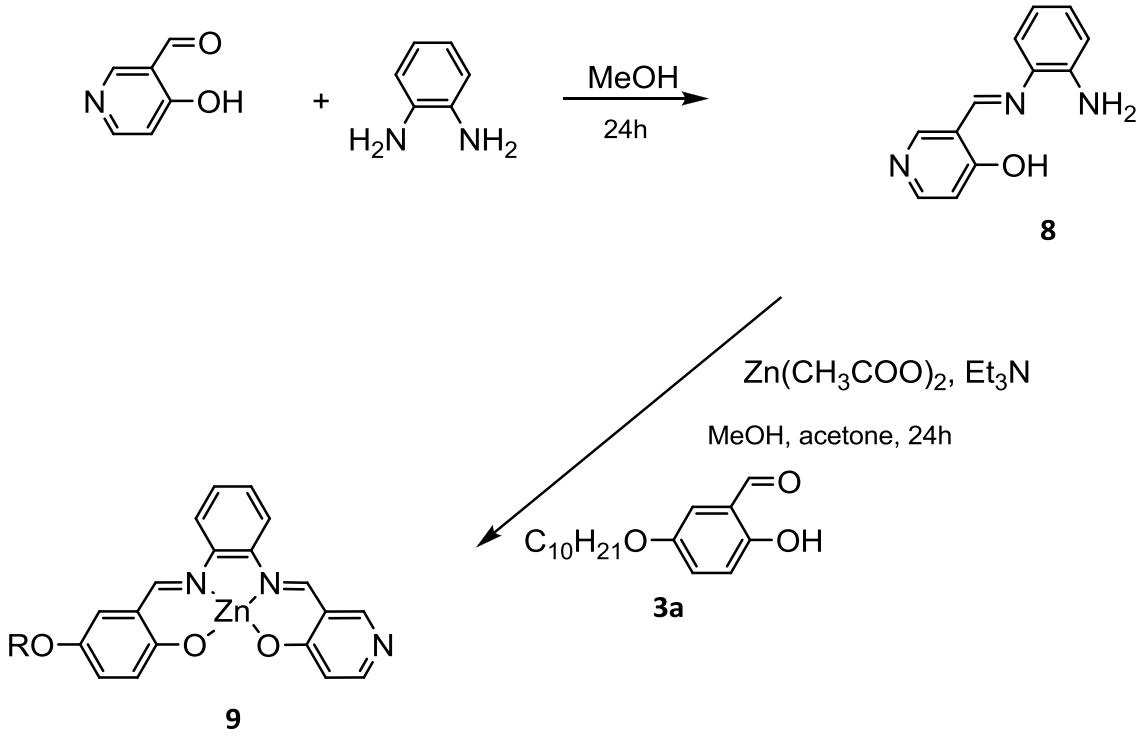

Scheme 1.6

The resulting isolated complex **9** revealed to be insoluble in the majority of common solvents, making difficult its spectroscopic characterisation.

e. Synthesis of Zn-salophen complex 13

As previously hypothesised, probably the complexes **5a**, **5b**, **7a** and **7b** didn't give the desired interaction because the pyridinic nitrogen was too hindered. For this reason we designed complex **13** (scheme 1.7).

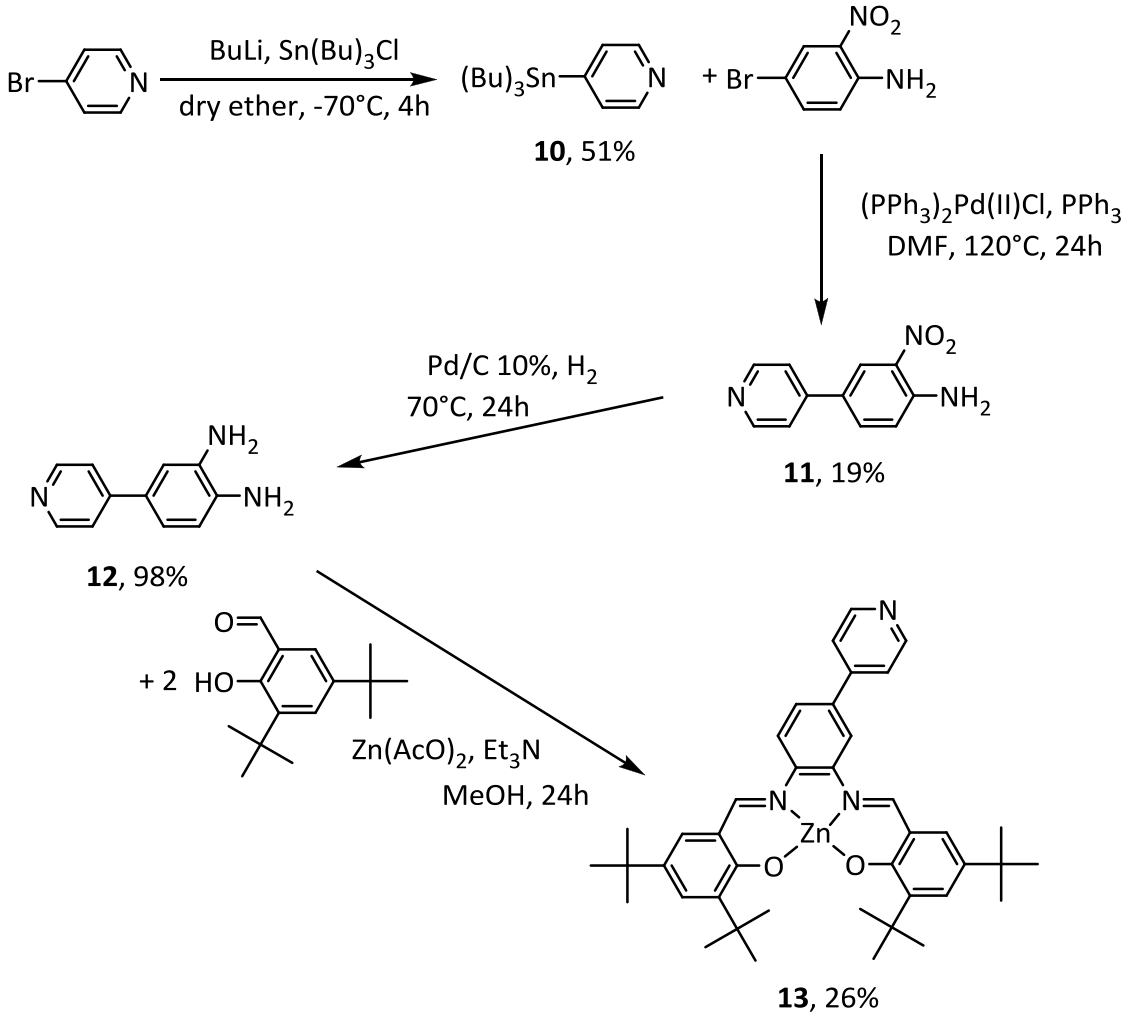

Scheme 1.7

The synthesis of the diamine **12** was first tried using the Suzuky coupling reaction[26] between 4-bromo-1,2-diaminobenzene and pyridylboronic acid, but it gave no product. Then we followed a longer synthetic path, which starts with the transformation of 4-bromo-pyridine in the organotin compound **10** (Stille reaction)[27]. This was coupled through a Suzuky reaction[28] with 4-bromo-2-nitro-aniline to give **11**, which was reduced to obtain **12**. The final step is the classical formation of a salophen and it is the condensation between the synthesized diamine and the 3,5-diterbutylsalicylaldehyde, a commercial product, in the presence of the Zinc acetate. The product was then isolated by filtration and characterised by NMR and mass spectra, but up to now all attempts done to grow single crystal failed.

[26] G. A. Morris, S.B. T. Nguyen, *Tetrahedron Lett.*, **2001**, *42*, 2093-2096.
[27] D. Peters, A.-B. Hörnfeldt, *J. Heterocycl. Chem.*, **1990**, *27*, 2165-2173.
[28] Q. Sun, B. Gatto, C. Yu, A. Liu, L. F. Liu, E. J. LaVoie, *J. Med. Chem.*, **1995**, *38*, 3638-3644.

1.3 Conclusion

We have reported the synthesis of a series of novel non-symmetrical Zn-salophen complexes (**5a**, **5b**, **7a** and **7b**) that in non coordinative solvents auto assembles and that in the solid state affords, in the presence of donor ligands, three-dimensional microporous coordination frameworks.

Also complexes **9** and **13** were synthesised, but the first one was very insoluble in common organic solvent and the second one gave problems in affording single crystals for x-ray diffraction.

1.4 Experimental section

1-(benzyloxy)-4-(decyloxy)benzene (1a)

In a 50mL flask 7,51g (0. 037 mol) of 4-benzyloxyphenol and 2.49g (0.044 mol) potassium hydroxide were combined with 15mL of water. The mixture were heated to reflux and 8.31g (0.037 mol) of *n*-decylbromide in 6mL of ethanol were added slowly. After 4h at reflux the reaction was stopped, cooled to room temperature and left at -24°C for 20'. The solid was filtered, washed with cold water and solubilised in 70mL of chloroform. The organic phase was washed two time with 10% potassium hydroxide solution and three time with water. It was then dried with sodium sulphate and evaporated to give a white solid. 7.85g (yield 61%) of the pure product was obtained by recrystallization from ethanol. **^{1}H-NMR** (300 MHz in $CDCl_3$), δ: 7.41-7.32 (m, 5H, CH), 6.90-6.79 (m, 4H, CH), 5.00 (s, 2H, CH_2), 3.88 (t, *J* = 6.6 Hz, 2H, CH_2), 1.78-1.69 (m, 2H, CH_2), 1.45-1.26 (m, 14H, CH_2), 0.88 (t, *J* = 6.3 Hz, 3H, CH_3).

1-(benzyloxy)-4-(hexadecyloxy)benzene (1b)

Procedure previously reported for product **1a**, 6.46g of product were obtained (yield of 30%). **^{1}H-NMR** (300 MHz in $CDCl_3$), δ: 7.44-7.35 (m, 5H, CH), 6.92-6.80 (m, 4H, CH), 4.98 (s, 2H, CH_2), 3.87 (t, *J* = 6.6 Hz, 2H, CH_2), 1.77-1.69 (m, 2H, CH_2), 1.46-1.25 (m, 26H, CH_2), 0.87 (t, *J* = 6.3 Hz, 3H, CH_3).

4-(decyloxy)phenol (2a)

0.26g of Pd/C (10%) were introduced in a 100mL two-neck flask and three argon-vacuum cycles were made. Then 50mL of degassed ethanol and 4.31g (0.013 mol) of 1-benzyloxy,4-*n*-decylbenzene were added. The mixture was kept at 70°C, in H_2 atmosphere for 16h. The state of the reaction was verified by TLC chromatography. The catalyst was removed by filtration on celite and after evaporation 3.20g of the pure product were obtained (yield of 95%). **^{1}H-NMR** (300 MHz in $CDCl_3$), δ: 6.75-6.71 (m, 4H, CH), 3.85 (t, *J* = 6.6 Hz, 2H, CH_2), 1.75-1.68 (m, 2H, CH_2), 1.42-1.25 (m, 14H, CH_2), 0.85 (t, *J* = 6.3 Hz, 3H, CH_3).

4-(hexadecyloxy)phenol (2b)

Procedure previously reported for product **2a**. 4.77g of product were obtained (yield of 94%). **^{1}H-NMR** (300 MHz in $CDCl_3$), δ: 6.74-6.73 (m, 4H, CH), 3.87 (t, *J* = 6.6 Hz, 2H, CH_2), 1.85-1.67 (m, 2H, CH_2), 1.45-1.23 (m, 26H, CH_2), 0.87 (t, *J* = 6.3 Hz, 3H, CH_3).

5-(decyloxy)salicylaldehyde (3a)

A flame-dried, two-necked, 100mL, round-bottomed flask equipped with an argon inlet and a magnetic stirbar was charged with 3.20g (0.012 mol) of 4-*n*-decyloxyphenol, 40mL of THF, 3.51mL (0.025 mol) of triethylamine and 2.61g (0.027 mol) of magnesium chloride. After 30' 2.12 g (0.071 mol) of paraformaldehyde were added. The mixture was heated to 70°C for 3h, then it was cooled to room temperature and 10mL of ethylacetate were added. The organic phase was washed three times with HCl 1N, one time with brine, dried on Na_2SO_4, filtrated and concentrated using a rotary evaporator. The residue was purified by flash column chromatography (silica gel, elution with petroleum ether:dichloromethane = 7:3). The fractions containing the product were collected to give 2.63g of a yellow solid (yield of 74%). **^{1}H-NMR** (200 MHz in $CDCl_3$), δ: 10.62 (s, 1H, CHO), 9.84 (s, 1H, OH), 7.16-6.88 (m, 3H, CH), 3.93 (t, *J* = 6.6 Hz, 2H, CH_2), 1.80-1.73 (m, 2H, CH_2), 1.42-1.26 (m, 14H, CH_2), 0.87 (t, *J* = 6.3 Hz, 3H, CH_3).

5-(hexadecyloxy)salicylaldehyde (3b)

Procedure previously reported for product **3a**. 4.94g of product were obtained (yield of 95%). **^{1}H-NMR** (200 MHz in $CDCl_3$), δ: 10.62 (s, 1H, CHO), 9.84 (s, 1H, OH), 7.15-6.89 (m, 3H,

CH), 3.93 (t, *J* = 6.6 Hz, 2H, CH_2), 1.80-1.73 (m, 2H, CH_2), 1.43-1.25 (m, 26H, CH_2), 0.87 (t, *J* = 6.3 Hz, 3H, CH_3).

Monoimine of 5-(decyloxy)salicylaldehyde (4a)

1.01 g (0.009 mol) of 2,3-diaminopyridine, 0.92g (0.003 mol) of 2-idroxy,5-*n*-decyloxybenzaldehyde and 18mL of methanol were introduced in a 50mL flask and stirred at room temperature. After 24h the mixture was filtered and the collected solid was purified by flash column chromatography (silica gel, elution with chloroform:ethylacetate = 7:3). 0.99g of the pure product were obtained with the yield of 82%. **^{1}H-NMR** (300 MHz in CD_3COCD_3): δ: 11.99 (s, 1H, OH), 8.77 (s, 1H, CH), 7.89 (dd, J_1 = 4.9 Hz, J_2 = 1.5 Hz, 1H, CH), 7.38 (dd, J_1 = 7.5 Hz, J_2 = 1.5 Hz, 1H, CH), 7.13 (d, *J* = 3.3 Hz, 1H, CH), 7.00 (dd, J_1 = 9 Hz, J_2 = 3.3 Hz, 1H, CH), 6.84 (d, *J* = 9 Hz 1H, CH), 6.64 (dd, J_1 = 7.5 Hz, J_2 = 4.9 Hz, 1H, CH), 5.45 (bs, 2H, NH_2), 3.94 (t, *J* = 6.3 Hz, 2H, CH_2), 1.42-1.26 (m, 16H, CH_2), 0.83 (t, *J* = 6.3 Hz, 3H, CH_3). **^{13}C-NMR** (300 MHz in CD_3COCD_3): δ: 163.81, 154.71, 152.61, 151.81, 146.28, 144.50, 130.90, 125.28, 121.81, 118.43, 117.83, 116.04, 113.94, 68.69, 31.62, 29.31, 29.29, 29.12, 29.04, 25.76, 22.41, 13.85. **Elementar Analysis**: *calc.* 11.37 N%; 71.51 C%; 8.46 H%; *found* 11.34 N%; 71.16 C%; 8.29 H%.

Monoimine of 5-(hexadecyloxy)salicylaldehyde (4b)

Procedure previously reported for product **4a**, 0.58g of product were obtained (yield of 46%). **^{1}H-NMR** (300 MHz in CD_3COCD_3): δ: 11.99 (s, 1H, OH), 8.77 (s, 1H, CH), 7.89 (dd, J_1 = 4.9 Hz, J_2 = 1.5 Hz, 1H, CH), 7.38 (dd, J_1 = 7.5 Hz, J_2 = 1.5 Hz, 1H, CH), 7.13 (d, *J* = 3.3 Hz, 1H, CH), 7.01 (dd, J_1 = 9 Hz, J_2 = 3.3 Hz, 1H, CH), 6.84 (d, *J* = 9 Hz, 1H, CH), 6.64 (dd, J_1 = 7.5 Hz, J_2 = 4.9 Hz,1H, CH), 5.45 (bs, 2H, NH_2), 3.95 (t, *J* = 6.3 Hz, 2H, CH_2), 1.45-1.24 (m, 26H, CH_2), 0.83 (t, *J* = 6.3 Hz, 3H, CH_3). **^{13}C-NMR** (300 MHz in CD_3COCD_3): δ: 166.45, 155.06, 152.11, 151.09, 134.81, 127.98, 123.52, 118.27, 117.87, 116.28, 112.89, 68.75, 31.63, 29.40, 29.31, 29.10, 29.06, 28.99, 25.74, 22.39, 13.82. **Elementar Analysis**: *calc.* 9.26 N%; 74.13 C%; 9.55 H%; *found* 8.69 N%; 73.24 C%; 9.30 H%.

Salophen (5a)

0.30g (0.0008 mol) of monoimine of 2-idroxy,5-*n*-decyloxybenzaldehyde was solubilized in 15mL of acetone, then 0.24g (0.001 mol) of 3,5-bis(*tert*-butyl) salicylaldehyde, 0.29g (0.0012

mol) of zinc acetate, 1.5mL of triethylamine and 30ml of methanol were added. The mixture was stirred for 24h at room temperature and the product is collected by filtration. 0.32g of an orange solid (m.p. 233°C) were obtained with a yield of 64%. **^{1}H-NMR** (300 MHz in CD_3COCD_3), δ: 9.40 (s, 1H, CH), 8.97 (s, 1H, CH), 8.35 (dd, J_1 = 4.9 Hz, J_2 = 1.5 Hz, 1H, CH), 8.16 (dd, J_1 = 8.1 Hz, J_2 = 1.5 Hz, 1H, CH), 7.37-7.31 (m, 2H, CH), 7.11 (d, J = 2.7 Hz, 1H, CH), 6.90-6.82 (m, 2H, CH), 6.61 (d, J = 9 Hz, 1H, CH), 3.85 (t, J = 6.3 Hz, 2H, CH_2), 1.71 (m, 2H, CH_2), 1.41 (s, 9H, CH_3), 1.40-1.27 (m, 23H, CH_2 and CH_3), 0.84 (t, J = 6.3 Hz, 3H, CH_3). **^{13}C-NMR** (300 MHz in CD_3COCD_3), δ: 172.29, 163.27, 150.69, 148.04, 145.95, 141.37, 134.45, 133.99, 129.61, 129.58, 124.74, 124.35, 123.49, 121.64, 118.5, 117.88, 116.57, 68.14, 34.95, 33.20, 31.45, 30.46, 25.66, 22.14. **Mass** (m/z): $[M + H]^+$ 649, $[2M + H]^+$ 1296.8. **Elementar Analysis**: *calc.* 6.47 N%; 68.45 C%; 7.61 H%; *found* 6.23 N%; 67.77 C%; 7.26 H%.

Salophen (5b)

Procedure previously reported for product **5a**. 0.42g of product were obtained (yield of 82%). **^{1}H-NMR** (300 MHz in CD_3COCD_3), δ: 9.38 (s, 1H, CH), 8.96 (s, 1H, CH), 8.35 (dd, J_1 = 4.9 Hz, J_2 = 1.5 Hz, 1H, CH), 8.15 (dd, J_1 = 8.1 Hz, J_2 = 1.5 Hz, 1H, CH), 7.36-7.32 (m, 2H, CH), 7.09 (d, J = 2.7 Hz, 1H, CH), 6.89-6.82 (m, 2H, CH), 6.58 (d, J = 9 Hz, 1H, CH), 3.84 (t, J = 6.6 Hz, 2H, CH_2), 1.71 (m, 2H, CH_2), 1.41 (s, 9H, CH_3), 1.37-1.25 (m, 35H, CH_2 and CH_3), 0.83 (t, J = 6.3 Hz, 3H, CH_3). **^{13}C-NMR** (300 MHz in CD_3COCD_3), δ: 172.35, 167.39, 163.63, 163.1, 150.67, 147.86, 145.85, 141.45, 134.43, 133.94, 129.57, 124.81, 124.30, 123.42, 121.59, 118.37, 117.87, 116.59, 68.19, 34.96, 33.20, 31.43, 30.48, 25.65, 22.13, 13.17. **Mass** (m/z): $[M + H]^+$ 733, $[2M + H]^+$ 1465.8.

Monoimine of 3,5-di-*t*-butylsalicylaldehyde (6)

Procedure previously reported for product **4a**. 0.56g of product were obtained (yield of 26%). **^{1}H-NMR** (300 MHz in CD_3COCD_3): δ: 13.24 (s, 1H, OH), 8.83 (s, 1H, CH), 7.90 (dd, J_1 = 4.9 Hz, J_2 = 1.5 Hz, 1H, CH), 7.49-7.41 (m, 3H, CH), 6.66 (dd, J_1 = 7.5 Hz, J_2 = 4.9 Hz, 1H, CH), 5.45 (bs, 2H, NH_2), 1.43 (s, 9H, CH_3), 1.30 (s, 9H, CH_3). **^{13}C-NMR** (300 MHz in CD_3COCD_3): δ: 165.11, 157.42, 152.09, 142.49, 140.63, 136.63, 131.06, 128.51, 126.52, 125.22, 117.57, 113.41, 34.48, 33.58, 30.75, 28.73. **Elementar Analysis**: *calc.* 12.91 N%; 73.81 C%; 8.36 H%; *found* 12.84 N%; 72.91 C%; 7.74 H%. **Mass** (m/z): $[M + H]^+$ 325.

Salophen (7a)

Procedure previously reported for product **5a**. 0.27g of product were obtained (yield of 70%).**^{1}H-NMR** (300 MHz in CD_3COCD_3), δ: 9.42 (s, 1H, CH), 9.00 (s, 1H, CH), 8.31 (dd, J_1 = 4.9 Hz, J_2 = 1.5 Hz, 1H, CH), 8.22 (dd, J_1 = 8.1 Hz, J_2 = 1.5 Hz, 1H, CH), 7.38-7.31 (m, 2H, CH), 7.13 (d, J = 2.7 Hz, 1H, CH), 6.94 (dd, J_1 = 9 Hz, J_2 = 3.3 Hz, 1H, CH), 6.88 (d, J = 3.3 Hz, 1H, CH), 6.68 (d, J = 9 Hz, 1H, CH), 3.93 (t, J = 6.6 Hz, 2H, CH_2), 1.73 (m, 2H, CH_2), 1.41 (s, 9H, CH_3), 1.40-1.25 (m, 23H, CH_2 and CH_3), 0.83 (t, J = 6.3 Hz, 3H, CH_3). **^{13}C-NMR** (300 MHz in CD_3COCD_3), δ: 171.29, 163.92, 162.73, 150.05, 147.75, 145.09, 141.32, 135.10, 133.74, 129.02, 128.99, 126.04, 124.76, 123.19, 122.15, 118.21, 117.70, 116.36, 68.10, 34.99, 33.20, 31.45, 30.53, 29.43, 29.03, 28.96, 27.89, 25.69, 22.14, 13.17. **Elementar Analysis**: *calc.* 6.47 N%; 68.45 C%; 7.61 H%; *found* 6.36 N%; 67.72 C%; 7.67 H%. **Mass** (m/z): $[M + H]^+$ 649, $[2M + H]^+$ 1298.

Salophen (7b)

Procedure previously reported for product **5a**. 0.44g of product were obtained (yield of 77%).**^{1}H-NMR** (300 MHz in CD_3COCD_3), δ: 9.43 (s, 1H, CH), 9.01 (s, 1H, CH), 8.30 (dd, J_1 = 4.9 Hz, J_2 = 1.5 Hz, 1H, CH), 8.23 (dd, J_1 = 8.1 Hz, J_2 = 1.5 Hz, 1H, CH), 7.38-7.32 (m, 2H, CH), 7.14 (d, J = 2.7 Hz, 1H, CH), 6.96 (dd, J_1 = 9 Hz, J_2 = 3.3 Hz, 2H, CH), 6.88 (d, J = 3.3 Hz, 1H, CH), 6.68 (d, J = 9 Hz, 1H, CH), 3.93 (t, J = 6.6 Hz, 2H, CH_2), 1.73 (m, 2H, CH_2), 1.41 (s, 9H, CH_3), 1.37-1.26 (m, 35H, CH_2 and CH_3), 0.84 (t, J = 6.3 Hz, 3H, CH_3). **^{13}C-NMR** (300 MHz in CD_3COCD_3), δ: 163.80, 162.52, 147.45, 145.03, 141.38, 135.08, 133.67, 129.03, 128.98, 126.27, 124.80, 123.18, 118.91, 117.35, 116.35, 68.16, 34.99, 33.20, 30.53, 25.67, 22.12, 13.16. **Mass** (m/z): $[M + H]^+$ 733, $[2M + H]^+$ 1465.8.

4-chloro-3-formylpyridine

A flame-dried, two-necked, 100mL, round-bottomed flask equipped with an argon inlet and a magnetic stirbar was charged with 0.80g (0.007 mol) of 4-chloropyridine, 6mL (0.009 mol) of LDA and 30mL of dry THF. The mixture was left at -70°C for 30’ and then 0.71mL (0.009 mol) of ethylformiate solubilised in 10mL of solvent were added. The flask was kept at -70°C for 3h and, when the temperature was increased up to -10°C, 10mL of water were added. The mixture was extracted with diethylether and the organic phase was dried and evaporated. 0.17g of the pure product (yield of 18%) were obtained after purification with column chromatography on silica gel (elution with chloroform). **^{1}H-NMR** (200 MHz in $CDCl_3$),

δ: 10.50 (s, 1H, CHO), 9.05 (s, 1H, CH), 8.69 (d, *J* = 5.2 Hz, 1H, CH), 7.47 (d, *J* = 5.2 Hz, 1H, CH). **Mass** (m/z): $[M + H]^+$ 141.

4-hydrossi-nicotinaldehyde

0.17g (0.0012 mol) of 4-chloro-3-formylpyridine, 3 drops of H_2O_2 (3%) and 13mL of HCl 3N were introduced in a stirred flask. After 6h at reflux the mixture was neutralised with 2g of $CaCO_3$, the solvent was evaporated and the solid was washed with absolute ethanol, which solubilises the product. The impurities were removed by filtration and 0.10g of a yellow solid were obtained (yield of 69%). **^{1}H-NMR** (300 MHz in $CDCl_3$), δ: 10.09 (s, 1H, CHO), 8.52 (d, *J* = 1.8 Hz, 1H, CH), 8.09 (d, *J* = 6.6 Hz, 1H, CH), 6.64 (d, *J* = 6.6 Hz, 1H, CH). **Mass** (m/z): $[M + H]^+$ 123.

Monoimine of 4-hydrossi-nicotinaldehyde (8)

0.03g (0.00027 mol) of *o*-phenylenediamine, 0.03g (0.00024 mol) of 4-hydrossi-nicotinaldehyde and 10mL of ethanol were introduced in a 50mL stirred flask. After 30' the solvent was evaporated and the product (0.05g) characterised. Some impurities were present, but the product was directly used in the following step.

Salophen (9)

A 25mL flask was charged with 0.05g (0.00022 mol) of the monoimine **8**, 0.06g (0.00025 mol) of Zinc acetate, 0.07g (0.00026 mol) of 2-idroxy,5-*n*-decyloxybenzaldehyde and 25mL of ethanol. After 2h at reflux the colour of the mixture was evidently changed and a solid was precipitated. The product was collected by filtration (0.12g), but characterisation and further purifications were not possible because of the low solubility.

4-(tributhylstannyl)pyridine (10)

To obtain 4-bromo-pyridine, 1.38g (0.0071 mol) of 4-bromo-pyridine-hydrochloride were treated with 10eq. of NaOH, and extracted with diethylether. After evaporation of the solvent, the reactant was introduced in a 25mL flame-dried flask with 11mL of dried ether. The flask is kept a -70°C and at this temperature 3.04mL (0.0076 mol) of butyllitium were slowly added. After 30' 1.93mL (0.0071 mol) of Bu_3SnCl solubilised in 4mL of solvent were added and the mixture was maintained in these conditions for still 4h. When the room

temperature was reached, 15mL of water are introduced in the flask. After three extractions with diethylether the organic phase was dried and evaporated. 1.34g of the pure product (yield of 51%) were obtained after purification with column chromatography (silica gel, elution with petroleum ether:dichlorometane = 9:1). **^{1}H-NMR** (300 MHz in $CDCl_3$), δ: 8.45 (d, *J* = 5.0 Hz, 2H, CH), 7.50 (d, *J* = 5.0 Hz, 2H, CH), 1.60-1.46 (m, 6H, CH_2), 1.33-1.24 (m, 6H, CH_2), 1.12-1.07 (m, 6H, CH_2), 0.86 (t, *J* = 7.2 Hz, 9H, CH_2).

2-nitro-4-(pyridin-4-yl)aniline (11)

0.30g (0.0014 mol) of 4-bromo-2-nitroaniline were solubilised in 9mL of DMF in a flame-dried 25mL flask. Then 0.50g (0.0014 mol) of **10**, 0.05g (0.000068 mol) of $PdCl_2(PPh_3)_2$ and 0.183g (0.00068 mol) of PPh_3 were added at this solution. The mixture was kept at reflux overnight. 1.18g of the crude product were obtained by evaporation and purified by flash chromatography (silica gel, elution with hexane:ethylacetate = 7:3). The pure product was isolated with a yield of 19% (0.05g). **^{1}H-NMR** (300 MHz in $CDCl_3$), δ: 8.53-8.49 (m, 2H, CH), 7.83 (m, 1H, CH), 7.70-7.53 (m, 3H, CH), 7.09 (d, *J* = 9.0 Hz, 1H, CH), 4.59 (bs, 2H, NH_2).

4-(pyridin-4-yl)benzene-1,2-diamine (12)

0.03g of Pd/C (10%) were introduced in a 100mL two-neck flask and three argon-vacuum cycles were made. Then 50 ml of degassed ethanol and 0.05g (0.00025 mol) of 2-nitro-4-(pyridin-4-yl)aniline were added. The mixture remained at 70°C, in H_2 atmosphere for 16 h. The state of the reaction was verified on TLC chromatography. The catalyst was removed by filtration on celite and, after evaporation, 0.05g of the pure product were obtained (98%). **^{1}H-NMR** (300 MHz in $CDCl_3$), δ: 7.67-7.61 (m, 3H, CH), 7.55-7.46 (m, 4H, CH), 1.59 (bs, 4H, NH_2).

Salophen of 4-(pyridin-4-yl)benzene-1,2-diamine (13)

A 50mL flask was charged with 0.05g (0.00027 mol) of **12**, 0.10g (0.00045 mol) of Zinc acetate, 0.14g (0.0006 mol) of 3,5-di-*t*-butylsalycilaldehyde, 0.3mL of triethylamine and 15mL of methanol. 0.05g of the product (yield of 26%) were collected by filtration. **^{1}H-NMR** (300 MHz in DMSO), δ: 9.19 (s, 1H, CH), 9.06 (s, 1H, CH), 8.64 (d, *J* = 6.3 Hz, 2H, CH), 8.31 (s, 1H, CH), 8.03 (m, 2H, CH), 7.88 (m, 2H, CH), 7.77-7.74 (m, 2H, CH), 7.28-7.22 (m, 2H, CH), 1.44 (s, 18H, CH_3), 1.25 (m, 18H, CH_3). **^{13}C-NMR** (300 MHz in CD_3COCD_3), δ: 187.85, 185.83, 150.34, 141.18, 129.99, 128.83, 124.88, 123.53, 118.42, 35.42, 31.59, 31.52, 31.26, 29.79, 22.59. **Exact Mass** (m/z): $[M + H]^+$ 680.3194 (*M calc.* 679.31).

Chapter 2

Functionalization of self-assembled supramolecular polymers

2.1 Introduction

a. Definition of gel

In the field of Materials Science there is always a lot of interest for the studies of systems which give gels.

The definition of *gel* is still subject of discussion. As a matter of fact at the beginning the problem was raised when, after the evaporation of a solvent, two different behaviours were observed: precipitation or formation of a gel. This latter one was defined as a solid elastic system, which embodied a large volume of liquid. This condition was "easier to recognize then to define"[29]. The definition has been improved during all the last century to arrive, with Rogovina et al. in 2008[30], at the last one: a gel is a solid composed by at least two components, one (polymer) which form a three-dimensional cross-linked network through covalent (chemical gel) or non-covalent bonds (physical gel) within a second one (liquid). The amount of this latter one should be from ten to a hundred times greater than the quantity of the polymer.

In conclusion the best way to recognize a gel remains the method of *"turning the vial"* (figure 2.1).

Figure 2.1

Depending on the nature of the liquid phase, gels can be classified as organogel (in organic solvent) or hydrogels (in water). And furthermore, depending on the nature of the bonds which form the network, it is possible to distinguish two families (figure 2.2):

- Chemical gels, based on covalent bonds and, as a consequence, usually irreversible
- Physical gels, based on non-covalent bonds and reversible.

The first one concerns classical synthetic methodology, which aim is the organization of the molecules (network) through covalent bonds (knots).

[29] D. J. Lloyd, *Colloid Chemistry*; J. Alexander Ed., *The Chemical Catalog Co:. New York*, **1926**, Vol. 1, p 767.
[30] L. Rogovina, V. Vasil'ev, E. Braudo, *Pol. Sci. Series C*, **2008**, 50 (1), 85-92.

Chemical gel *Physical gel*

Figure 2.2 Schematic representation of two classes of gels: chemical and physical.

In the second family, because of the reversibility of the interactions, there is a continuous interchange between the connections. The contribution of an additional force is necessary to obtain a stable system: the cooperativity. This means that the energetic formation barrier of an interaction will decrease after the formation of the same connection in the neighborhood.

Also if the definition of physical network is simple, the area of research involved in these studies is really wide. In fact the enormous variety of interactions that can occur among the molecules removes almost all the limits to the scientist's imagination. For example it is possible to design a molecule that, through expected interaction, leads to the encapsulation of a guest.

b. Applications and examples of physical gels

Numerous articles concerning physical gel are well known and widely spread in the literature. The starting approach is the design of molecular structures, which are capable of assembling into functional nano-scale architectures. The development of low-molecular-weight building blocks can lead to self-assembling gel, through non-covalent interactions. A lot of supramolecular polymers belong to this class of compounds.

To form a physical gel it is possible to exploit all the weak interactions characteristic of the supramolecular chemistry, to which this kind of gel belongs. Obviously gel classification derives directly from this strict connection. In the next few pages for each kind of gel we will show some example, also concerning the formation of *containers*, subject strictly related to our work.

Electrostatic

These gels are characterized by a bond energy comprised between 50-400 kJ/mol, isotropy and presence of a precise proportion between the two species. The limit is the sensitivity to

every change that will influence the strength of the electrostatic interaction (change of pH or ionic force, presence of chelating agent).

As shown in figure 2.3, Guenet et al.[31] have designed a building block based on a propargylamine skeleton which organizes itself in a supramolecular pH- and thermo-responsive system. The presence of hydrochloric acid induces the formation of self-supporting structures, which were observed by SEM and SANS. The experiments confirmed the importance of protonation of the amine, of the presence of chloride anion and of the role of the alkyne substituent on the nitrogen.

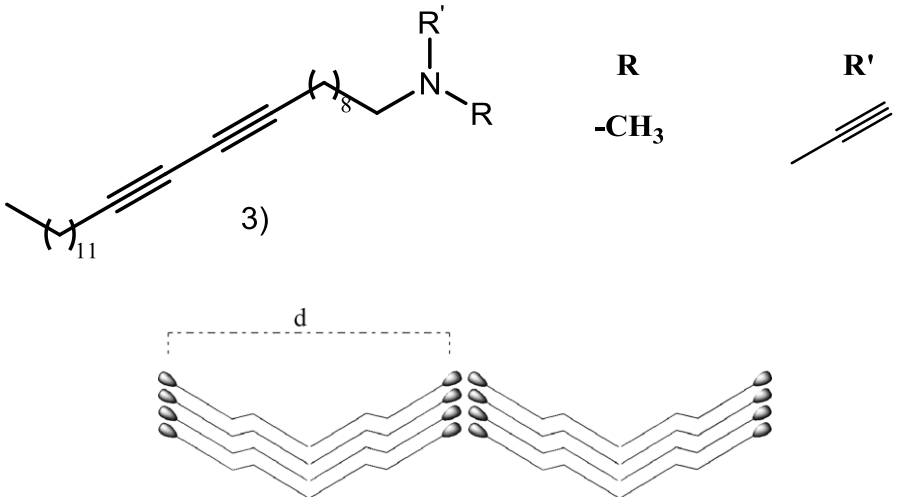

Figure 2.3 Sketch of the possible chevron-like arrangement of **3)** accounting for the 4.9 nm spacing distance (*d)* observed by Small Angles Neutron Scattering.

Complexation

This kind of interaction is the most energetic (50-200kJ/mol) and is really selective, because it depends on a two-way interaction between the components. The limit is the amount of product required, which is greater than the other cases (usually about 1-2% in mass, here is comprised between 15-25% in mass).

The next example[32] shows how it is possible to obtain viscous jellies from the cooling of an hot solution, exploiting the encapsulation of a metal ion (Cu^{2+}) by a ditopic ligand (ethyl-2-hexanoate), which forms filaments similar to polymeric chains (figure 2.4).

[31] E. Morin, J.-M. Guenet, D. D. Dıaz, J.-S. Remy, A. Wagner, *J. Phys. Chem. B* **2010,** *114,* 12495–12500.

[32] D. Lopez, J.-M. Guenet, *J. Phys. Chem. B,* **2002,** *106,* 2160-2165.

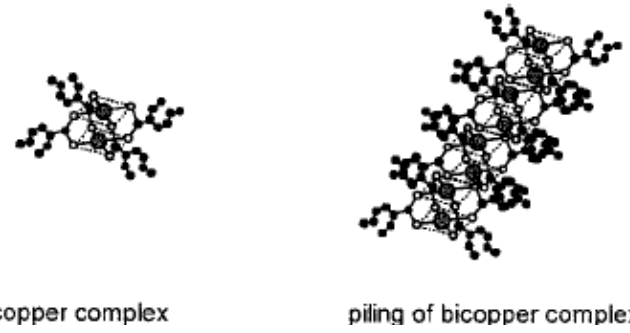

Figure 2.4 Schematic drawing of a bicopper complex molecule (left), and the way these molecules pile up to form long monomolecular filament (right). The chemical formula is $Cu_2(O_2C\text{-}C_7H_{15})_4$.

This system, like many others, is in continuous equilibrium between the breaking of existing filaments and formation of new ones. An important property associated to this complex is the possibility to act as an heterogeneous nucleation agent for the formation of the fibrils of iPS (isotactic polystyrene) gel and to cause an increase in gelation threshold.

A particular feature for this mixed system is the dependence not only on the nature of solvent, but also on its configuration. Indeed the gel forms in trans-decaline but not in cis-decaline.

Encapsulation of a metal ion was exploited also by S.Arai et al[33], who obtained gels by the self-assembly of mono-urea derivatives and Ag^+ in organic solvents, like benzene, xylene and tetralin. In this structure there are two active sites:

- a pyridyl substituent, which interacts with silver in 2:1 proportion,
- the urea groups, which form intermolecular hydrogen bonds, fundamental for the fibrous self-assembly.

It is only the combination of the two effect which leads to gelation.

π – π stacking

This kind of interaction brings to the formation of anisotropic aggregates, thus it is widely used in supramolecular design. It is not too much energetic (1-50 kJ/mol), but its strength lies in the large number of connections which can be formed.

Nijenhuis et al.[34] started from an idea concerning the conductivity of electronic charge through self-organized columnar assemblies and developed a diskotic sidechain polymer. The

[33] S. Arai, K. Imazu, S. Kusuda, I. Yoshihama, M. Tonegawa, Y. Nishimura, K.-I. Kitahara, S. Oishi, T. Takemura, *Chem Lett.*, **2006**, *vol. 35*, p. 634 – 635.

gel formation depends on the face-to-face interaction among the mesogens, which are characterized by an extended aromatic wall.

From calculation it results that almost all the mesogens linked to the polymeric chain are in a free state.

a) b)

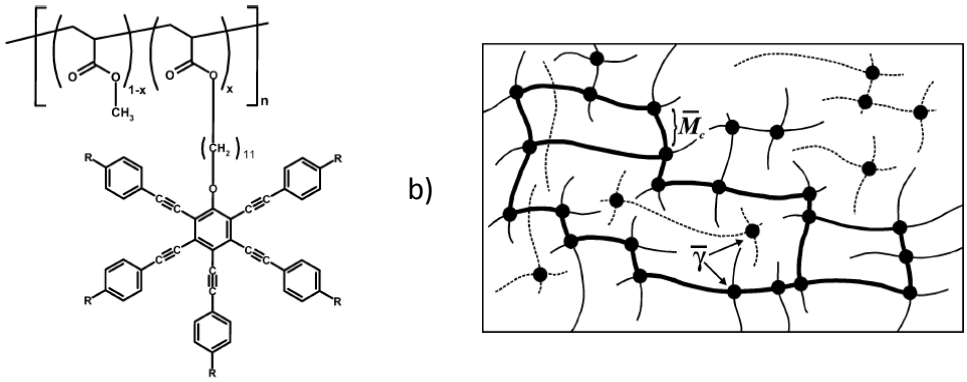

Figure 2.5 a) Chemical structure of mesogen, b) Representation of gel network.

The majority of the rest of mesogens, those that create crosslinks, are organized in groups of two disks, and only a small fraction in groups of three or four disks.

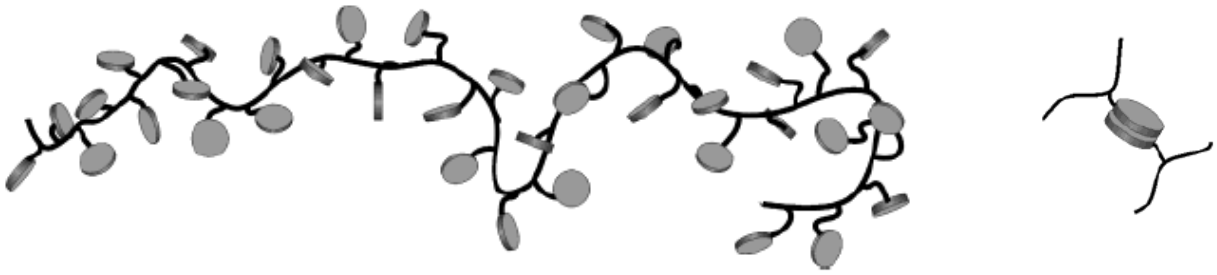

Figure2.6 Schematic representation of the diskotic side-chain polymers.

Hydrogen bond

It has an energy of 5-120 kJ/mol and a good selectivity. This last property is fundamental because it permits to have a great control over the organisation. Its limit lies in the nature of the solvent. Indeed in water there is a strong competition with solvent molecules, so it is much simpler to work in organic solvents. An important application derives from the possibility to build containers, which can bring an insoluble molecule into the solution.

[34] M. W. C. P. Franse, K. te Nijenhuis, J. Groenewold and S. J. Picken, *Macromolecules* **2004,** *37,* 7839-7845.

Between all the possible weak interactions which could be responsible for the formation of these systems, a big class of products rely on the formation of hydrogen bond. Several commercial applications are known for these materials (cosmetic, medical, etc) and for this reason the research is still ongoing to discover structures with new and better properties.

Recently Khan et al.[35] synthesized a two-component organogel, which can encapsulate metal nanoparticles and organic molecules within his hollow fiber structure.

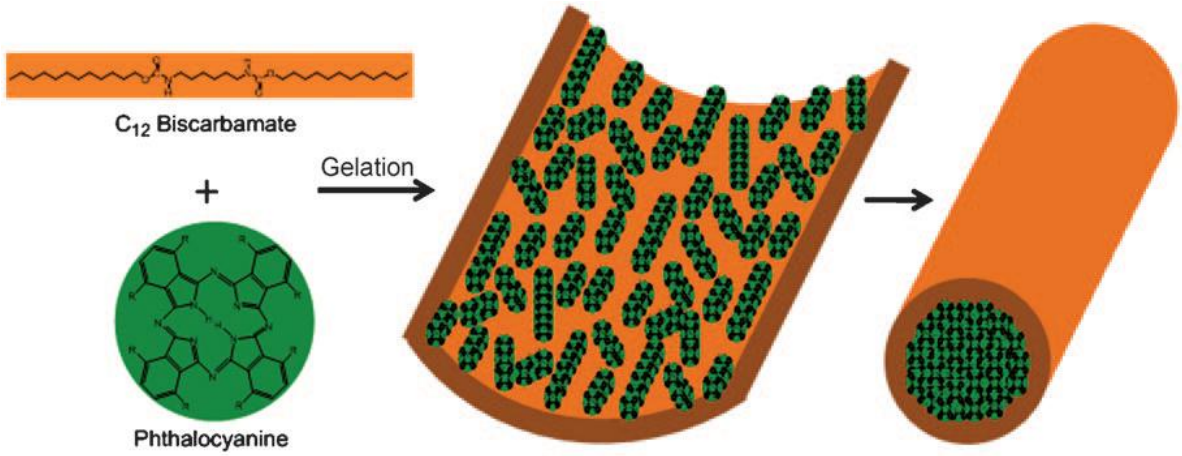

Figure2.7 Proposed model for the encapsulation of phthalocyanine (Pc) in the tubes of biscarbamate gel.

As reported in figure 2.7, the basic component of the gel network is C_{12} biscarbamate, which exploits both Van der Waals interactions between the long chains, and hydrogen bonds between the carbamate moieties. After inclusion of silver or Pc into the hollow fibers, the change of gel morphology was confirmed by microscopic experiments. It is evident that the encapsulation of some guests has a great influence on the self-assembling of the supramolecular aggregate.

The next example introduces us to the core of my project, because it concerns the class of compounds developed in the laboratory where I worked in Paris (Université Pierre et Marie Curie).

Prof. Bouteiller and his group have largely studied a family of molecules containing two ureido moieties[36] (figure 2.8), which can lead to the formation of four hydrogen bonds. The basic structure contains a rigid spacer to prevent intramolecular interactions.

[35] M. K. Khan and P. Sundararajan, *Chem. Eur. J.*, **2011**, *17*, 1184 – 1192.
[36] V. Simic, L. Bouteiller and M. Jalabert, *J. Am. Chem. Soc.*, **2003**, Vol. 125, *43*, 13148-13154.

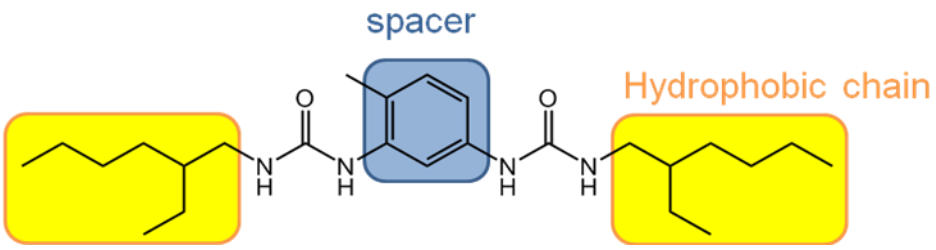

Figure 2.8 2-Ethylhexyl-3- [3-(3-(2-ethylhexyl)ureido)-4-methylphenyl] urea (EHUT).

Bis-urea EHUT self assembles into two distinct high molecular weight structures: simple filaments and nanotubes[37,38]. The filaments form viscous solutions, whereas the nanotubes form viscoelastic gels. The equilibrium among the three species is shown in figure 2.9.

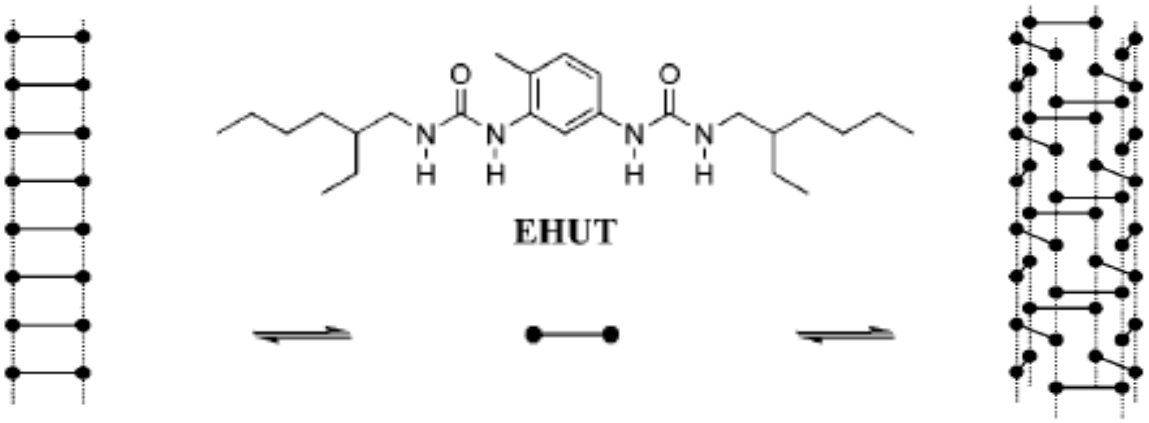

Figure 2.9 EHUT monomer and schematic structures for filaments and tubes. Hydrogen bonds are represented by dotted lines connecting the urea functions (black circles).

These nanotubes can be micrometers long and are in dynamic exchange with the monomer and with simple hydrogen-bonded filaments. By analogy with hydrogen-bonded molecular capsules, self-assembled nanotubes are really interesting because they can temporarily isolate guest molecules from the solution.

The equilibrium among the three species has been studied with nano-DSC, FTIR and ITC and, by these analysis, it was possible to draw the pseudophase diagram of EHUT (figure 2.11).

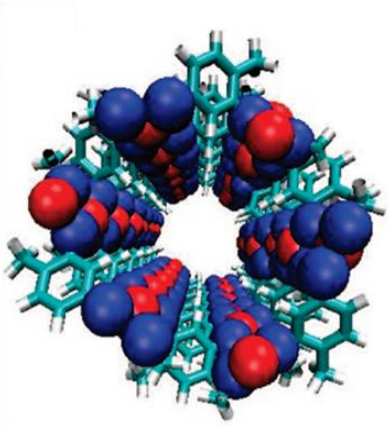

Figure 2.10 Tubular geometry.

[37] M. Bellot and L. Bouteiller, *Langmuir* , ***2008,*** *24,* 14176-14182.
[38] L. Bouteiller, O. Colombani, F. Lortie, P. Terech, *J. Am. Chem. Soc.*, **2005**, *127*, 8893-8898.

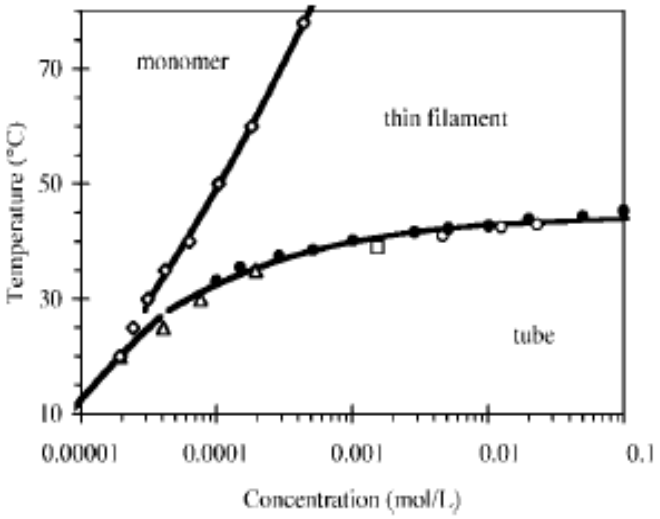

Figure 2.11 Pseudophase diagram of EHUT in toluene.

This system was also embodied in a photo-polymerised polyacrylate film in order to obtain porous material[39]. The main feature of this kind of material is the independence of the porosity from the matrix mechanical properties, indeed it depends only on the self-assembling of the nanotubes.

c. Aim of the research

In the literature concerning supramolecular chemistry a very large quantity of self-assembling structures is known. Among them *supramolecular containers* offer an exceptional opportunity to study the effects of solvation. They create, as a matter of fact, a space in which a *guest* is temporarily isolated from the solution.

The most used interaction for this purpose is hydrogen bond, which, thanks to its high thermodynamic stability and selectivity, leads easily to the formation of two types of aggregates: globular or tubular.

The synthesis and the study of tubular aggregates formed from bis-urea monomer are the object of this chapter. This kind of system shows two big advantages:

- the possibility to host a larger number of guest molecules, thanks to their high internal capacity (length of the order of micrometer),
- high selectivity, which can be obtained by modifying the monomer and tuning the section of the tube, to be specific for a specific guest.

[39] F. Ouhib, E. Bugnet, A. Nossov , J.-L. Bonardet and L. Bouteiller, *Polymer*, **2010**, *51*, 3360-3364.

As already said the research group of Professor Bouteiller has optimized EHUT system, which is characterized by an equilibrium among monomer, filament and nanotube. It was demonstrated that the stability of the tube is related to the possibility for solvent molecules to fit inside the tubular cavity. The diameter of the cavity, which is really small (about 7 Angstrőm) can be finely tuned by introducing a modified monomer in controlled amount[40].

In this chapter we'll describe the tentative of functionalization of the tube cavity to build a specific host-guest couple. We tried to introduce a fluorine atom on the monomer bis-urea skeleton, and in that way we hope to obtain nanotubes which can encapsulate fluorinated molecules selectively. Indeed perfluorinated compounds are normally insoluble in all non-fluorinated solvents, so we hope to succeed in creating within the cavity an environment adapted to host this kind of molecules.

Summarising the objective is to synthesize and study bis-urea **t**, however, because C-F is a weak hydrogen bond acceptor, we will first synthesize simple halogenated bis-ureas. On this series of molecules we will investigate if halogen atom in ortho position to the urea is compatible with the formation of urea-urea intermolecular hydrogen bond and we should confirm the feasibility of our designed system **t**.

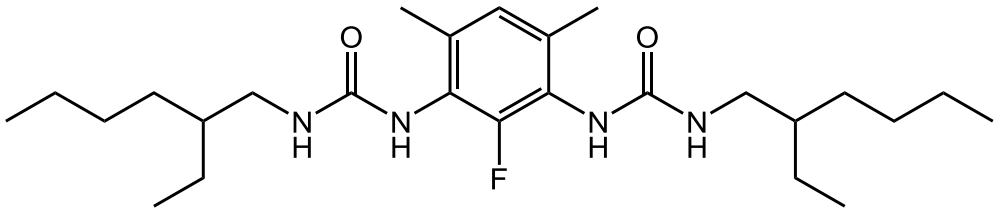

t

[40] B. Isare, M. Linares, R. Lazzaroni and L. Bouteiller, *J. Phys. Chem. B*, **2009,** *113,* 3360–3364.

2.2 Results and discussion

a. Synthesis of halogenated bis-ureas

Firstly, we began with some preliminary studies on simpler molecules containing three identical halogen atoms. In this way it was possible to evaluate the influence of such electronegative substituents on the properties of our system.

It was necessary to follow two different synthetic paths depending on available starting materials.

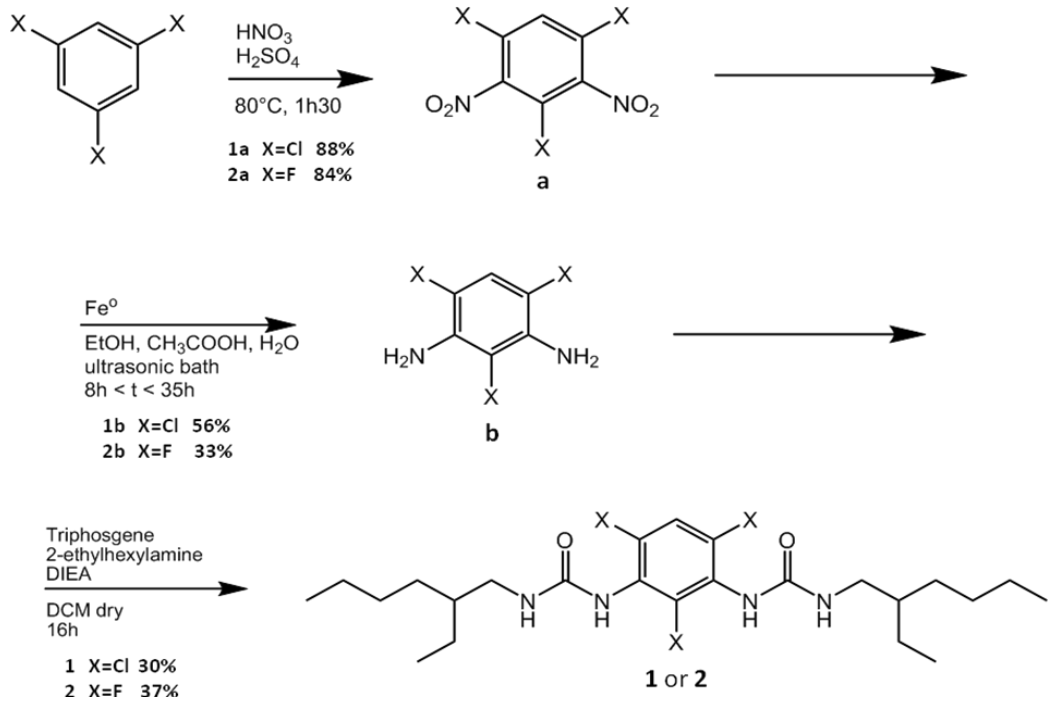

Scheme 2.1

For the molecules containing chlorine (**1**) and fluorine (**2**), the starting reactant was the tri-halogenated benzene and the first step was a di-nitration[41]. Obviously the choice of the experimental conditions was oriented to avoid per nitration. The nature and purity of products were then verified through TLC, NMR and melting point. The di-nitrate **a** was then reduced[42] in presence of iron using a mixture of ethanol, water and acetic acid, under sonication. Also in this case it was not easy to obtain the completely reduced product, and the purification was difficult because of the formation of the iron oxide.

[41] E. H. Huntress, F. H. Carten, *J. Am. Chem. Soc.*, **1940**, 511-514.
[42] A. B. Gamble, J. Garner, C. P. Gordon, S. M. J. O'Conner, P. A. Keller, *Synthetic Comm.*, **2007**, *37*, 2777-2786.

The last step is the formation of the bis-urea derivatives. A first attempt was made letting to react the aromatic diamine **b** with the aliphatic isocyanate, but this did not work. So we prepared the isocyanate of **b** by using triphosgene, and let it react with the 2-ethyl-hexylamine[43].

This synthesis worked out nicely and products **1** and **2** were obtained pure after crystallisation in 30% and 37% yields respectively.

For the synthesis of the product with three bromine substituents we started with the bromination of the *meta*-phenylenediamine[44]. The reference for this reaction was very old and not really accurate. Therefore we had to find the right conditions to perform it (see experimental section). After the isolation of the product, **c**, we transformed it in the corresponding bis-urea **3** (yield of 40%).

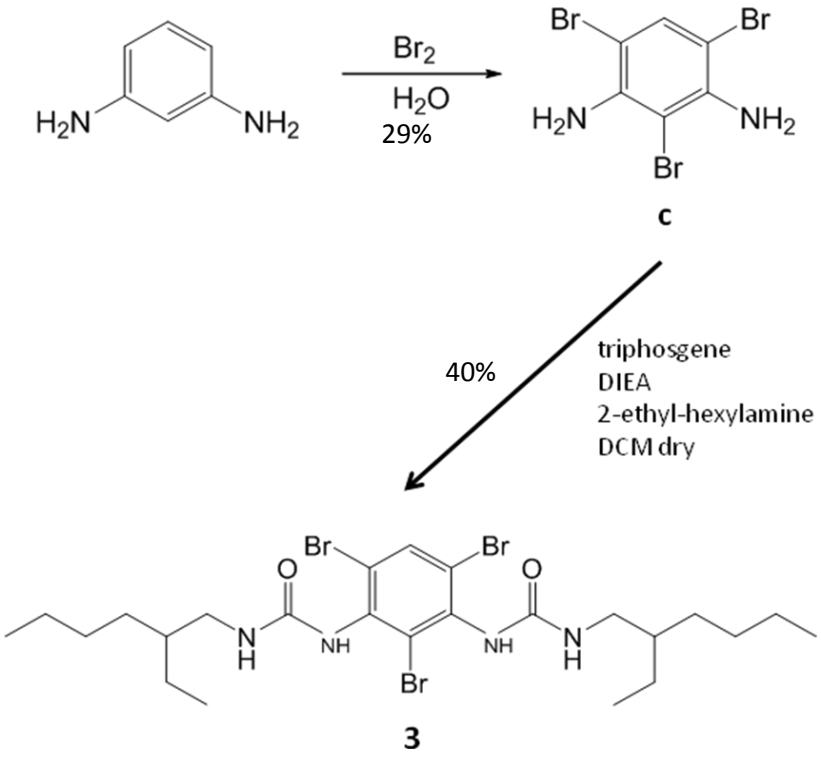

Scheme 2.2

First tests of solubility carried on the products **1 – 3 showed** that none of these formed gels in the most common solvents. May be this can be ascribed to the presence of a substituent between the two urea moieties (position 2). So, to continue the series of halogenated

[43] S. Boileau, L. Bouteiller, F. Laupretre, F. Lortie, *New. J. Chem.*, **2000**, *24*, 845-848.
[44] C. L. Jackson, S. Calvart, *Am. Chem. J.*, **1896**, *18*, 465-489.

monomer, we designed another molecule containing two chlorine atoms and having the position 2 free.

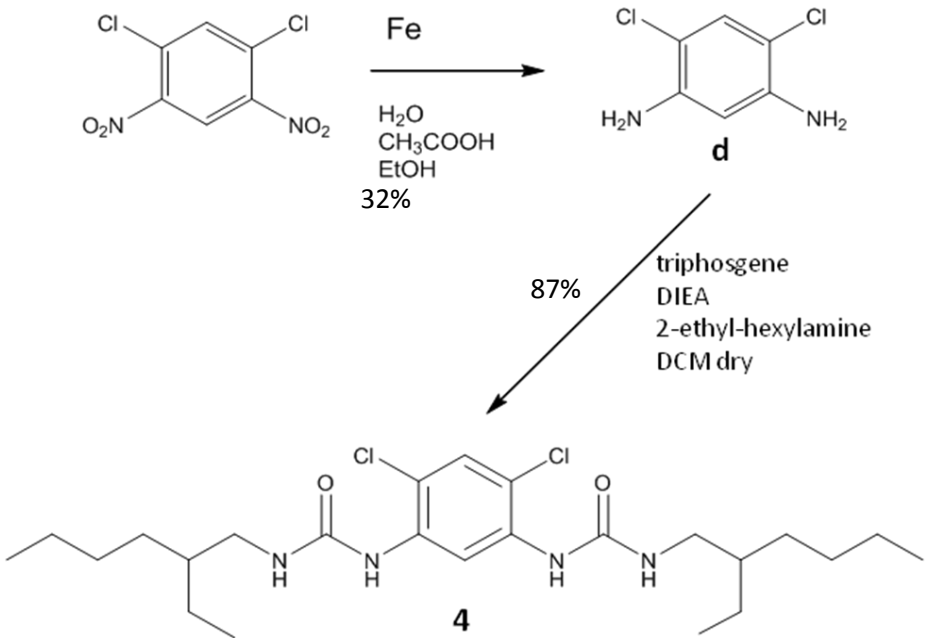

Scheme 2.3

b. Characterization

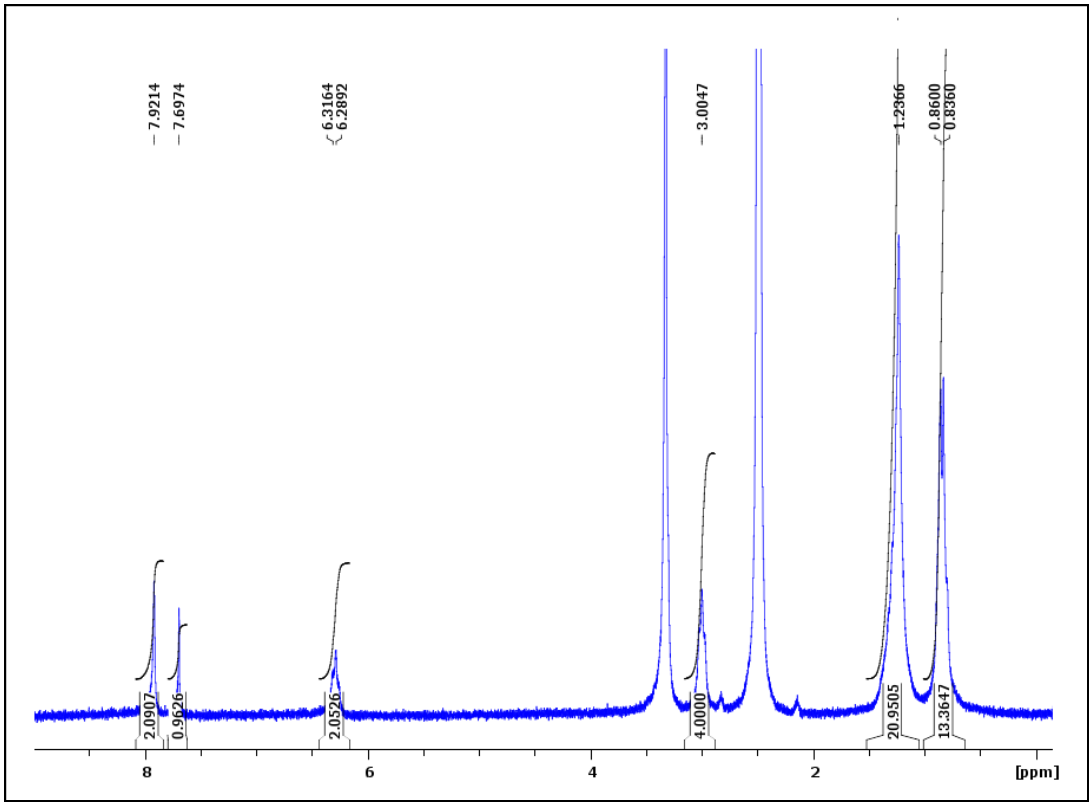

Figure 2.12 ^{1}H-NMR spectrum of **1** in DMSO.

Products **1 – 4** were characterised by ^{1}H-NMR in DMSO. In such polar solvent all the associations among bis-urea moieties are prevented, so that it is possible to obtain a better resolved spectra.

In figure 2.12 we show here only one spectrum, which is representative for all the others.

c. Solubility and viscosity

Their solubility was then tested in three apolar solvents: chloroform, toluene and cyclohexane. They proved to be soluble in all the solvents, but only the product with two chlorine gave gels.

Table 2.1 Results of tests of solubility for the products **1-4** in three different solvents (solution 10 mM obtained without heating, S = soluble, G = gel).

	toluene	c-hexane	$CHCl_3$
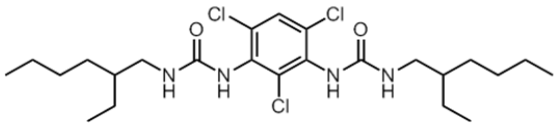 **1**	S	S	S
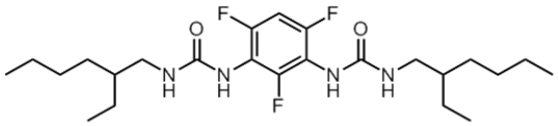 **2**	S	S	S
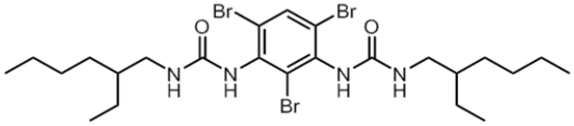 **3**	S	S	S
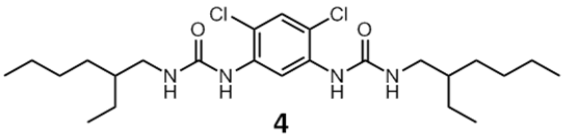 **4**	G	G	G

To confirm the nature of the aggregation, measurements of viscosity were made on our products solubilised in cyclohexane (Figure 2.13). The instrument used to this purpose is a rolling bead viscometer, based on the Stoke's Law, in which the fluid is stationary in a glass tube. A metallic bead of known size and density is allowed to descend through the liquid and a series of measures are made changing the angle of the tube. The relative viscosity is obtained by comparing the time the sphere takes to descend and pass through the sample,

and that the sphere uses to pass through the solvent alone. The same measurements in the same solvent were done on two reference compounds: EHUT, which is known to aggregate to give tubes, and EHUTMB (2,4,6-trimethyl EHUT), which gives only filaments. After simple comparison between the viscosity of our products and that obtained for the two references, we concluded that :

- Product **1**-**3**, having viscosity values similar to that of EHUTMB, are probably self-organised in filaments.
- Product **4** instead, whose viscosity is higher than that of EHUT, is probably organised in tubes.

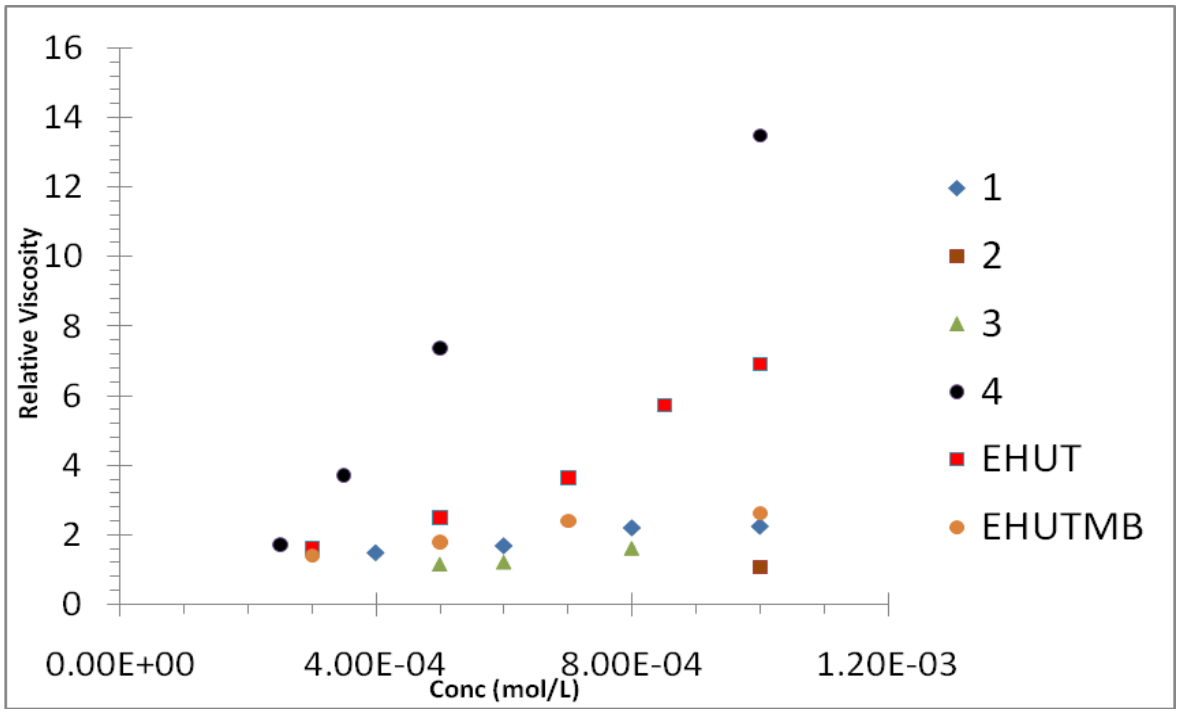

Figure 2.13 Viscosity of **1**, **2** , **3**, **4**, EHUT and EHUTMB measured in cyclohexane with an angle of 30° at 20°C.

d. Small Angle Neutron Scattering (SANS)

This analysis is used to define the organisation and the structure of *objects* spread in an homogeneous medium. These *objects* can be pores of a solid or, like in our case, polymers in a solution.

During a SANS experiment a beam of neutrons is directed towards the sample. The neutrons behave at the same time as waves and particles, and thus they are characterized by energy values and wavelength. The wavelength of the beam of neutron is selected through a monochromator and then collimated under vacuum within a distance variable between two

and seven meters. In this way it is possible to obtain a beam parallel enough for small angle scattering. The neutrons are then diffused by the sample atoms in different directions with a specific scattering angle. It is really important to note that the scattering caused by hydrogen is distinct from that of deuterium, and for this reason the experiments are performed in deuterated solvents. In this way the only hydrogens observed belong to the solute.

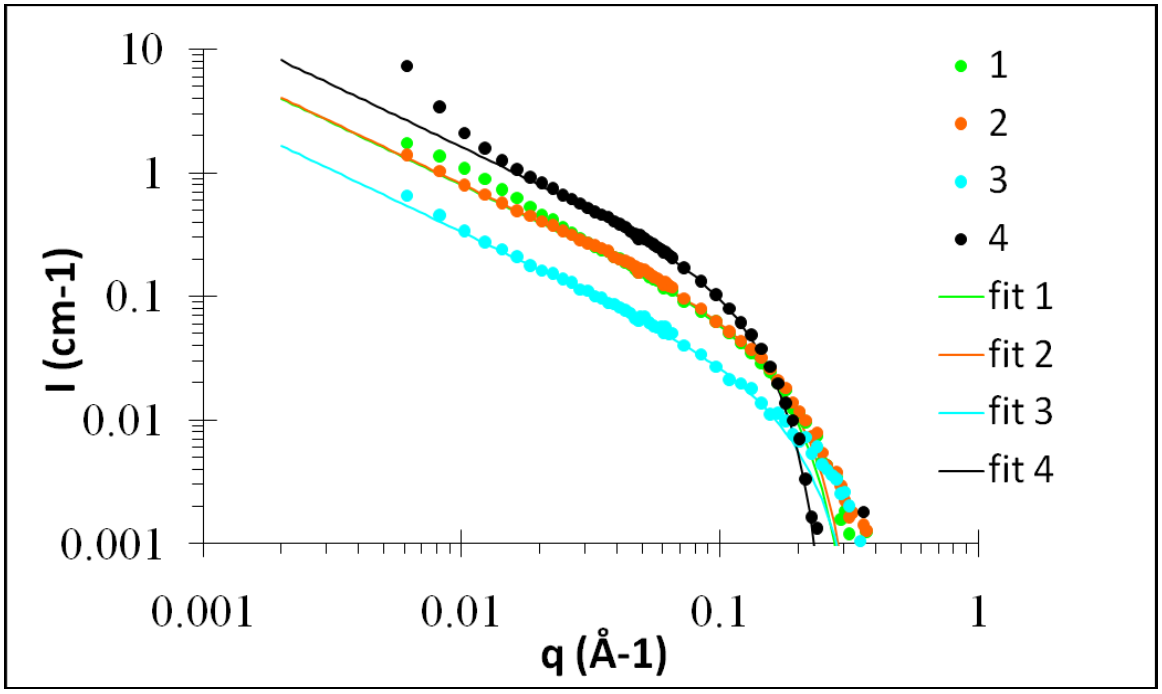

Figure 2.14 SANS curves of solution of the products in deuterated cyclohexane.

The fit of the experimental curves with the shape factor for infinitely long and rigid cylinders is shown on figure 2.14. The model yields 2 parameters: the radius of the cylinder and its density (that yields the number of molecules in the cross-section of the cylinder). The values obtained in deuterated cyclohexane are reported in table 2.2.

Table 2.2 Value of radius and density of the cylinder measured in deuterated cyclohexane at 21°C.

	r (Å)	**d (number of molecules)**
1	11.3	1.2
2	10.9	1.2
3	10.0	0.6
4	14.5	2.2

The analysis of these values confirms the results previously obtained. Only bisurea **4** gives gels.

Table 2.3. Results of SANS analysis on compounds **1**-**4**.

	Cyclohexane (10mM, 21°C)	Toluene (10mM, 21°C)	Chloroform (10mM, 21°C)
1	Filament	Filament	Filament
2	Filament	Filament	Filament
3	Filament	Filament	Filament
4	Tube	Tube	Tube

e. Spectroscopy FT-IR

Other informations can be obtained through FTIR, indeed this spectroscopy can show the presence of hydrogen bonds. It distinguishes between free and bound N-Hs. So we analysed all the products in the same solvents used for the solubility tests at 10mM concentration to see if the hydrogen on N was free or bound. In all the analysis, at this concentration, it was clear that hydrogen bonds were formed (signals of N-H stretching at 3360 cm^{-1} and 3240 cm^{-1}).

In order to study the strength of hydrogen bonds dilution experiments of were performed.

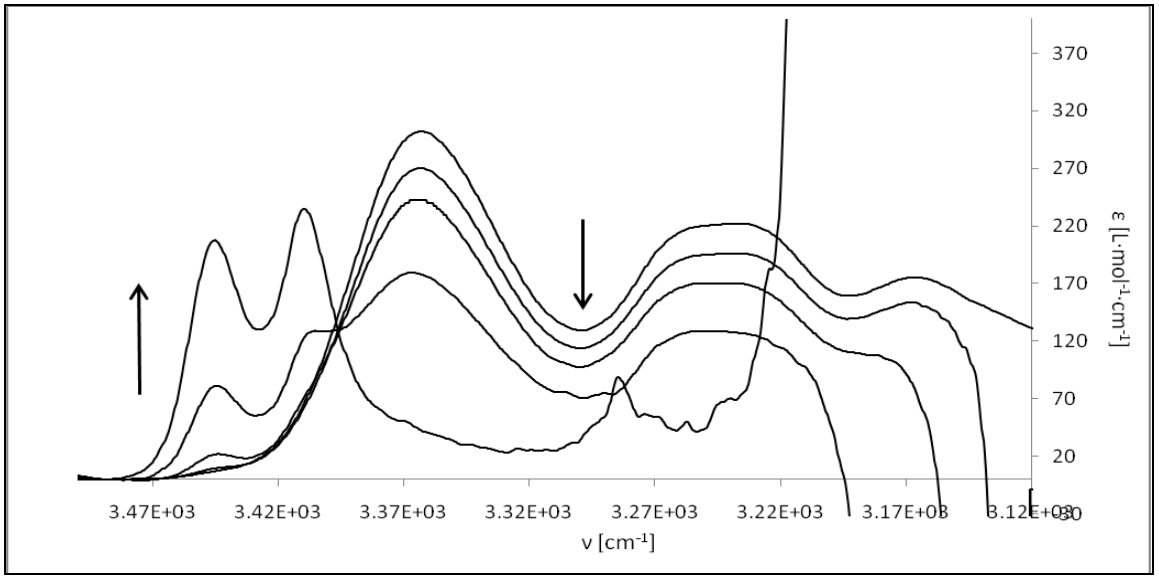

Figure 2.15 Experimental FT-IR curves for the dilution experiment performed on product **1** in chloroform, showing N-H stretching signals. Arrows indicate the direction of change with decreasing concentrations (10mM, 2mM, 0.4mM, 0.08mM, 0.02mM).

The experimental conditions were the same for all the products: range of concentration between 10mM and 0.02mM in chloroform. In figure 2.15 we report the experiment relative to compound **1**.

At high concentrations it is possible to see that N-H is hydrogen bound to C=O, while this does not happen at low concentrations. Indeed the shift of the N-H stretching at 3410 cm^{-1} and 3440 cm^{-1} reveals the presence of free N-H.

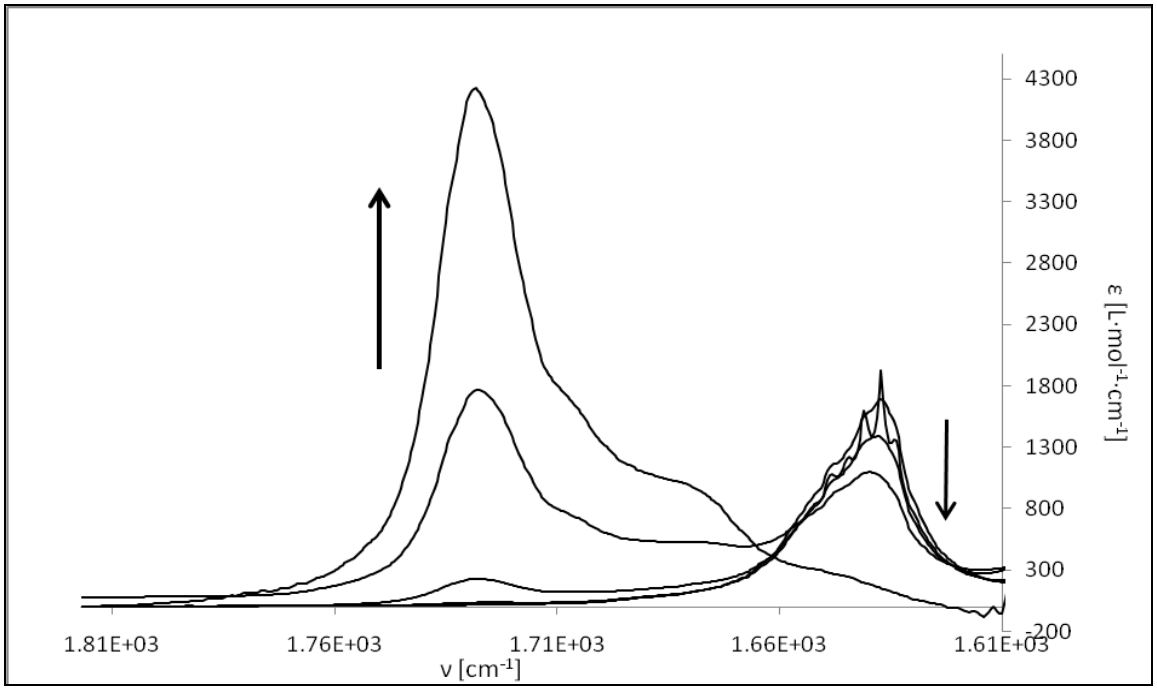

Figure 2.16 Experimental FT-IR curves for the dilution experiment performed on product **1** in chloroform, showing C=O stretching signals. Arrows indicate the direction of change with decreasing concentrations (10mM, 2mM, 0.4mM, 0.08mM, 0.02mM).

Reporting on a graphic the FTIR spectra of all the diluted samples (0.02mM), from the comparison it is possible to draw some conclusions:

- At such concentration all the compounds are present as monomer.
- They all show to posses two different signals for N-Hs.
- One signal is characterised by the same wavenumber in all the spectra, while the other changes significantly.

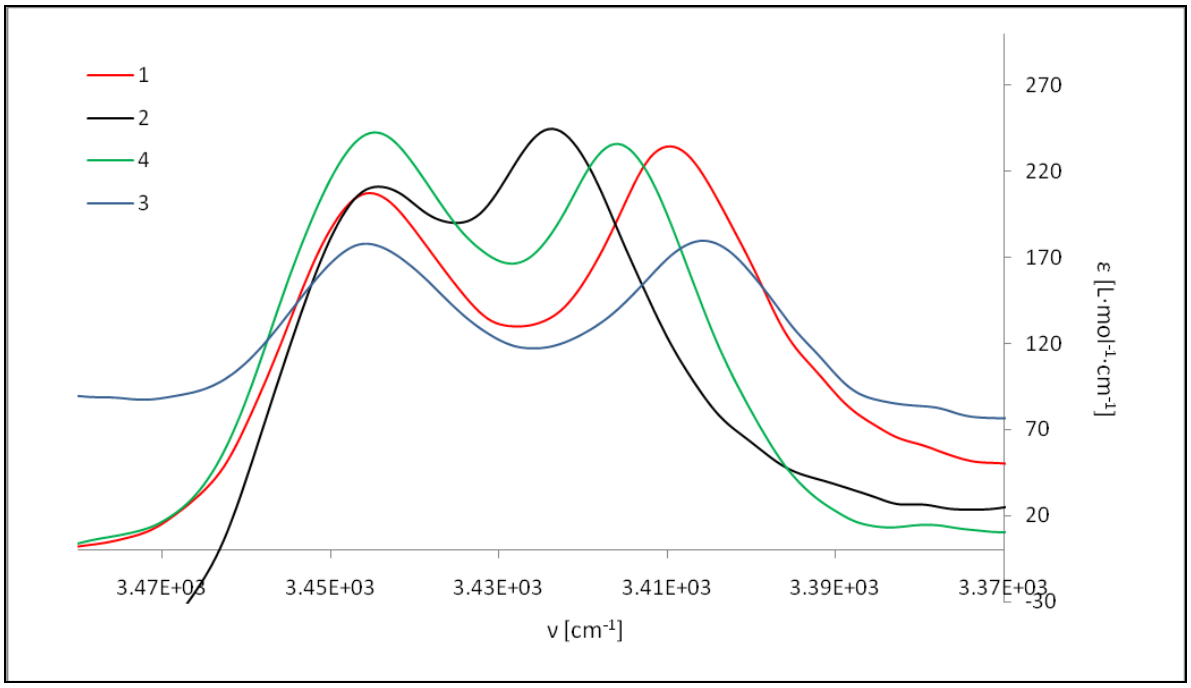

Figure 2.17 Experimental FT-IR curve for all the products at the minor concentration (0.02mM) in chloroform, signals of N-H stretching.

To rationalise these observations some calculations were performed on the reference compound showed below. These were carried out with the computational program Gaussian 03, which allows to calculate energy, molecular structures, vibrational frequencies and several other properties for chemical systems by using functionals. In our case a semiempirical method deriving from the density functional theory (DFT) was applied, which name is b3lyp/aug-cc-pvdz.

The calculations were made also on a reference methyl-substituted urea that cannot form intramolecular hydrogen bond.

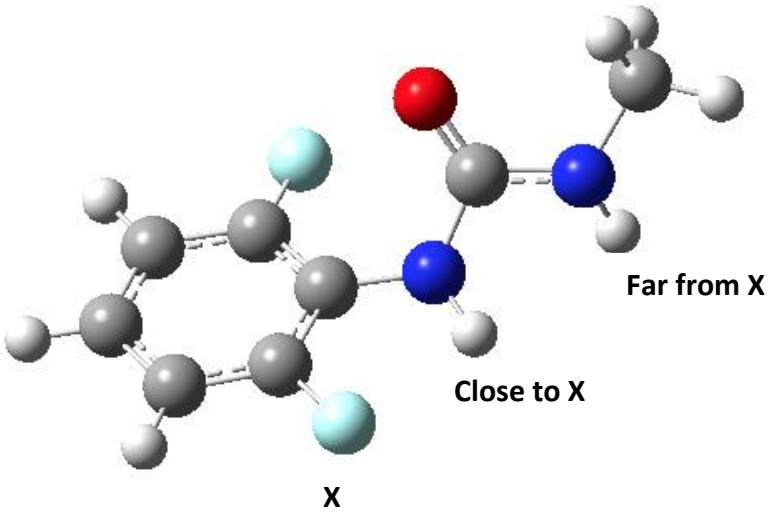

Table 2.4 Comparison between the results of the calculations relative to N-H stretching IR frequency, made on X-substituted mono-urea and the experimental values.

Substituent X	$\tilde{\nu}$ *N-H far*$_{calc}$	$\tilde{\nu}$ *N-H far*$_{exp}$	$\tilde{\nu}$ *N-H close*$_{calc}$	$\tilde{\nu}$ *N-H close*$_{exp}$
-CH_3	3608	3445	3591	3426
-F	3614	3446	3589	3430
-Cl	3615	3448	3572	3418
-Br	3615	3449	3564	3411

Even though the absolute experimental values are significantly different from the calculated ones, the comparison has to be done only among the general trend of each series of values. These trends are quite similar for the calculated values and the experimental ones. So it becomse clear that the $\tilde{\nu}$ *N-H far* is the same for all the products, while $\tilde{\nu}$ *N-H close* changes in presence of Cl or Br, which form intramolecular hydrogen bonds.

We can then explain all the results saying that the signal at the higher wavenumbers is generated by the *N-H far* from the aromatic ring, and this is also far from the halogen substituent. The other is generated by the *N-H close* to the aromatinc ring, which can form intramolecular hydrogen bond with the halogen[45,46].

So the differences observed depend on the fact that products containing chlorine and bromine form an hydrogen bond, whereas the product with fluorine atoms remains with both its N-Hs free.

f. Isothermal Titration Calorimetry (ITC)

ITC is a quantitative technique used to determine the thermodynamic parameters of weak interactions in solution. An isothermal titration calorimeter is composed of two identical cells made of a highly efficient thermal conducting and chemically inert material, surrounded by an adiabatic jacket. Sensitive thermocouple circuits are used to detect temperature differences between the reference cell (filled with the solvent alone) and the sample cell. Our experiments were carried in order to measure the strength of the interactions among the monomers as a function of concentration.

During the experiment, calculated amounts of the supramolecular polymer were introduced into the cell, full of chloroform. These additions cause heat to be released,

[45] V. Simic, L. Bouteiller, M. Jalabert, *J. Am. Chem. Soc.*, **2003**, *125*, 13148-13154.
[46] Y. Mido, C. Furusawa, *J. Of Mol. Struct.*, **1982**, *82*, 23-28.

because of the hydrogen bond breaking. Measurements consist of the time-dependent input of power required to maintain equal temperatures between the sample and reference cells. As a result, the experimental raw data consists of a series of spikes of heat flow (power), with each spike corresponding to one sample injection.

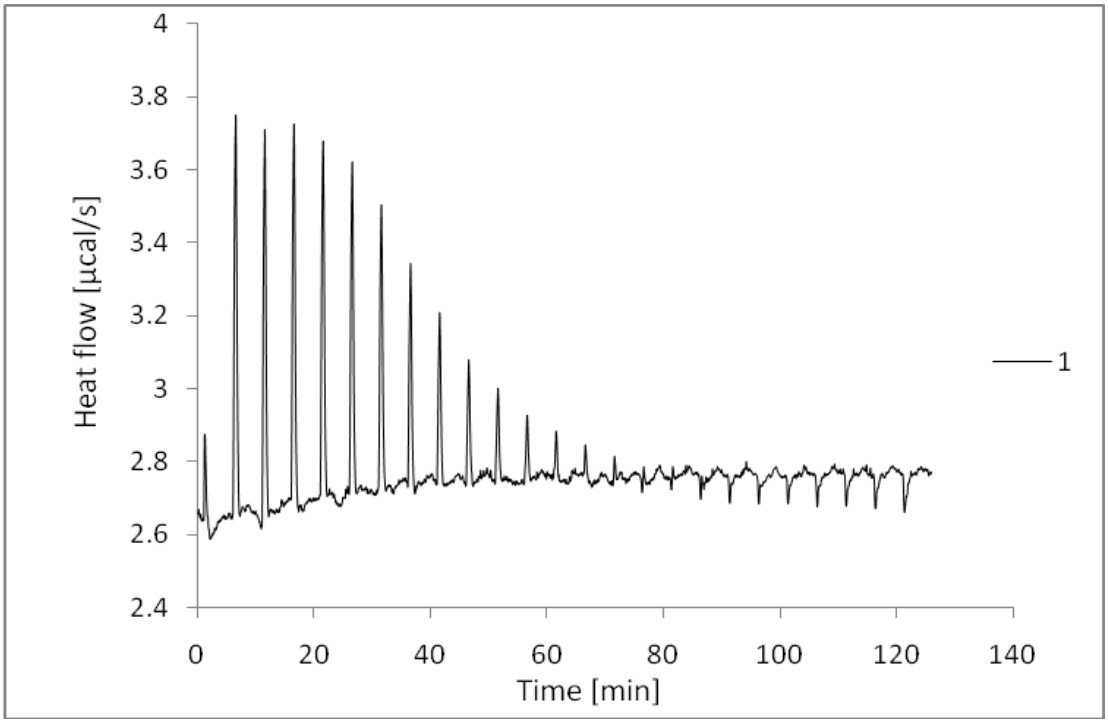

Figure 2.18 Experimental calorimetric titration data for subsequent addition of 12µL of **1** solution 0.3mM in chloroform at 20°C.

These heat flow spikes are integrated as a function of time, giving the total heat exchanged per injection. The pattern obtained can be analyzed to give the thermodynamic parameters of the interactions under investigation.

In figure 2.19 the inflexion point represents the trasition from the monomeric form to the filament. Indeed the first aliquots introduce only a small amount of polymer, which dissociates completely into free monomers. As the number of the additions increases the concentration of polymer increases as well and the amount of solvent becomes too small to keep the molecules of monomer separated. Under these conditions the supramolecular chains do not aggregate anymore and the subsequent additions do not cause heat release.

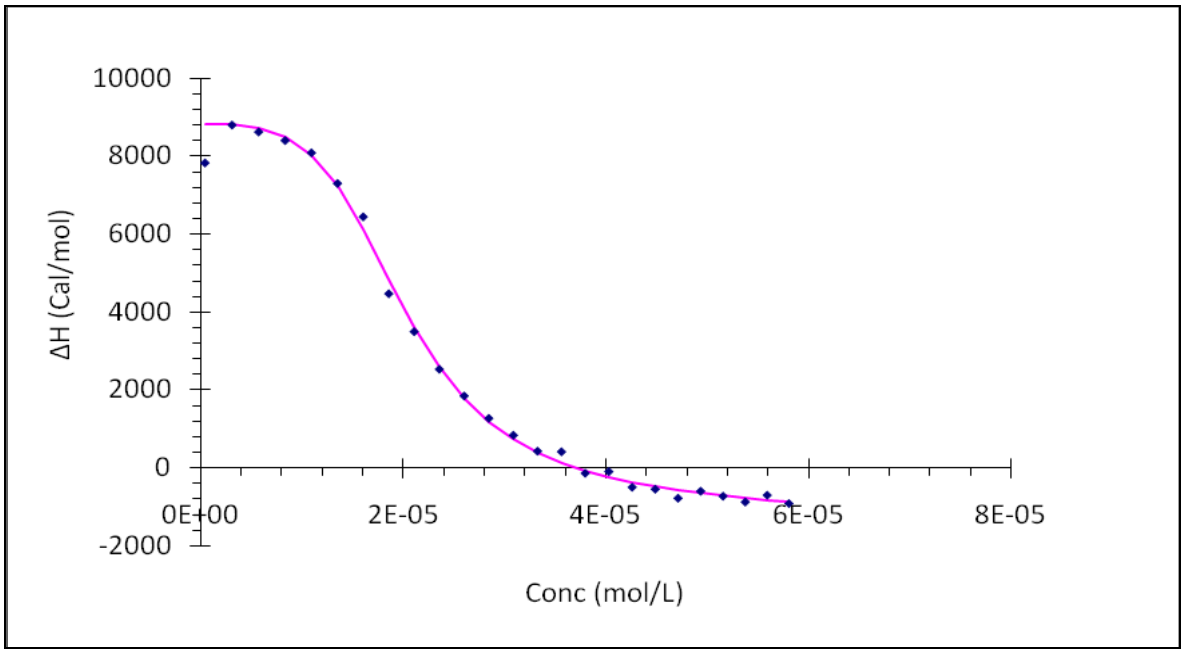

Figure 2.19 Experimental ITC enthalpogram for a 0.3mM solution of **1**in chloroform injected into pure chloroform, versus total **1** concentration in the cell at 20°C.

In the analysis of product **4** it is possible to recognize two distinct steps. The first one still represents the passage from monomers to filaments, and the second one indicates the transition between filaments and tubes.

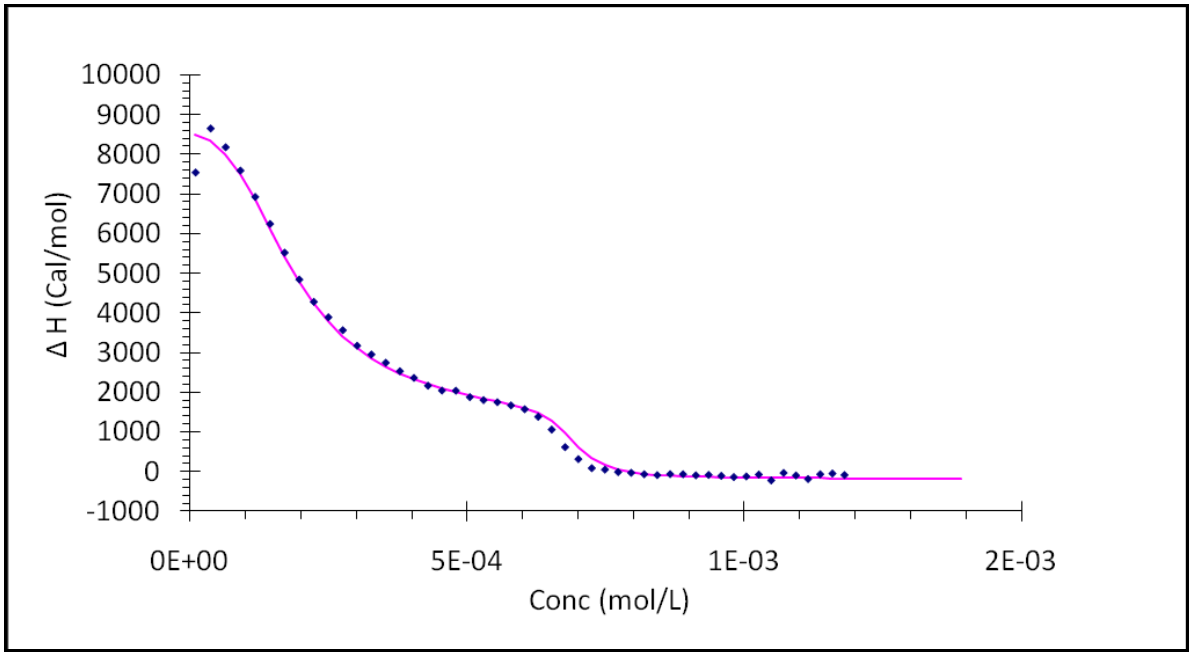

Figure 2.20 Experimental ITC enthalpogram for a 6mM solution of **4** in chloroform injected into pure chloroform, versus total **4** concentration in the cell at 20°C.

Because of the dependence of the polymer length on the chosen conditions (concentration, solvent, temperature), the best way to describe our system is a theoretical model, *association model*, which considers all the possible self-assembled species and all the relative equilibriums[47].

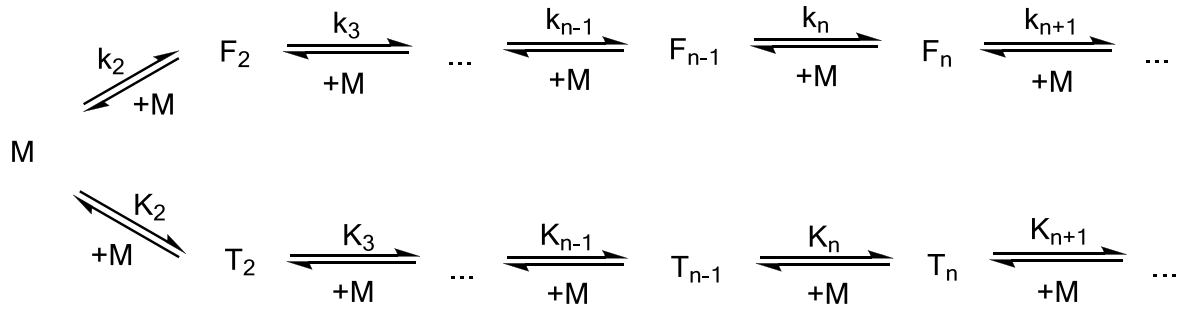

Scheme 2.4 Association equilibria between monomer (M) and two supramolecular polymers: filament (F_n) and tube (T_n). Each equilibrium is characterised by its own constant (K_n).

This model takes into account also of the cooperativity of the system. So it is possible to say that the dimerization step is less favored than the subsequent association steps ($k_n>k_2$ or $K_n>K_2$). We also assume that the subsequent association steps are equivalent: $K_n=K$ and $k_n=k$ for n>2.

Starting from this model a series of equations has been written, which correlates the heat exchanged during the experiments with K_2, k_2, K, k, ΔH_2, ΔH, Δh_2, Δh, $\Delta H_{dilution}$. Knowing the exact concentration of the polymer solution is a necessary condition to compute all the parameters.

The meaning of the parameters is:

- K_2 (k_2), constant of formation of dimer for the tube (filament),
- K (k), constant of formation of *n*-mer for the tube (filament),
- ΔH_2 (Δh_2), enthalpy of dissociation of dimer for the tube (filament),
- ΔH (Δh), enthalpy of dissociation of *n*-mer for the tube (filament),
- $\Delta H_{dilution}$, enthalpy of dilution for the tube (filament).

The most relevant data obtained from this analysis are reported in Table 2.5.

[47] M. Bellot and L. Bouteiller, *Langmuir , **2008, 24,*** 14176-14182.

Table 2.5 Results of ITC analysis in chloroform at 20°C. The values measured for **1**, **2**, **3**, **EHUT**, **EHUTMB** are referred to the transition from filament to monomer (k_2, k, Δh). The values measured for **4**, are referred to the transition between tube, filament and monomer (k_2, k, Δh, K_2, K, ΔH). Because of the large number of adjustable parameters in the case of bis-urea 4, the fit was performed simultaneously on experimental data obtained at 6 different temperatures between 10 and 35°C.

	k_2 (and K_2) [L/mol]	K (and K) [L/mol]	Δh (and ΔH) [Kcal/mol]
1	1300	43000	12
2	2500	15000	12
3	700	29500	8
4	700 (0.07)	7000 (9000)	9 (9)
EHUT	60	1700	8
EHUTMB	9	3200	7

Among the bis-ureas with substituents in 2,4,6 position, the strength of the self-association increases in the order **EHUTMB** < **2** < **3** < **1**. The fact that the halogenated compounds self-associate more efficiently than the methylated one may be due to an electron withdrawing effect making the N-H groups more acidic and thus better hydrogen bond donors. However, the fact that **1** self-associates more strongly than **2** is unusual, first because chlorine is less electronegative than fluorine, and secondly because FTIR experiments have shown that **1** forms intramolecular hydrogen bonds whereas **2** does not. This is surprizing because usually, when an atom is involved in an intramolecular H bond, the intermolecular interaction is usually weakened.

However the formation of an intramolecular interactions also modifies the dihedral angle among the atoms involved, and this in turn has an influence on the intermolecular interaction. Indeed to have hydrogen bonding between two monomers, the urea moieties must be precisely oriented (almost perpendicular to the aromatic plane).

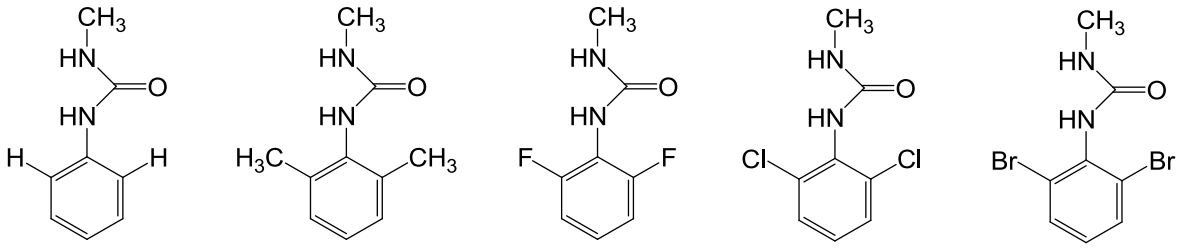

Figure 2.21

Calculations of the potential energy as a function of the phenyl-urea dihedral angle were made on the reference structures showed in figure 2.21, to point out the influence of the different substituents.

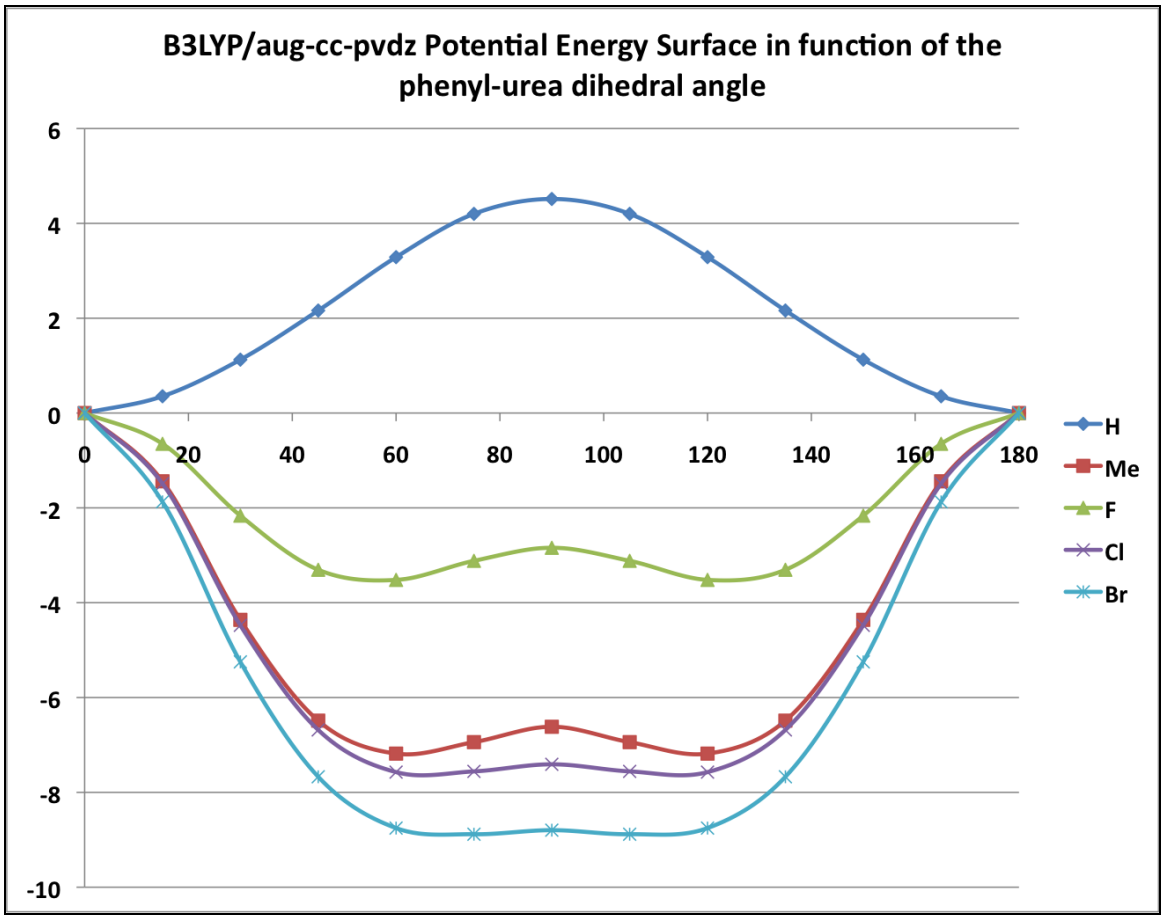

Figure 2.22

By analysing these calculations we can say that:

- in the absence of ortho substituent the most stable conformation comprise the urea in the same plane as the phenyl,

- for all the substituents the most stable conformation is non-coplanar, with a significant barrier to rotation,

- for F and Me: the most stable dihedral angle is 60° with a small barrier (1kcal/mol) corresponding to a 90° angle,

- for Cl and Br, the barrier at 90° disappears: a large range of angles are allowed (60 to 120°).

The intramolecular H bond with Cl is responsible for a different conformation (more perpendicular). This may explain the stronger intermolecular interaction since it may preorganize better the C=O and the N-H far from Cl for intermolecular hydrogen bonding. In

the literature, halo-aromatic trisubstituted mono-urea systems are already known[48], but they do not aggregate because of the formation of an intramolecular hydrogen bond. Our system apparently overcomes this problem thanks to the presence of a second N-H group on the urea moiety.

For product **4** ITC measurements were performed at different temperature (10°C, 15°C, 20°C, 25°C, 30°C, 35°C), in order to obtain a pseudo-phase diagram (Figure 2.23), that summarises the conditions (temperature and concentration) at which **4** is self-assembled. This diagram is really similar to the phase diagram of EHUT in toluene (figure 2.11).

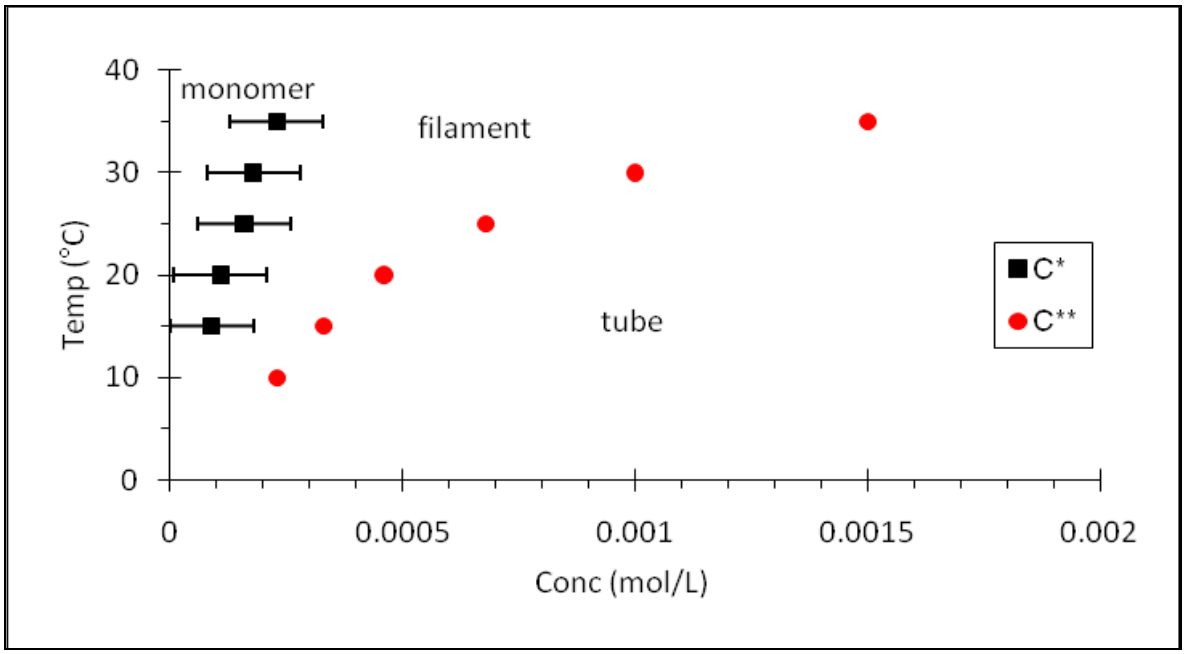

Figure 2.23 Pseudo-phase diagram for **4** solution in chloroform. Transition between the species determined by ITC.

In conclusion we can say that the presence of fluorine in the ortho positions prevents the formation of intramolecular hydrogen bonds and this let us think that the bis-urea **t** will self assemble easily since its N-Hs are all free. On the other hand –Cl or –Br substituents in the ortho positions form intramolecular hydrogen bonds, that seem to favour intermolecular ones.

[48] Y. Mido and C. Furusawa, *J. of Mol. Struct.*, **1982**, *82*, 23-28.

g. Synthesis of mono-fluorinated bis-urea

The first target of this project was the functionalization of the bis-urea monomer on position 2 with a fluorine atom (**t**). In order to obtain a gel the presence of methyl substituents was necessary.

The first attempt was made following the synthetic path outlined in scheme 2.5. It implies the reduction of 2,4-dimethyl-5-nitroaniline in the presence of hydrazine[49], and the subsequent protection of the amino groups as acetyl derivatives[50].

The subsequent step was the fluorination with Selectfluor. This is a fluorinating agent which should introduce a fluorine atom on the aromatic ring through electrophilic substitution.

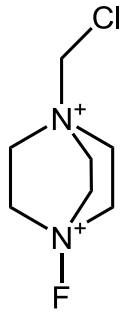

Selectfluor

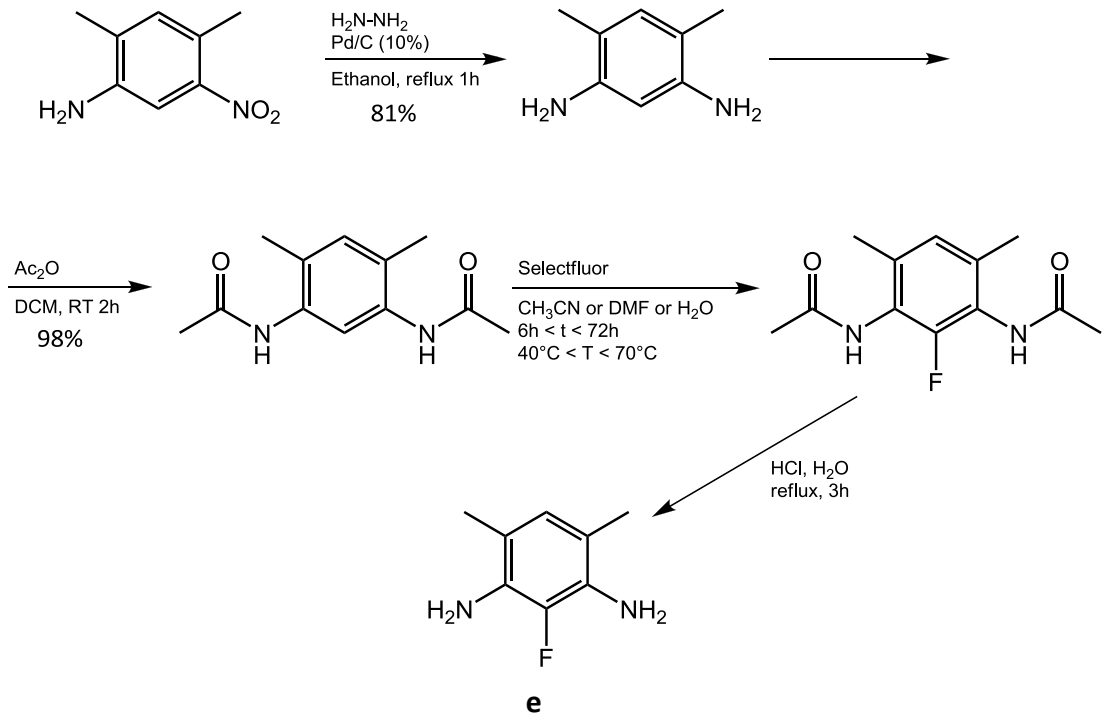

e

Scheme 2.5

In the literature the reactivity and the orientation of this reaction are reported to be similar to a normal electrophilic aromatic substitution[51,52,53,54].

[49] Bavin, *Can. J. Chem.*, **1958**, *36*, 238-243.
[50] D. R. Stuart, M. Bertrand-Laperle, K. M. N. Burgess and K. Fagnou, *J. Am. Chem. Soc.*, **2008**, *130*, 16474-16475.
[51] M. Zupan, J. Iskra, S. Stavber, *Tetrahedron*, **1996**, *52*, 11341-11348.
[52] R. P. Singh, J. M. Shreeve, *Chem. Comm.*, **2001**, 1196-1197.
[53] A. J. Poss, G.A. Shia, *Tetrahedron Lett.*, **1999**, *40*, 2673-2676.

The first attempt was made in a mixture of DMF and acetonitrile, kept at 70°C for two days. No result was achieved. Then we changed various conditions:

- the solvent (water, methanol...),
- temperature (room temperature and reflux),
- time (several days).

At the end of these series of unsuccessfully experiments we changed the strategy using as starting material a compound that bears already a fluorine atom.

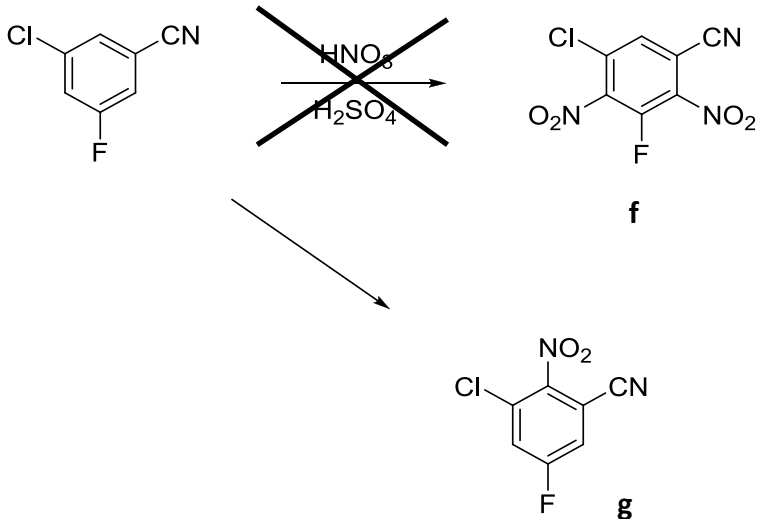

Scheme 2.6

3-fluoro-5-chloro-benzonitrile was chosen as starting material. This product was nitrated, to obtain of di-nitrated derivatives, but only the mononitrated compound **g** was obtained.

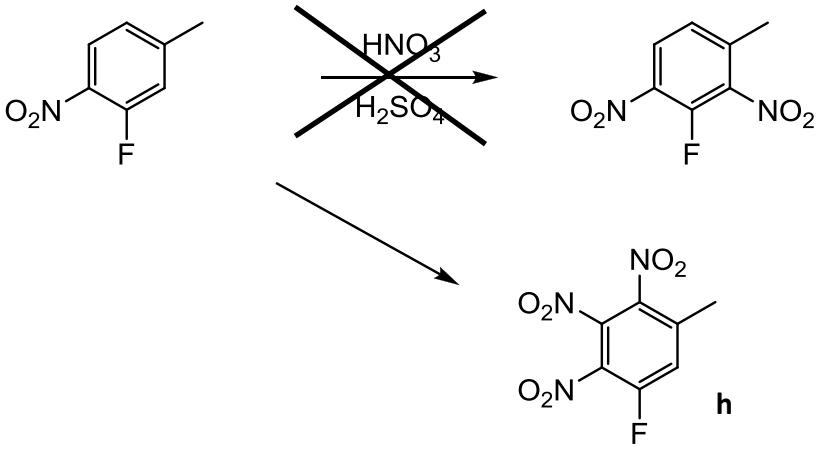

Scheme 2.7

[54] R. E. Banks, M.K. Besheesh, S.N. Mohialdin-Khaffaf, I. Sharif, *J. Chem. Soc. Perkin Trans.1*, **1996**, 2069-2076.

The nitration[55] was performed also on the 2-fluoro-4-methyl-nitrobenzene. But also in this case only the undesired product, **h**, was obtained. After all these attempts it was evident that we have to protect position 5, to avoid nitration in that position. The easiest solution is to start from a molecule having that position already occupied.

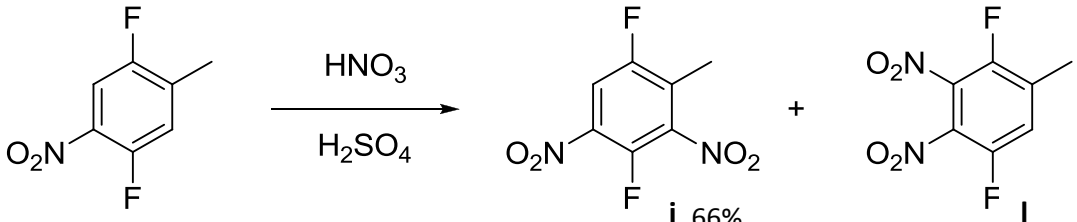

Scheme 2.8

So this time the starting material was 2,5-difluoro-4-methyl-nitrobenzene. The reaction leads to the formation of a mixture of **i**(93%) and **l**(7%), which were then separated through flash column chromatography. To verify the nature of the two products an NMR-COSY experiment was performed. It confirmed that the undesired product was only present in 7% yield of the mixture.

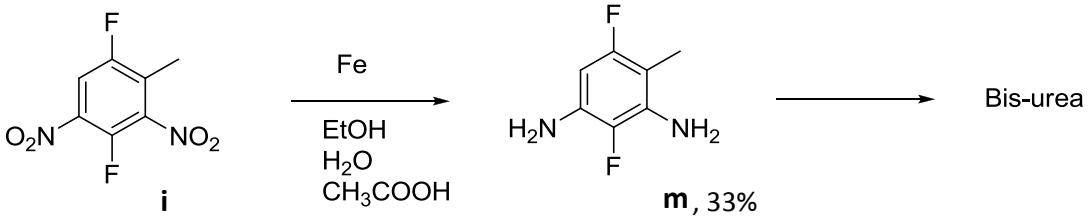

Scheme 2.9

i was then reduced and used in the synthesis of the bis-urea **t2**. The ^{1}H-NMR analysis showed the presence of the product and of some impurities. The purification and the analysis on this derivative have still to be carried out.

2.3 Conclusion

In this chapter we reported the synthesis of a series of new bis-urea monomers, functionalised with halide atoms. The properties of these compounds were then studied by NMR spectroscopy, viscometry, SANS, FT-IR and ITC.

[55] S. Seravanan, P. C. Srinivasan, *Synthetic Comm.*, **2001**, *31*, 823-826.

From these analysis we have verified that the fluorine atom in ortho position does not make intramolecular hydrogen bond. chlorine and bromine atoms in the same position instead give intramolecular hydrogen bond, and surprisingly that reinforces intermolecular urea hydrogen bond.

Among the synthesised products, **4** seemed to be the most promising, because it is the only bis-urea derivative which forms tubes instead of filaments in chloroform (Fig. 2.22 pseudo-phase diagram).

Many attempts were made to obtain the target molecule **t**, but only at the end of my working period a feasible way was found. All the synthetic paths that we tried are here reported.

2.4 Experimental Section

2,4,6-trichloro-1,3-dinitrobenzene (1a)

5,27g (0.029mol)of 1,3,5trichlorobenzene were dissolved in 15mL of HNO_3 and the flask was kept at 40°C for 15 minutes. 13,5mL of H_2SO_4 were added and the temperature was gradually increased till 80°C in 90 minutes. The mixture was slowly poured on 350mL of water (exothermic reaction with evolution of nitrogen oxides) and this caused the precipitation of the product, which was then filtered and washed.

7.59g of a yellow powder were obtained. TLC analysis confirmed the presence of only one compound, whose ^{1}H-NMR showed a single signal. To verify the nature of the product (mono- or di-nitrate) the melting point was measured: 129°C (lit. 129-130°C[56]). The yield was 96%. **Gas cromatography-Mass**: single peak with $[M+H]^+$ 270 (100%), 272 (97%), 274 (31%). **^{1}H-NMR** (250MgHz, $CDCl_3$) δ: 7.61 (s, 1H, CH).

2,4,6-trichloro-1,3-diaminobenzene (1b)

In a 500mL flask 6.03g (0.022mol) of **1a** were solubilised in 25mL of water, 50mL of acetic acid and 80mL of ethanol. Then 7.60g (0.136mol) of iron powder were added. The flask was sonicated for 30h, and the reaction was followed by TLC. The brown mixture was filtered on silica and then washed with ethyl acetate. The filtrate was extracted two times with 200mL of

[56] R. B. Moodie, M. A.Payne, K. Schofield, *Journal of the Chemical Society, Perkin Transactions 2: Physical Organic Chemistry (1972-1999)*, **1985**, 1457-1464.

KOH 2M, and this solution was diluted with 200mL of ethylacetate used to wash the aqueous layer. The organic phase was dried on Mg_2SO_4 and evaporated to give a pale yellow solid. It was crystallized by hexane to give 2.90g (yield 62%) of the pure product. **Gas cromatography-Mass**: single peak with $[M+H]^+$ 210 (100%), 212 (97%), 214 (31%). **^{1}H-NMR** (250MHz, $CDCl_3$) δ: 7.09 (s, 1H, CH), 4.11 (broad s, 4H, NH_2).

2,4,6-trifluoro-1,3-dinitrobenzene (2a)

As for compound **1a** a 50mL flask containing 2.13g (0.016mol)of 1,3,5trifluorobenzene and 9mL of HNO_3 was kept at 40°C for 15 minutes. Then 8mL of H_2SO_4 were added and the temperature was gradually increased till 55°C in 90 minutes. The mixture was poured on 100mL of water and this caused the separation of the product, a dense liquid at the bottom of the beaker. This was isolated, washed three times with water and after this it precipitated. It was filtered, solubilised in 40mL of ethylacetate and washed with 2x40mL of brine. The solution was dried and evaporated. 2.11g of a yellow solid were obtained (yield 58%). Melting point: 54-55°C (lit. 53-55°C[57]). **Gas cromatography-Mass**: single peak with $[M+H]^+$ 222 (100%). **^{1}H-NMR** (250MgHz, $CDCl_3$) δ: 7.16 (double triplet, 1H, coupling with *p*-F J_1 = 1.9 Hz, coupling with *o*-F J_2 = 7.2 Hz, CH). **^{19}F-NMR** (250MHz, $CDCl_3$) δ: 122.37 (1F, s), 106.67 (2F, s).

2,4,6-trifluoro-1,3-diaminobenzene (2b)

1.98g (0.009) of **2a** were solubilised in a mixture of solvents (11mL of water, 22mL of acetic acid and 33mL of ethanol). After solubilisation 2.43g (0.056mol) of iron powder were added. The flask was left for 24h in the ultrasonic bath, and the reaction was followed by TLC. The brown mixture was filtered on silica and then washed with ethylacetate. The filtrate was evaporated and purified by flash column chromatography (silica gel, elution with ethyl acetate:hexane = 1:4). The fractions containing the product were collected to give 0.48g of a yellow solid (yield of 33%). **^{1}H-NMR** (250MHz, $CDCl_3$) δ: 6.60 (double triplet, 1H, coupling with *p*-F J_1 = 1.9 Hz, coupling with *o*-F J_2 = 7.2 Hz, CH), 3.38 (broad s, 4H, NH_2).

[57] R. H. Shiley, J.L. Forsberg, R.S. Perry, D.R. Dickerson, G.C. Finger, *Journal of Fluorine Chemistry*, **1975**, 371-373.

2,4,6-tribromo-1,3-diaminobenzene (c)

5.07g of *m*-phenilenediamine were solubilised in 200mL of water and bromine was added drop by drop. Immediately a grey solid appeared in the solution. After the addition of 1mL of Br_2 the mixture was filtered. This operation has been repeated twelve times on the same solution. At the end 19.33g of the crude product (black) were obtained, still containing unreacted bromine. This excess was removed by solubilisation in chloroform and filtration on celite. After evaporation of the solvent 3.63g of the pure product were isolated (yield of 29%). **^{1}H-NMR** (250MHz, $CDCl_3$) δ: 7.43 (s, 1H, CH), 4.50 (broad s, 4H, NH_2). **^{13}C-NMR** (250MHz, $CDCl_3$) δ: 141.67, 132.24, 96.32, 95.30.

4,6-dichloro-1,3-diaminobenzene (d)

1.07g (0.0045) of 1,3-dichloro-4,6-dinitrobenzene were solubilised in a mixture of three different solvents (6mL of water, 12mL of acetic acid and 20mL of ethanol). After solubilisation 1.35g (0.024mol) of iron were added. The flask was left for 10h in the ultrasonic bath, and the reaction was followed by TLC. The work-up was previously described for product **1b**. After crystallisation 0.24g of the product were obtained (yield of 32%). **^{1}H-NMR** (250MHz, $CDCl_3$) δ: 7.11 (s, 1H, CH), 6.17 (s, 1H, CH), 3.90 (broad s, 4H, NH_2). **^{13}C-NMR** (250MHz, $CDCl_3$) δ: 142.38, 127.13, 109.10, 101.99.

Bis-ureas (1, 2, 3, 4, t)

In a dry 100mL flask under nitrogen atmosphere 20mL of dichloromethane and 0.0015mol of triphosgene were introduced. Then 0.002mol of the aromantic amine and 0.004mol of diisopropilethylamine (DIEA), solubilised in 15mL of dry dichloromethane were added by a syringe pump (speed 2.5mL/h). The syringe was washed with other 7mL of solvent (speed 3.5mL/h). This mixture was kept stirring for one hour and then 0.004 mol of 2-ethyl-hexylamine and 0.004 mol of DIEA in 12mL of solvent were added. After one night the solvent was evaporated. The raw crude appears to be a paste, which we crystallise from acetonitrile.

2-Ethylhexyl-3- [3-(3-(2-ethylhexyl)ureido)-2,4,6-trichlorophenyl] urea (1)

^{1}H-NMR (0.24g, yield of 30%), (250MHz, DMSO) δ: 7.92 (s, 2H, NH), 7.70 (s, 1H, CH), 6.29 (broad t, 2H, NH), 3.00 (broad t, 4H, CH_2), 1.23 (m, 18H, CH/CH_2), 0.83 (m, 12H, CH_3). **^{13}C-**

NMR (250MHz, DMSO) δ: 154.28, 133.83, 133.34, 130.44, 126.79, 41.85, 29.94, 27.91, 23.28, 21.86, 13.19, 10.21. **Mass ESI-TOF:** $[M+Na]^+$ 543.00.

2-Ethylhexyl-3- [3-(3-(2-ethylhexyl)ureido)-2,4,6-trifluorophenyl] urea (2)

^{1}H-NMR (0.27g, yield of 37%), (250MHz, DMSO) δ: 7.70 (s, 2H, NH), 7.21 (double triplet, 1H, CH), 6.30 (broad t, 2H, NH), 3.00 (broad t, 4H, CH_2), 1.24 (m, 18H, CH/CH_2), 0.84 (m, 12H, CH_3). **^{13}C-NMR** (250MHz, DMSO) δ: 156.65.07, 135.63, 134.98, 131.41, 43.45, 31.56, 29.60, 24.85 23.72, 15.15, 11.99. **Mass ESI-TOF:** $[M+Na]^+$ 495.07.

2-Ethylhexyl-3- [3-(3-(2-ethylhexyl)ureido)-2,4,6-tribromophenyl] urea (3)

^{1}H-NMR (0.52g, yield of 40%), (250MHz, DMSO) δ: 7.99 (s, 2H, NH), 7.90 (s, 1H, CH), 6.26 (broad t, 2H, NH), 3.00 (broad t, 4H, CH_2), 1.24 (m, 18H, CH/CH_2), 0.83 (m, 12H, CH_3). **^{13}C-NMR** (250MHz, DMSO) δ: 154.07, 136.63, 133.11, 127.41, 121.28, 41.77, 29.97, 27.94, 23.27, 21.89, 13.23, 10.23. **Mass ESI-TOF:** $[M+Na]^+$ 677.05.

2-Ethylhexyl-3- [3-(3-(2-ethylhexyl)ureido)-4,6-dichlorophenyl] urea (4)

^{1}H-NMR (0.58g, yield of 87%)**,** (250MHz, DMSO) δ: 8.93 (s, 1H, CH), 7.95 (s, 2H, NH), 7.46 (s, 1H, CH), 6.91 (broad t, 2H, NH), 3.03 (broad t, 4H, CH_2), 1.25 (m, 18H, CH/CH_2), 0.88 (m, 12H, CH_3). **^{13}C-NMR** (250MHz, DMSO) δ: 154.90, 136.32, 130.44, 126.80, 41.20, 30.94, 28.89, 23.28, 22.98, 14.44, 11.24. **Mass ESI-TOF:** $[M+Na]^+$ 509.24.

1,3-diamine-4,6-dimethylbenzene

In a 500mL flask 5.55g (0.033mol) of 2,4-dimethyl-5-nitroaniline, 21mL of H_2N-NH_2 (0.669mol), 0.55g of Pd/C 10% and 200mL of ethanol were introduced. The reaction was kept at reflux for two days. Then the mixture was filtered on celite and washed with dichlorometane. After evaporation of the solvent, the product was solubilised in ethylacetate and washed with water (3x150mL). The organic phase was dried and evaporated to obtain 3.70g of the pure product (yield of 81%). **^{1}H-NMR** (250MHz, $CDCl_3$) δ: 6.72 (s, 1H, CH), 6.10 (s, 1H, CH), 3.29 (broad s, 4H, NH_2), 2.07 (s, 6H, CH_3).

N,N'-(4,6-dimethyl-1,3-phenylene)diacetamide

In a 250mL flask 3.61g (0.026mol) of 1,3-diamino-4,6-dimethylbenzene, 6.5mL (0.069mol) of acetic anhydride and 75mL of dry dichlorometane were introduced. The reaction was stirred at room temperature for two days. 5.71g of the product, purified by filtration, were obtained with a yield of 98%. **^{1}H-NMR** (250MHz, $CDCl_3$) δ: 9.23 (s, 2H, NH), 7.37 (s, 1H, CH), 6.98 (s, 1H, CH), 2.09 (s, 6H, CH_3), 2.00 (s, 6H, CH_3). **^{13}C-NMR** (250MgHz, $CDCl_3$) δ: 168.05, 134.13, 131.57, 128.47, 121.95, 23.21, 17.30.

2-fluoro-4,6-dimethyl-1,3-diaminobenzene (e)

1mmol of N,N'-(4,6-dimethyl-1,3-phenylene)diacetamide, 1mmol of Selectfluor and 20mL of solvent (acetonitrile or dimethylformamide or water or methanol) were introduced in a 50mL flask and the mixture was kept at room temperature (but also, in different experiments, at 40°, 55°C, 70°C, or at reflux), during 1 night (or 2). The NMR analysis on the crude mixture showed in all the cases the formation of unknown products.

2-fluoro-4-cyano-6-chloro-1,3-dinitrobenzene (f)

0.51g (0.003mol) of 3-cyano-5-chloro-fluorobenzene were solubilised in 3mL of fuming nitric acid at 40°C in 15 minutes. Then 2.5mL of sulphuric acid were added and the mixture was kept at 80°C for 90 minutes. The mixture was poured in 50mL of water and this caused the precipitation of the product, which was then filtered and washed. 0.47g of a white solid were collected and ^{1}H-NMR analysis confirmed it was the 3-cyano-4-nitro-5-chloro-fluorobenzene (g). **^{1}H-NMR** (250MHz, $CDCl_3$) δ: 7.62 (dd, J_1 = 9.7 Hz, J_2 = 3.2 Hz, 1H, CH), 7.50 (dd, J_1 = 9.7 Hz, J_2 = 3.2 Hz, 1H, CH).

2-fluoro-4-methyl-1,3-dinitrobenzene

2-fluoro-4-methyl-nitrobenzene (1.02g, 0.006mol) was solubilised in 4mL of sulphuric acid and 2mL of nitric acid were added drop by drop. After 30 minutes at 90°C the mixture was poured on ice. 1.09g of a solid were isolated by filtration. The nature of the product was verified by ^{1}H-NMR and it has been possible to identify it as 2-fluoro-4-methyl-1,5,6-trinitrobenzene (h) thanks to the coupling constant with the fluorine atom . **^{1}H-NMR** (250MHz, $CDCl_3$) δ: 8.89 (d, 1H, coupling with *o*-F J_2 = 8.5 Hz, CH), 2.69 (s, 3H, CH_3).

2,5-difluoro-4-methyl-1,3-dinitrobenzene (i)

2.24g (0.013) of 2,5-difluoro-4-methyl-nitrobenzene, 6mL of nitric acid and 6mL of sulphuric acid were introduced in a 25mL flask and kept at 70°C for 24h. The mixture was poured in water and extracted with ethylacetate. The organic phase was then washed with NaOH 2N, with water and dried with Mg_2SO_4. After evaporation the product was purified by flash column chromatography (silica gel, elution with ethyl acetate:hexane = 2:5, **i** RF = 0.8, **l** RF = 0.4). Two different products were separated: 1.85g of **i** (yield of 66%) and 0.15g of **l**. **^{1}H-NMR** (250MHz, $CDCl_3$) δ: 7.97 (dd, 1H, coupling with *m*-F J_1 = 5.0 Hz, coupling with *o*-F J_2 = 6.8 Hz, CH), 2.40 (d, *J* = 2 Hz, 3H, CH_3). **^{19}F-NMR** (250MgHz, $CDCl_3$) δ: -112.37 (1F, d), -132.09 (1F, d). **^{13}C-NMR** (250MHz, $CDCl_3$) δ: 157.65, 154.31, 147.15, 143.57, 128.67, 115.11, 11.71.

2,5-difluoro-4-methyl-1,3-diaminobenzene (m)

1.56g (0.007) of **i** were solubilised in a mixture of three different solvents (7.5mL of water, 15mL of acetic acid and 15mL of ethanol). After solubilisation 2.52g (0.045mol) of iron were added. The flask was left for 20h in the ultrasonic bath, and the reaction was followed by TLC. The brown mixture was filtered on silica and then washed with ethylacetate. The filtrate was evaporated and purified by flash column chromatography (silica gel, elution with ethylacetate:hexane = 1:4). The fractions containing the product were collected to give 0.39g of a white-yellow solid (yield of 35%). **^{1}H-NMR** (250MHz, $CDCl_3$) δ: 5.94 (dd, 1H, coupling with *m*-F J_1 = 9.2 Hz, coupling with *o*-F J_2 = 13.2 Hz, CH), 3.64 (broad s, 4H, NH_2), 1.98 (d, *J* = 2 Hz, 3H, CH_3).

2-Ethylhexyl-3- [3-(3-(2-ethylhexyl)ureido)-2,5-difluoro-4-methylphenyl] urea (t2)

To be characterised.

Chapter 3

Synthesis of new [2]-rotaxanes systems

3.1 Introduction

a. Definition

Rotaxanes were synthesised for the first time in 1967 by Schill and Zollenkopf[58] in a multistep synthesis and by Harrison and Harrison[59] in a statistical approach. For a long time these species were considered laboratory curiosities only accessible in low yields[60]. It was only in the 80's, after the works of Sauvage and Stoddart on template synthesis[61], that they became obtainable in preparative yields and really raised interest in the chemical community.

Rotaxanes (figure 3.1b) are systems composed of a bead-like macrocycle trapped on a linear component terminated at both ends by bulky stoppers in the shape of a dumbbell. The ring and the axle are not covalently linked, but it is a mechanical bond which holds the components together.

(a) (b)

Figure 3.1 Examples of pseudo-rotaxane (a) and rotaxane (b) systems[62].

Pseudo-rotaxanes (figure 3.1a) are the precursors of rotaxanes, indeed, since no intercomponent mechanical bond exists in these supramolecular species, their separate components are free to dissociate. The template-directed synthesis of this class of compounds requires the presence on the components of particular units able to master the self-assembling processes.

[58] G. Schill, H. Zollenkopf, *Nachr. Chem. Tech.,* **1967**, *15,* 149-151.
[59] T. Harrison, S. Harrison., *J. Am. Chem. Soc.*, **1967,** *89*, 5723-5724.
[60] G. Schill, *Catenanes, Rotaxanes and Knots*; Academic: New York, NY, **1971.**
[61] C . O. Dietrich-Buchecker, J.-P. Sauvage, J. P. Kintzinger, *Tetrahedron Lett.*, **1983**, 24, 5095 -5098; C. 0. Dietrich-Buchecker, I-P. Sauvage, *Chem. Rev.,* **1987**, 87, 795-810.
[62] J. Araki, K. Ito, *Soft Matter,* **2007**, *3*, 1456-1473.

Everyday new efficient methods to assemble such systems are explored, but there are two main synthetic approaches, which are known as "*clipping*" and "*threading and stoppering*" methods.

In the former the axle is previously synthesised and the macrocycle is closed around it (figure 3.2).

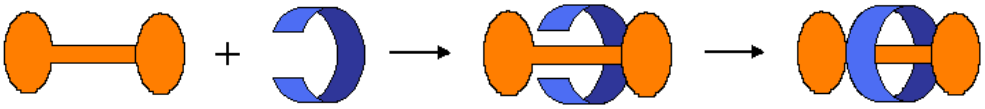

Figure 3.2 Schematic representation of the *clipping* method.

The latter is based on the formation of the axle directly within the cycle (figure 3.3).

Figure 3.3 Schematic representation of the *threading and stoppering* method.

Without a strong driving force none of these reactions would be possible and usually non-covalent interactions are exploited at this scope

b. Method of synthesis

In recent years various examples of rotaxanes, pseudorotaxanes, catenanes and other types of molecular links with three or more mechanical bonds or components have been described. These systems are known to have unique dynamic behaviour and intense research has been focused on the use of external stimuli to influence their dynamics. The control may be exercised for example by guest binding.

In a recent work[63] a rare case of [3]-rotaxane (§ in figure 3.4-c-), comprising two axles passing through the same ring, is achieved by the *threading and stoppering* method. This system is exceptional also because to interlock *n* components, normally *n* – 1 template sites are required, but in this case only a single site (*n* - 2) is present, which induces the formation

[63] S. M. Goldup, D. A. Leigh, P. R. McGonigal, V. E. Ronaldson, A. M. Z. Slawin, *J. Am. Chem. Soc.*, **2010**, *132*, 315-320.

of both the threads. The strategy is build around a macrobicyclic ligand, that, coordinating a metal (Cu^{+}), works as a catalyst for the formation of the axles in two steps.

Starting from this basic scheme it is possible to develop similar approaches. Indeed if the second thread is formed more slowly than the first, it is possible to stop the reaction at the step of [2]-rotaxane and change the metal center. In this way at the end a system of three different components is formed. Another variation may be introduced by forming the second axle in an inverted position with respect to the cycle plane, as a consequence two different diastereoisomers will be obtained.

(a)

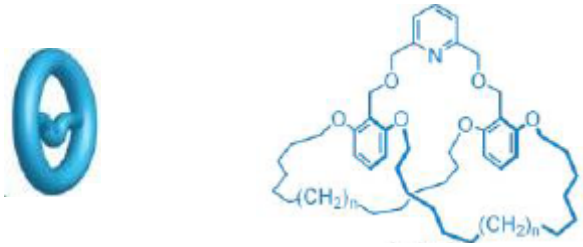

(b)

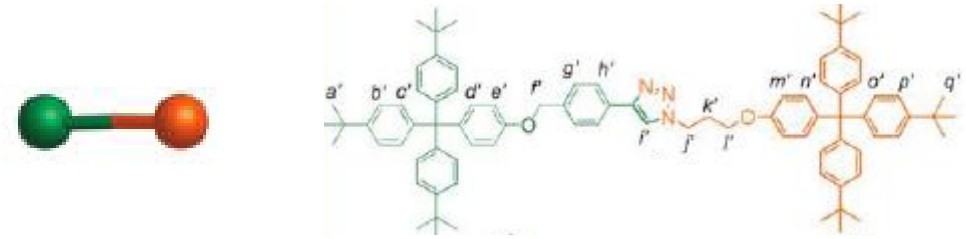

(c)

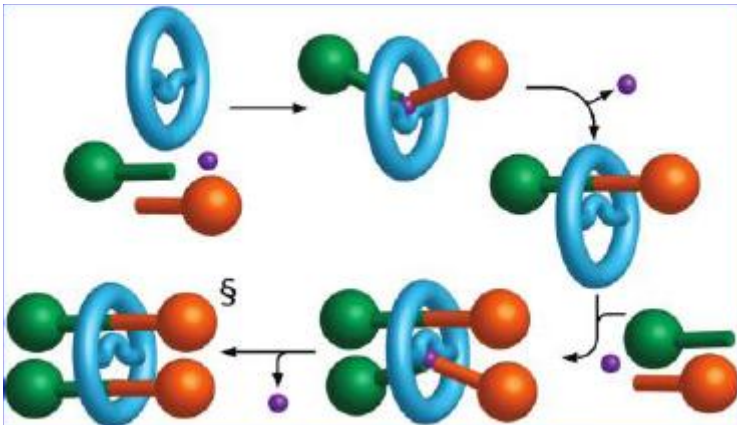

Figure 3.4 Structures of the building blocks (a and b). Scheme of the template synthesis of macrobicyclic [3]-rotaxanes.

The majority of the examples that imply the use of the *clipping* method are based on the formation of irreversible covalent bonds[64,65]. However recently big progresses have been

[64] R. Jäger, F. Vogtle, *Angew. Chem.*, **1997**, *36*, 930-944.

made in the field of reversible dynamic covalent chemistry (DCC). A reversible reaction often employed for this purpose is the imine bond formation[66,67].

Y. Liu et al. described a system synthesised through a [2+3] clipping reaction[68]. The five units of the macrocycle react in the presence of the axle to give a single product, the rotaxane (figure 3.6). Without the template effect of the axle, a mixture of different products is obtained.

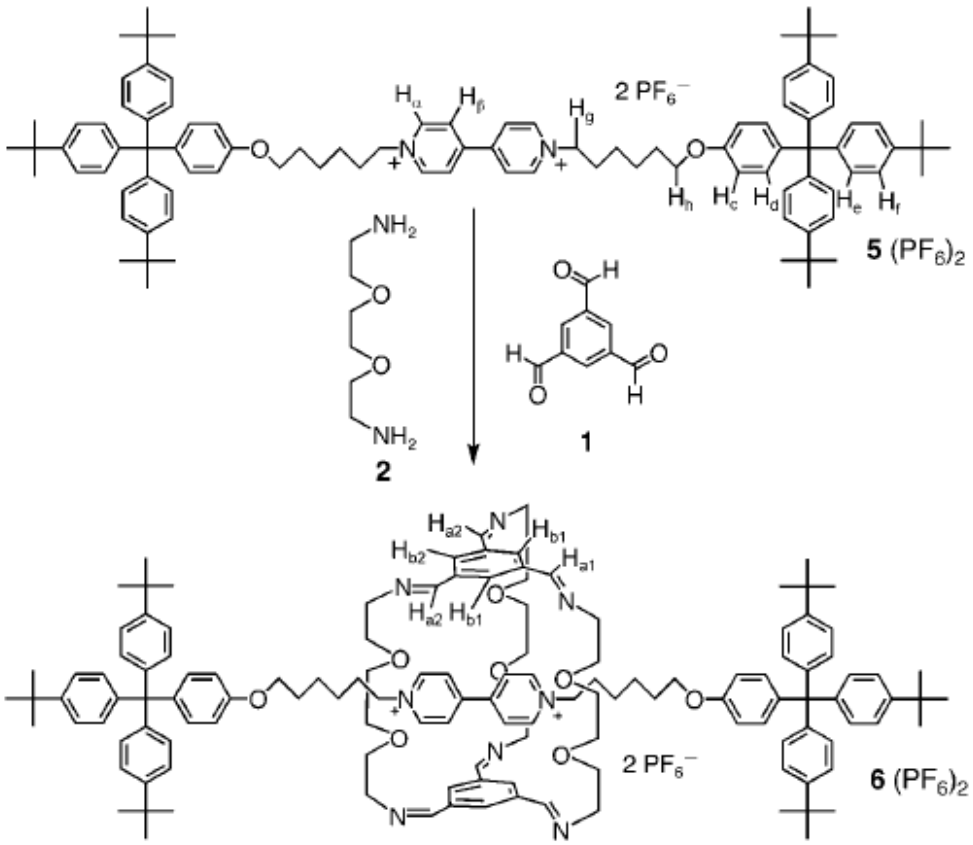

Figure 3.6

The rotaxane **6**$(PF_6)_2$ is an example of cryptand, i.e. a three-dimensional host capable of including ions and small molecules. In particular this one dues its properties to the flexibility and to the polar binding sites of the ethylene glycol pillars.

[65] A.G. Johnston, D. A. Leigh, A. Murphy, J. P. Smart, M. D. Deegan, *J. Am. Chem. Soc.*, **1996**, *118*, 10662-10663.
[66] X.-Z. Zhu, C.-F. Chen, *J. Am. Chem. Soc.*, **2005**, *127*, 13158-13159.
[67] O.Molokanova, A. Bogdan, M. O. Vysotsky, M. Bolte, T. Ikai, Y. Okamoto, V. Boehmer, *Chem. Eur. J.*, **2007**, *13*, 6157-6170.
[68] L. M. Klivansky, G. Koshkakaryan, D. Cao, Y. Liu, *Angew. Chem. Int. Ed*., **2009**, *48*, 4185-4189.

c. Uses of rotaxanes systems

The most investigated field for these systems is that of molecular machines (MM). Indeed like macroscopic machines also MM typically are made up by two or more movable parts, which aim is the production of useful work. Under a classification point of view there are two types of synthetic MM: molecular motors and molecular shuttles. The formers are characterised by a capability of unidirectional rotational motion powered by external energy input (as light). The latters undergo to change of state, usually through an internal translational movement and then they return to the original position. Classical examples of molecular shuttles are interlocked systems, as rotaxanes and catenanes. Indeed, by virtue of the mechanical bond characteristic of a rotaxane, the ring can "shuttle" along the linear component, which possesses appropriate recognition sites that act as station. The "shuttling" process can be controlled reversibly by external stimuli (pH, temperature, an electrical courrent, the presence of a ligand, some reactions etc.).

Shuttle systems are investigated also in the field of molecular electronics. The ring of the rotaxane showed in figure 3.7 can pass from the OFF position, ground state and less conductiong, to the ON position, metastable state and more conducting[69]. The stimuli that controls the shuttling is the oxidation or the reduction of the ring.

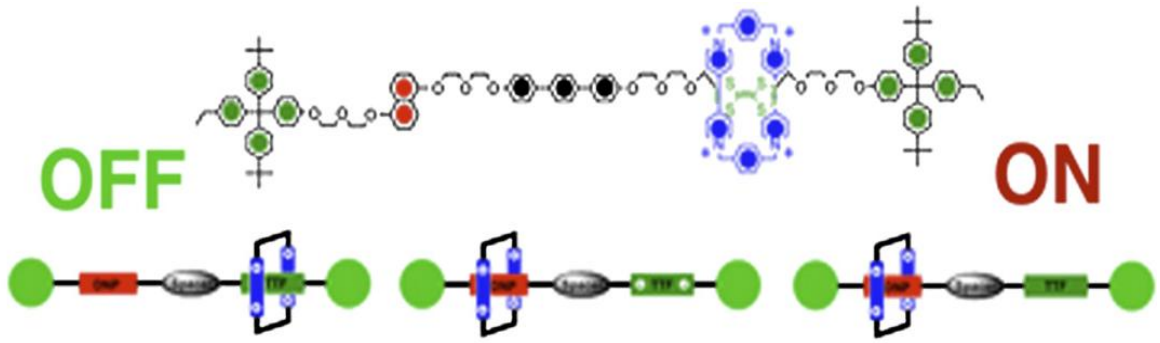

Figure 3.7 Structure of a switchable [2]-rotaxane responding to an electrical stimuli.

Also pseudorotaxane systems can show switching properties. A particularly fertile line of research uses a 4,4'-bipyridinium dication as axle, and crown ethers containing π-electron donors units as macrocycle.

[69] J. F. Stoddart , H. M. Colquhoun, *Tetrahedron*, **2008**, *64*, 8231-8263.

An example of this family is reported by J. F. Stoddart et al.[70] (figure 3.8). It is verified that the four cations present on the thread pair off with the binding sites of the macrocycles. From this selective coupling a series of multicomponent pseudorotaxanes are generated. The switch between dethreaded and rethreaded species is induced by acid-base stimuli.

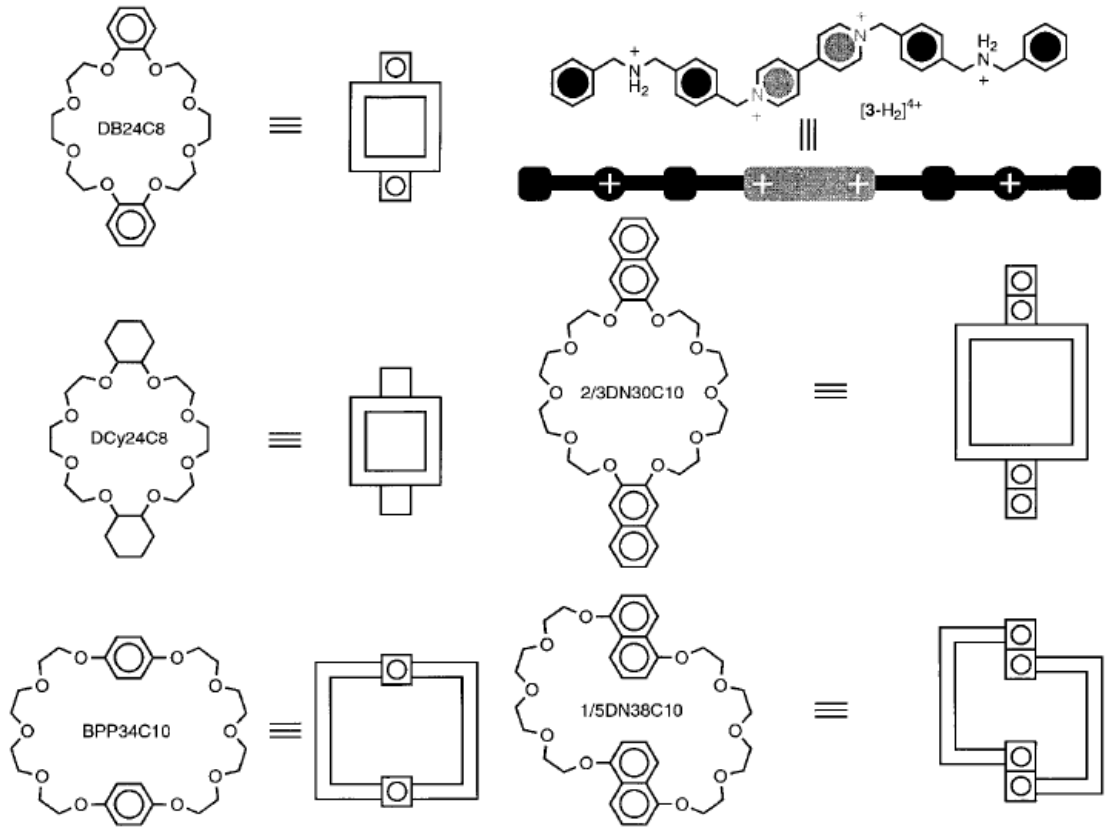

Figure 3.8 Molecular structure of the building blocks of the pseudorotaxanes.

Studies carried out in my laboratory lead to the synthesis of a pseudorotaxane system (figure 3.9), which can work as a molecular machine[71].

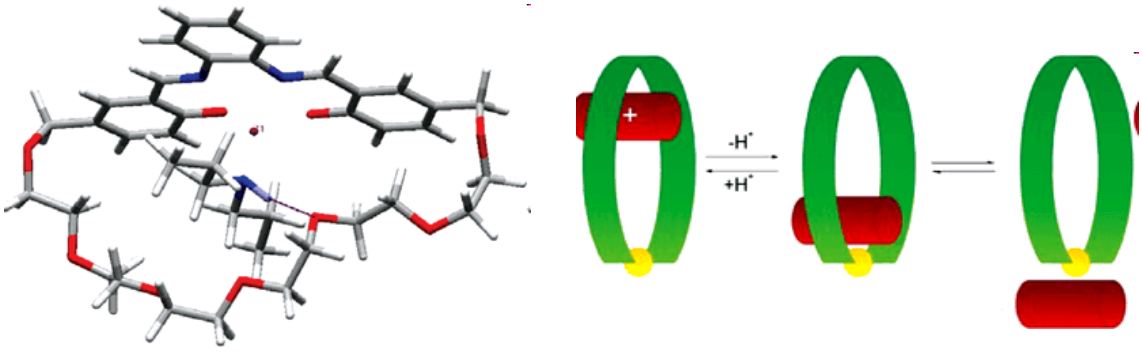

Figure 3.9 Pseudorotaxane structure and its working as molecular machine.

[70] P. R. Ashton, R. Ballardini, V. Balzani, M. C. T. Fyfe, M. T. Gandolfi, M.-V. Martínez-Díaz, M. Morosini, C. Schiavo, K. Shibata, J. F. Stoddart, A. J. P. White, D. J. Williams, *Chem. Eur. J.*, **1998**, *4*, 2332-2341.
[71] A.Dalla Cort, L. Mandolini, C. Pasquini, L. Schiaffino, *Org. Biomol. Chem.,* **2006**, 4543-4546.

This system is composed by a crown ether macrocycle containing a Zn-salophen unit, the wheel, and by a diisopropylamine axle. Calculations on the structure of the salophen complex confirmed that the apical binding site of the Zinc is oriented inside the cavity pointing towards the chain. Thus the dibenzylammonium cation can translate between the two stations, the crown ether oxygens and the metal center, responding to pH variations.

d. Aim of the research

Therefore part of my work has been focused on the development of the corresponding salophen-based rotaxane system. The introduction of appropriate stoppers at the end of the amine axle should give life to the formation of an locked system.

Among the most commonly used stoppers there are tetrarylmethane-based derivatives, because of their bulkiness and the easy synthetic introduction[72,73,74]. Thus we decided to develop an axle containing a secondary amine function, decorated with two trityl-stoppers.

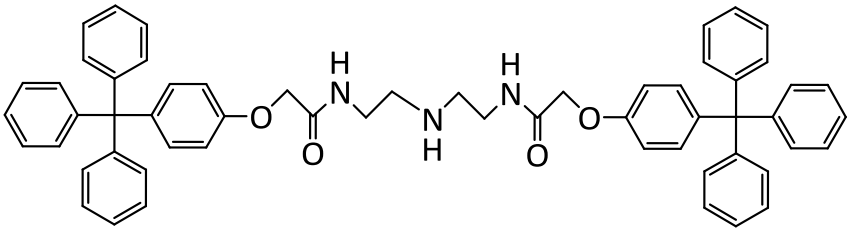

axle c

The method we decided to apply to obtain the rotaxane was the *clipping* one, i.e. closing the macrocycle directly around **axle c**.

[72] R. Ballardini, V. Balzani, W. Dehaen, A. E. Dell'Erba, F. M. Raymo, J. F. Stoddart, M. Venturi, *Eur. J. Org. Chem.*, **2000**, 591-602.
[73] L. M. Hancock, P. D. Beer, *Chem. Eur. J.*, **2009**, *15*, 42-44.
[74] S. M. Goldup, D. A. Leigh, P. J. Lusby, R. T. Mc Burney, A. M. Z. Slawin, *Angew. Chem. Int. Ed.*, **2008**, *47*, 6999-7003.

3.2 Results and discussion

The preparation of axle **c** follows the synthetic path reported in scheme 3.1.

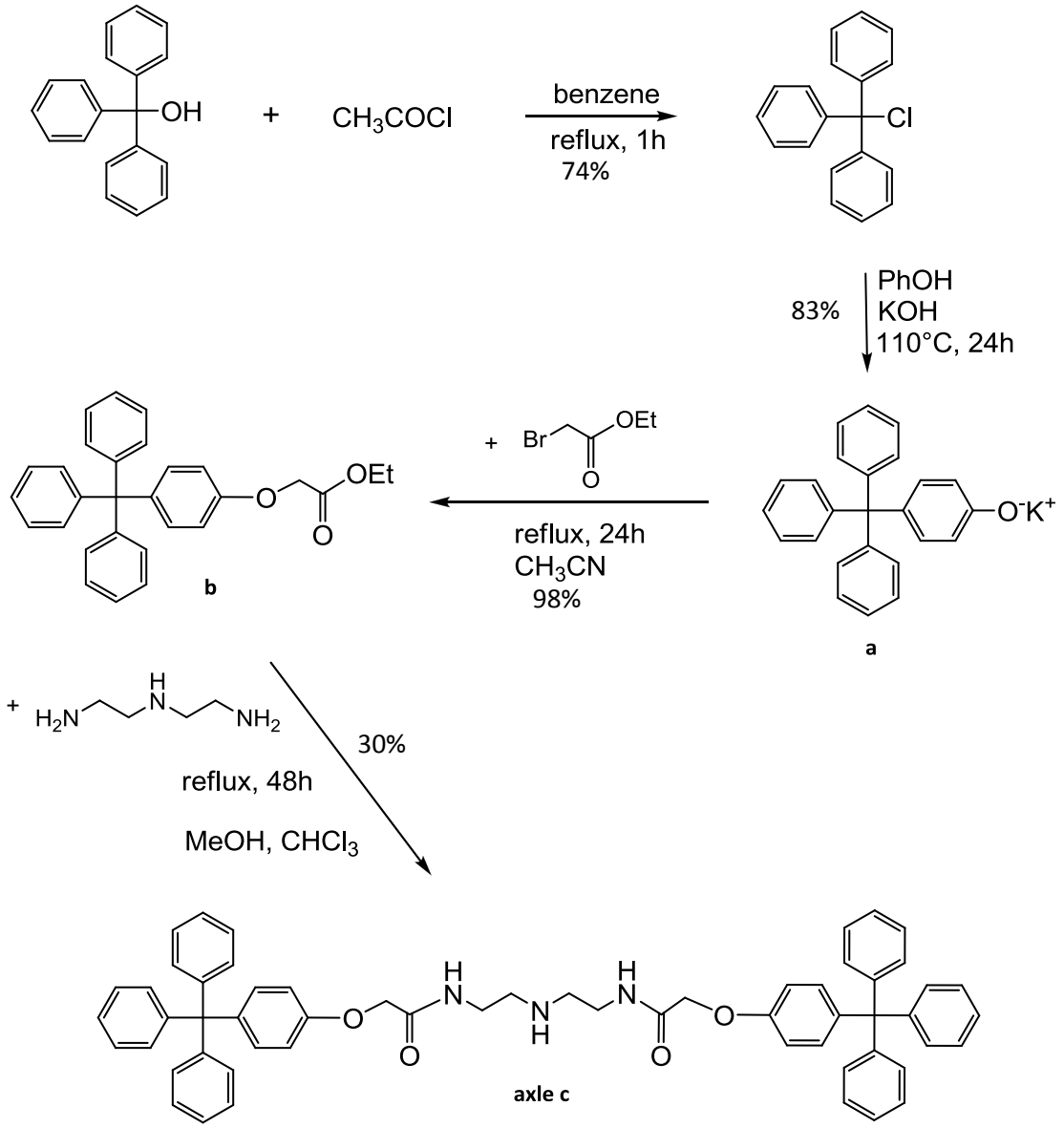

Scheme 3.1

The first two steps[75] are two subsequent substitutions on triphenylmethanol, to introduce firstly a chorine atom, and then a potassium phenolate group.

Compound **a** will easily react with ethyl bromoacetate to give the corresponding ether **b**[76]. This stopper unit was allowed to react[77] with the bis-(2-aminoethyl)amine affording the

[75] P. R. Ashton, R. Ballardini, V. Balzani, M. Belohradsky, M. T. Gandolfi, D. Philp, L. Prodi, F. M. Raymo, M. V. Reddington, N. Spencer, J. F. Stoddart, M. Venturi, D. J. Williams, *J. Am. Chem. Soc.*, **1996**, *118*, 4931-4951.

expected bis amide in low yield after column chromatography purification. The synthesis of the dialdehyde necessary for the Zn-salophen macrocycle is the following (scheme 3.2).

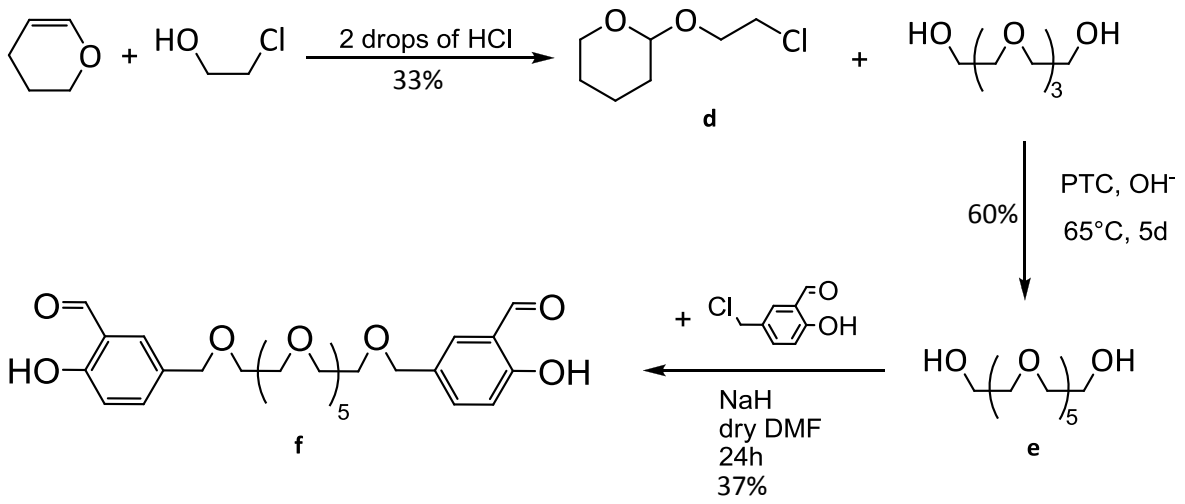

Scheme 3.2

The first step is the protection of the hydroxyl group of 2-chloroethanol with 3,4-dihydro-2H-pyran[78]. In this way **d** can react with tetraethyleneglycol and forms the protected esaethyleneglycol. The subsequent deprotection is performed in the same pot[79]. The major limitation of these products is the purification, which resulted to be often difficult and leading to a decrease of the yields.

The dialdehyde **f** is obtained from the reaction of **e** with 2 equivalents of the previously synthesised 5-chloromethyl-2-hydroxybenzaldehyde.

Before trying the synthesis of the rotaxane, some preliminary studies were performed to verify the feasibility of the system. UV-Vis titration experiments were conducted on a model system constituted by a simple Zn-salophen complex and **axle c**, to measure the association between the metal center and the secondary amine nitrogen of the axle. The binding constant resulted to be $K_1 = 5000 \pm 200\ M^{-1}$, thus confirming the good affinity between the components.

Therefore we tried the rotaxane synthesis following the procedure here described, procedure a. Axle **c** was solubilised in methanol and 1 equivalent of methansulphonic acid was added to protonate the amine function of the axle. In this way the nitrogen will form

[76] V. Balzani, J. Becher, A. Credi, M. B. Nielsen, F. M. Raymo, J. F. Stoddart, A. M. Talarico, M. Venturi, *J. Org. Chem.*, **2000**, *65*, 1947-1956.
[77] I. Korendovych, M. Cho, P. L. Butler, R. J. Staples, E. V. Rybak-Akimova, *Org. Lett.*, **2006**, *8*, 3171-3174.
[78] A. Buzas, C. Egnell, M. Moczar, *Chem. Soc. Fr.*, **1962**, 267-271.
[79] R. A. Bartsch, C. V. Cason, B. P. Czech, *J. Org. Chem.*, **1989**, *54*, 857-860.

hydrogen bonds with the polyoxyethylenic chain of the dialdehyde favouring the preorganization of the precursors. The flask containing this solution was charged with the dialdehyde **f** (1 eq.), zinc acetate dihydrate (1.3 eq.) and *o*-phenylenediamine (1 eq.). The reaction was stirred at 50°C for 3 days, the solvent evaporated and the product analysed by ESI-TOF mass spectrometer (figure 3.10).

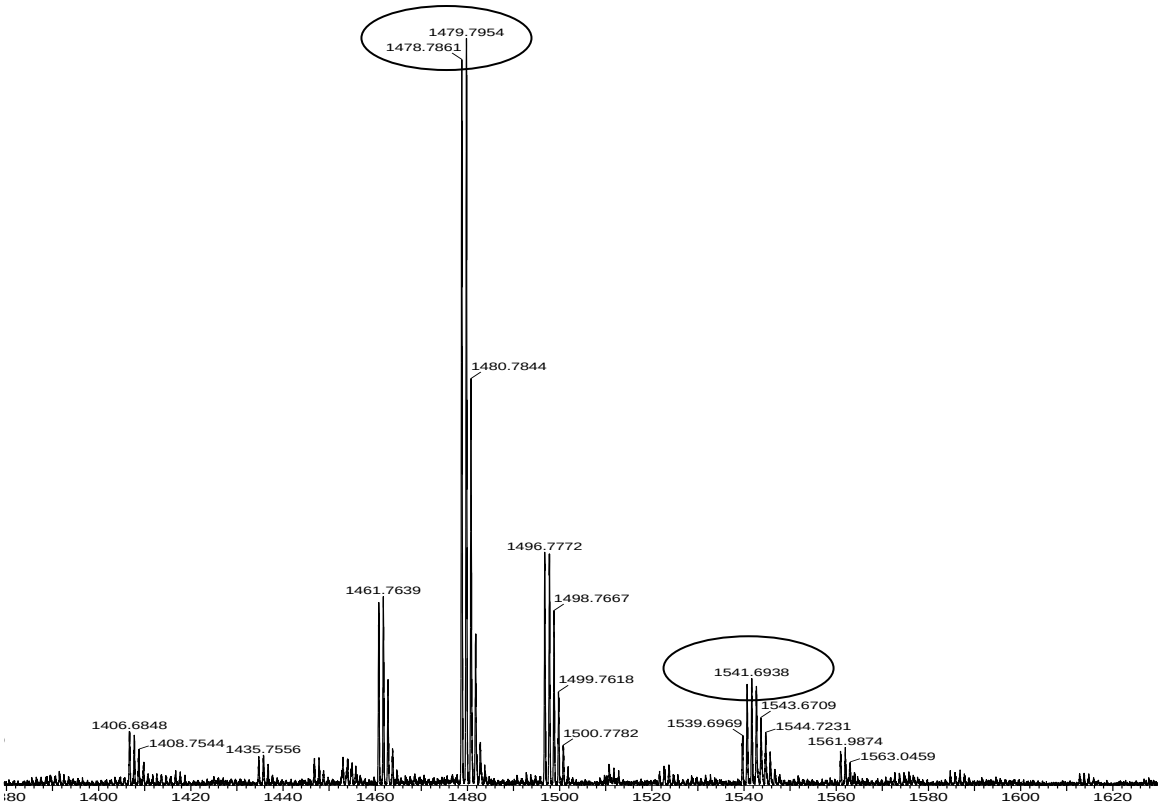

Figure 3.10 Zoom enlargement of mass spectrum of the crude product obtained with procedure a, in methanol at 20°C.

The mass spectrum showed the peaks corresponding to the reactants, and among them the base peak being that referred to the axle. Two peaks of very low intensity confirmed the formation of rotaxane **1**, at [m/z] = 1541.69 $[M+H]^+$, and of the demetalated rotaxane at [m/z] = 1479.79 $[M-Zn]^+$. It is indeed reported in the literature the tendency of Zn-salophen to lose the zinc cation in the presence of acid impurities[80].

An attempt to overcome this problem was made by avoiding the addition of acid. The reaction was carried out in this way, procedure b: to a zinc solution in methanol at reflux were subsequently added 1eq. of *o*-phenylenediamine, 1 eq. of axle **c** and slowly at the end 1 eq. of dialdehyde **f**. The mixture was kept at reflux for 3 days, then the solvent was

[80] E. C. Escudero-Adàn, J. Benet-Buchholz, A. W. Kleij, *Dalton. Trans.*, **2008**, 734-737.

evaporated and the product analysed. This time the peak of the demetalated product was absent, but the peak corresponding to rotaxane **1** still represents only a small percentage of the total.

Still to prevent demetalation we designed a different axle in which a pyridine unit is present (**axle g**). As already reported in chapter 1, the interaction N_{pyr}-Zn is really strong and should stabilise the rotaxane. On the other hand we knew that this might prevent the possibility for the axle to shuttle between the two stations. Nevertheless we want to see if the rotaxane can still be formed.

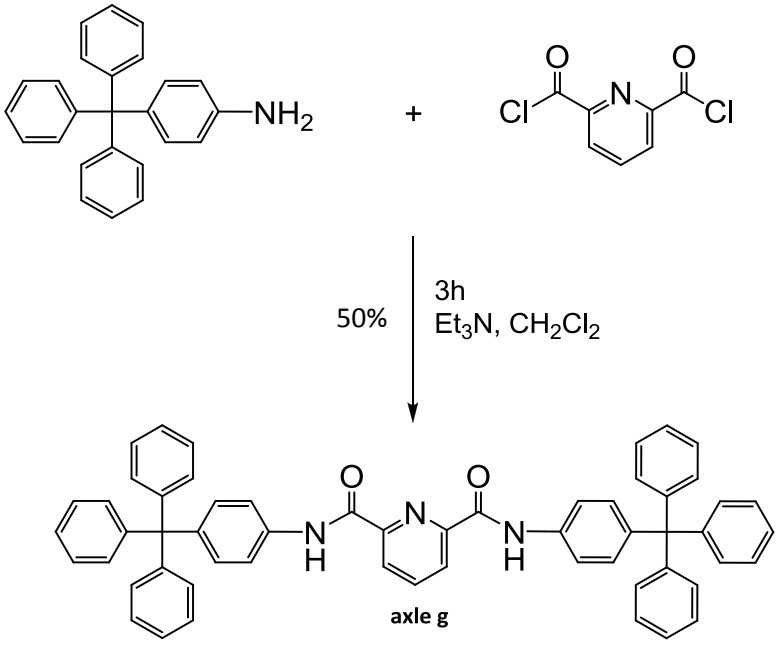

axle g

Scheme 3.3

Axle g is easily obtained by the formation of two amide bonds between 4-tritylaniline and 2,6-pyridindicarbonylchloride[81]. This reaction gives good yields of the product and this fact suggested to us to change the synthetic route and to employ the *threading and stoppering* method. This means that the macrocycle has to be previously synthesised and isolated.

[81] F. Vögtle, F. Ahuis, S. Baumann, J. L. Sessler, *Liebigs Ann.*, **1996**, 921-926.

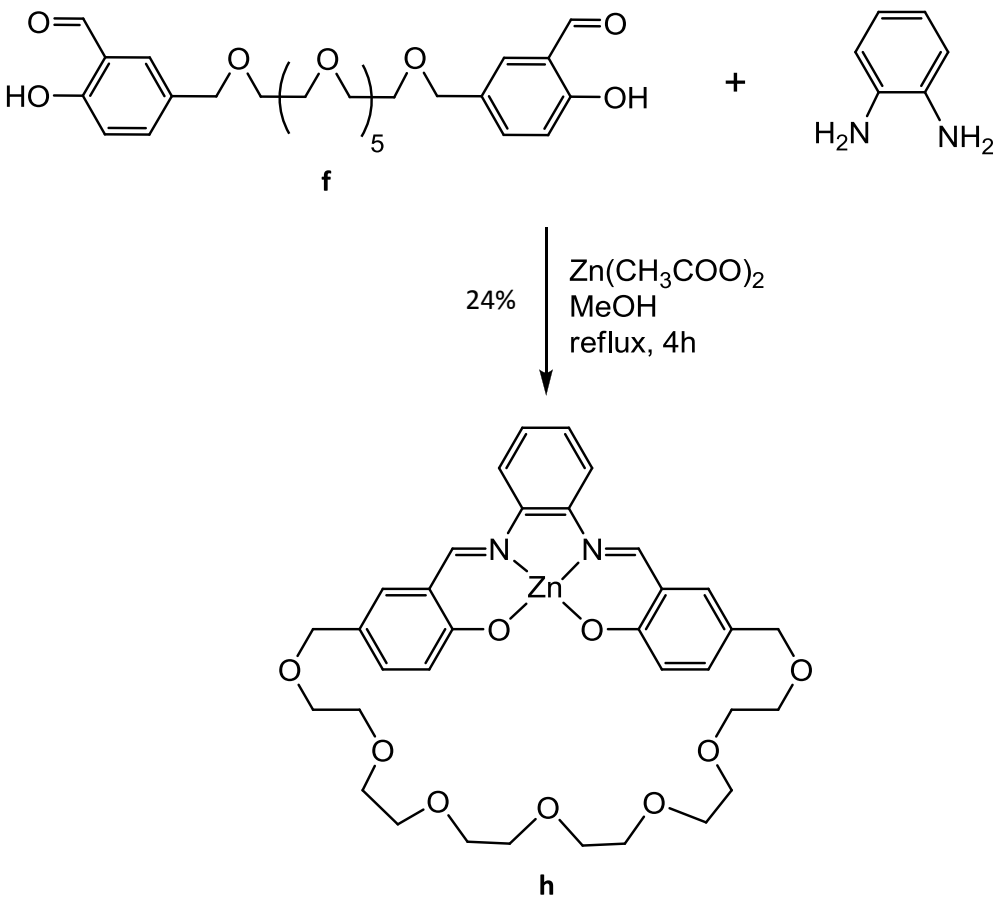

Scheme 3.4

The macrocyclisation reaction has to be performed under controlled conditions. In general the synthesis of macrocyclic compounds implies the formation of an open intermediate, which can give intramolecular (ring closure) or intermolecular reaction (formation of linear polymers or higher order cyclo-olygomers). To promote the intramolecular reaction with respect to the intermolecular one, it is necessary to work at concentration lower than the effective molarity (EM) of the system. EM is defined by the equation 3.1[82], where k_{intra} and k_{inter} are the specific rates of analogous intra- and intermolecular reactions run under identical conditions.

$$EM = k_{intra}/k_{inter} \qquad \textbf{3.1}$$

[82] C. Galli, L. Mandolini, *Eur. J. Org. Chem.,* **2000**, 3117-3125.

The EM value for macrocycles of this size is in the order of 10^{-2}M, this means that to promote the intramolecular reaction the synthesis has to be carried out at concentrations < 10^{-2}M. To obtain this condition it is necessary to use the influx technique.

Preliminary UV-Vis titrations were carried out with **axle g** and the basic Zn-salophen complex to test the affinity between the metal center and the pyridinic unit. A binding constant was obtained (K_2 = 20000 ± 600M^{-1}), and it resulted significantly higher than K_1, that measured for the secondary amine based axle (**axle c**), as expected.

The synthesis was pursued following procedure c: 1 eq. of 2,6-pyridindicarbonylchloride and 1 eq. of macrocycle **h** were solubilised in dichloromethane. A solution of 2 eq. of tritylaniline was added by a syringe pump over a period of 8h. At the end of the addition the mixture was stirred for 12h. Then the solvent was evaporated and the crude product analysed by ESI-TOF (figure 3.12). Also this time the peak of the rotaxane is present, but it still represents a small percentage of the total.

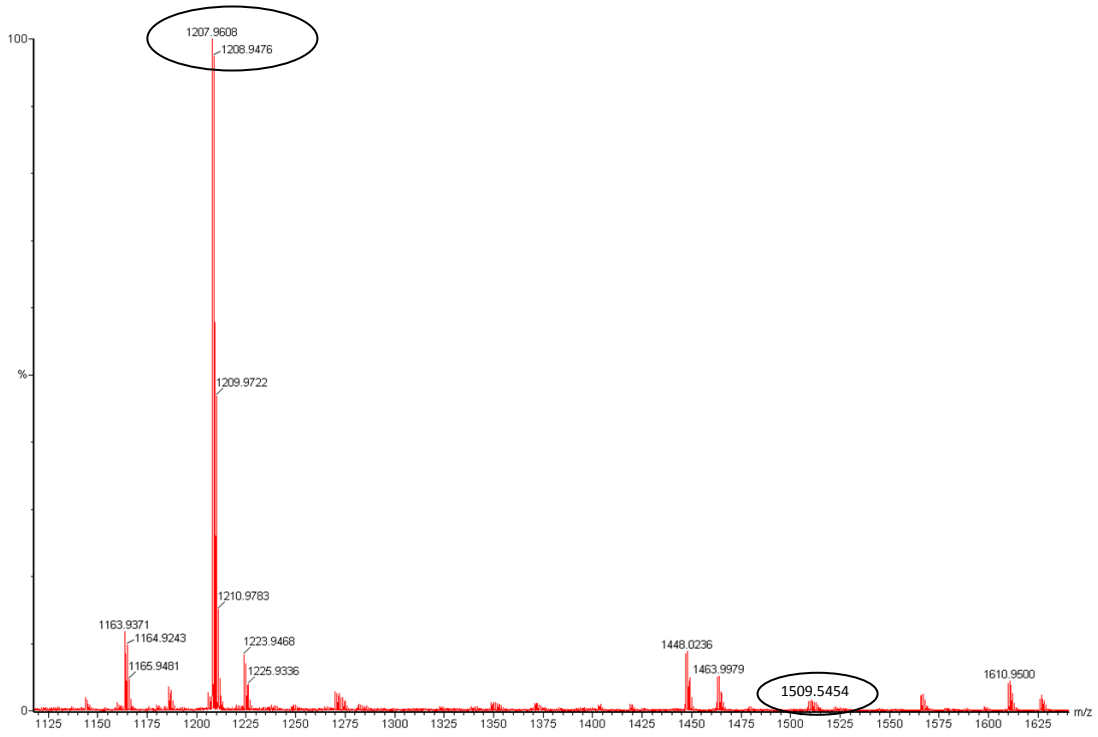

Figure 3.12 Mass spectrum of the crude product obtained with procedure c, in methanol at 20°C.

By now the base peak is no more that of the axle, as in the previous case, but it is a peak at [m/z] = 1207.92, which corresponds to the formation of a new compound. This mass value is that of the pseudorotaxane composed by the macrocycle and the axle with only one stopper.

This result leads us to think that the wheel (**h**) is too small to host the axle. For this reason we synthesised a larger macrocycle, for which a dialdehyde containing one more ethylene glycol unit is needed (scheme 3.5).

As in the previous case, the first step is the protection of one of the terminal hydroxyl functions. The starting material is the diethyleneglycol, which is mono-protected (**i**) and reacted with the triethyleneglycol bis-tosylate using a Phase Transfer Catalyst (PTA). The resulting product **l** undergoes to an acid-catalysed deprotection to give the epthaethylene glycol **m**. The last step is the reaction with 5-chloromethyl-2-hydroxybenzaldehyde to produce the dialdehyde necessary for the macrocycle formation.

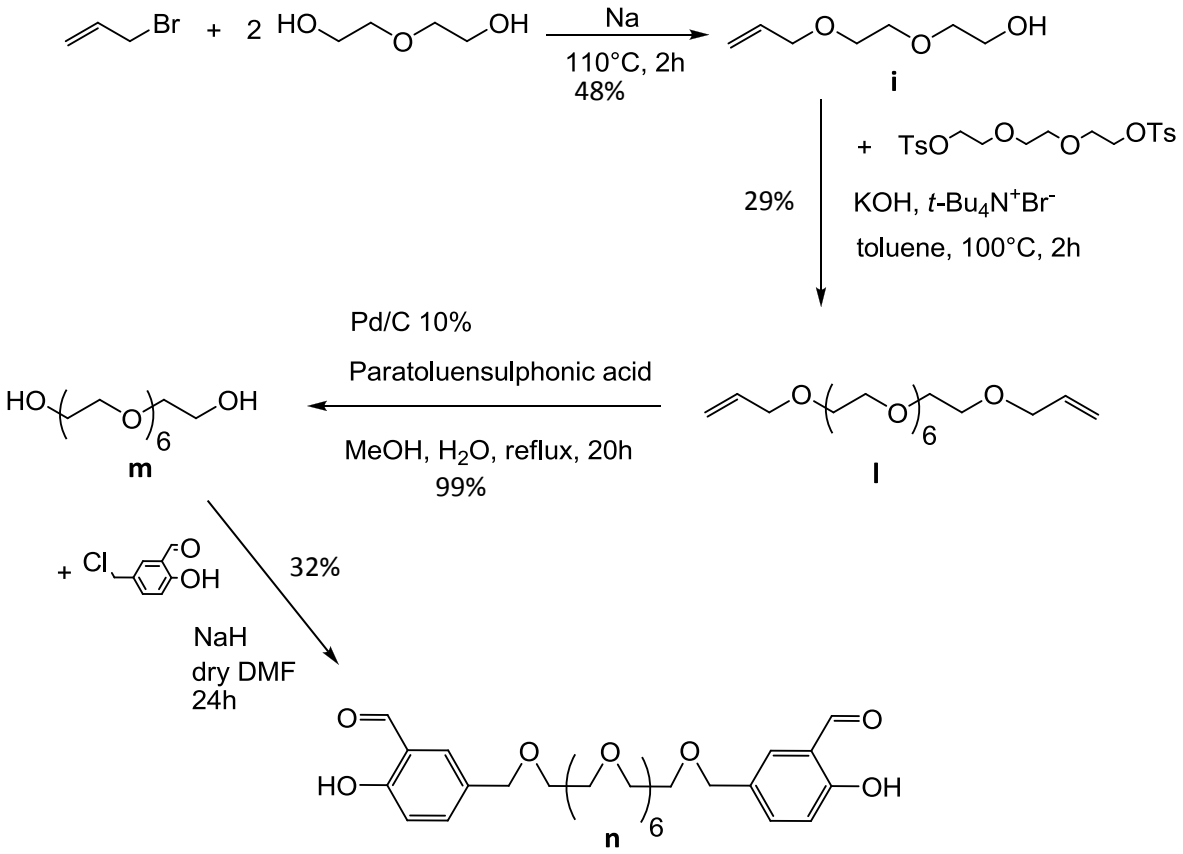

Scheme 3.5

This time the dialdehyde **n** was employed for the synthesis of a macrocyclic uranyl-salophen to be used as a wheel.

The choice is due to the well known robustness of such complexes, then UO_2-salophen macrocycles of three different dimensions were synthesised. The macrocyclisations were performed under high dilution conditions.

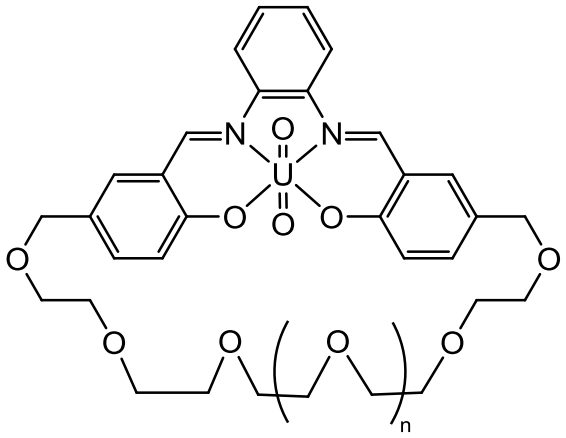

A (n = 1), 92%
B (n = 2), 90%
C (n = 3), 63%

UV-Vis titration experiments were carried out on a model system constituted by an simple UO_2-salophen and the axle (**c** or **g**), to measure the affinity between the metal center and the nitrogen atoms of the axles. The measures provided respectively the binding constants K_3 = 10000 ± 200 M^{-1} and K_4 = 17000 ± 400 M^{-1}. As in the case of zinc-salophen complexes, also for the uranyl-salophen ones the interaction with the axle **g** is stronger than with the axle **c**.

We employed the *threading and stoppering* method on the macrocycles (**A**, **B** and **C**) combined with **axle g**: in a 1:1 methanol-chloroform mixed solvent the macrocycle was solubilised with 1eq. of 2,6-pyridindicarbonylchloride. Then 2eq. of stopper, 4-tritylaniline, were added and the mixture was stirred for 24h. Unexpectedly the ESI-TOF mass analysis showed the formation of unknown compounds and the complete absence of the rotaxane peaks.

3.3 Conclusion

We have reported our attempts to synthesize [2]-rotaxane systems employing a metal-salophen macrocycle as a wheel. Our attempts were supported by UV-Vis preliminary studies, which confirmed the feasibility of the designed targets. We have explored many possible combinations, changing: synthetic method (*clipping* or *threading and stoppering*), dimension of the cycle (five, six or seven ethylene glycol units), type of axle (bearing a secondary amine function or a pyridyl one), nature of the complexed metal (zinc or uranyl). None of these attemps led to the isolation of the rotaxane. Only with procedure a and

procedure b (*clipping* method) it was possible to recognize the molecular peak of the **rotaxane 1** by mass analysis (ESI-TOF). This synthesis has to be optimised to obtain the rotaxane in sucha quantity to be isolated.

The last attempts with uranyl-salophen macrocycles did not work probably because of the different orientation of the binding site, which is not directed inside the cavity.

3.4 Experimental Section

Tritylchloride

A 100ml flask is charged with 5.11 g (0.02 mol) of triphenylmethanol, 13mL of benzene and 3.7mL (0.05 mol) of acetyl chloride. The solution was kept at reflux for 1h, then cooled and diluted with 60mL of hexane. The flask was left at -24°C overnight and then the white precipitate was collected by filtration (4.05g, yield of 74%). **^{1}H-NMR** (200 MHz in $CDCl_3$), δ: 7.39-7.29 (m, 15H, CH).

Potassium 4-tritylphenolate (a)

In a 50 ml flask 10,27 g (0.11 mol) of phenol were melted at 110°C to work as solvent, then 4.05g (0.014 mol) of tritylcloride were added. The mixture was kept at 110°C overnight, then cooled and mixed with 150mL of a NaOH solution 40%$_w$. Immediately a white solid began to precipitate. It was collected by filtration to give 4.54g (yield of 83%) of the pure product. **^{1}H-NMR** (200 MHz in $CDCl_3$), δ: 7.40-7.28 (m, 15H, CH), 7.10 (d, *J* = 10.7 Hz, 2H, CH), 6.74 (d, *J* = 10.7 Hz, 2H, CH).

Ethyl 2-(4-tritylphenoxy)acetate (b)

A flame-dried, two-necked, 1 L, round-bottomed flask equipped with an argon inlet and a magnetic stirbar is charged with 2.36g (0.007 mol) of **a**, 17.43g (0.126 mol) of K_2CO_3 and 420mL of dry acetonitrile. At this mixture at reflux 2.63g (0.015 mol) of ethyl bromoacetate were added and it was maintained at 70°C for 24h. Then it was filtered and the solution evaporated. The solid obtained was solubilised in dichloromethane, washed two times with water and one time with brine and dried over Na_2SO_4. The product was then purified by flash column chromatography (silica gel, elution with petroleum ether:chloroform = 1:1). The fractions containing the product were collected to give 2.53g of a white solid (yield of 98%).

^{1}H-NMR (200 MHz in $CDCl_3$), δ: 7.25-7.15 (m, 15H, CH), 7.10 (d, *J* = 10.7 Hz, 2H, CH), 6.74 (d, *J* = 10.7 Hz, 2H, CH), 4.58 (s, 2H, CH_2), 4.29-4.22 (m, 2H, CH_2), 1.28 (t, *J* = 6.0 Hz, 3H, CH_3).

N,N'-(2,2'-azanediylbis(ethane-2,1-diyl))bis(2-(4-tritylphenoxy)acetamide) (axle c)

1.55g (0.004 mol) of **b**, 0.2 mL (0.002 mol) of bis-(2-aminoethyl)amine, 20 mL of methanol and 30mL of chloroform were introduced in a 100mL flask and kept at reflux for 72h. By evaporation of the solvent 1.86g of crude product were obtained and then purified by flash column chromatography (silica gel, elution with chloroform and 1% methanol). 0.47g of pure product were isolated (yield of 30%). **^{1}H-NMR** (200 MHz in $CDCl_3$), δ: 7.40-7.19 (m, 50H, CH), 7.10 (d, *J* = 10.7 Hz, 4H, CH), 6.74 (d, *J* = 10.7 Hz, 4H, CH), 4.64 (s, 4H, CH_2), 3.45 (m, 4H, CH_2), 2.84 (m, 4H, CH_2). **^{13}C-NMR** (300 MHz in $CDCl_3$), δ: 168.66, 154.83, 146.49, 140.32, 132.15, 130.74, 127.23, 125.68, 113.29, 67.00, 64.03, 47.83, 37.74.

2-(2-chloroethoxy)tetrahydro-2H-pyran (d)

8.8mL (0.126 mol) of 3,4-dihydro-2H-pyran and 11.2mL (0.128 mol) of 2-chloroethanol were introduced in a 50mL flask and two drops of HCl were added. The mixture was stirred for 3h30', then 50mL of diethylether were added. The organic phase was extracted two times with 50mL of NaOH 2N and a third time with water, then it was dried over Na_2SO_4 and evaporated. 6.78g of the pure product was collected by distillation at 97°C and identified by gas chromatography-mass (yield of 33%). **^{1}H-NMR** (300 MHz in $CDCl_3$), δ: 4.65 (t, *J* = 3.3 Hz 1H, CH), 3.95-3.47 (m, 6H, CH_2), 1.81-1.53 (m, 6H, CH_2). **Mass** (m/z): $[M]^+$ 164.

Hexaethyleneglycole (e)

A 50mL flask was charged with 6.08g (0.037 mol) of e39, 1.4mL (0.008 mol) of tetraethyleneglycole, 0.22g (0.0006 mol) of tetrabutylammonium hydrogen sulfate as Phase Transfer Catalyst. 15mL (0.130 mol) of a solution of NaOH 10M were added to this mixture and then the flask was kept at 65°C for 5 days. The crude product was diluted with 45mL of dichloromethane, washed three times with water, dried over Na_2SO_4 and filtered on silica to remove the impurities. This workup was followed by an acid-catalysed deprotection (performed with HCl) which gave 1.37g of pure hexaethyleneglycole (yield of 60%). **Gaschromatography-Mass** (m/z): 89 (rt = 24.67 mins, compared with tetraethyleneglycole rt = 18.32 mins).

5-Chloromethyl-2-hydroxybenzaldehyde

A 500mL flask is charged with 7.55mL (0.095 mol) of *p*-formaldehyde acq. and 95mL of HCl. At this solution 10mL (0.095 mol) of salicylaldehyde were slowly added and the mixture was stirred overnight at room temperature. The product was collected by filtration and then recrystallised from ethanol. 6,01g of the pure product were isolated, with a yield of 37%. **^{1}H-NMR** (200 MHz in $CDCl_3$), δ: 11.04 (s, 1H, CHO), 9.88 (s, 1H, OH), 7.55 (m, 2H, CH), 6.99 (m, 1H, CH), 4.57 (s, 2H, CH_2).

5,5'-(2,5,8,11,14,17,20-heptaoxahenicosane-1,21-diyl)bis(2-hydroxybenzaldehyde) (f)

A flame-dried, two-necked, 25mL, round-bottomed flask equipped with an argon inlet and a magnetic stirbar was charged with 1.25g (0.031 mol) of NaH, which was then washed three times with hexane and suspended in 4mL of dry DMF. The flask was introduced in an ice bath and 0.95g (0.003 mol) of **e** solubilised in 4mL of anhydrous DMF were slowly added. After the evolution of hydrogen had ceased 1.25g (0.007 mol) of 5-chloromethyl-2-hydroxybenzaldehyde were also added. The mixture was stirred overnight, then was poured over ice and neutralised with HCl. This aqueous phase was extracted three times with dichloromethane, dried over Na_2SO_4 and evaporated. 5.50g of the crude product was then purified by flash column chromatography (silica gel, elution with diethylether:acetone = 9:1). The fractions containing the product were collected to give 0.69g of a yellow oil (yield of 37%). **^{1}H-NMR** (300 MHz in $CDCl_3$), δ: 10.97 (s, 2H, CHO), 9.88 (s, 2H, OH), 7.55-7.47 (m, 4H, CH), 6.97-7.94 (m, 2H, CH), 4.51 (s, 4H, CH_2), 3.62 (m, 24H, CH_2).

***N*^{2},*N*^{6}-bis(4-tritylphenyl)pyridine-2,6-dicarboxamide (axle g)**

In a 500mL flask 0.34g (0.001 mol) of 4-tritylaniline and 0.10g (0.0005 mol) of 2,6-pyridindicarbonylchloride were solubilised in 250mL of dichloromethane in the presence of 0.14mL of triethylamine. The reaction was followed by TLC, and after 4h it was stopped, filtered through silica and evaporated. 0.40g of the pure product were obtained with a yield of 50%. **^{1}H-NMR** (200 MHz in $CDCl_3$), δ: 9.46 (bs, 2H, NH), 8.49 (d, *J* = 7.8 Hz, 2H, CH), 8.12 (t, *J* = 7.8 Hz, 1H, CH), 7.62-7.59 (m, 4H, CH), 7.39-7.23 (m, 34H, CH). **^{13}C-NMR** (300 MHz in $CDCl_3$), δ: 160.95, 148.93, 146.34, 143.61, 139.44, 134.82, 131.72, 130.80, 130.69, 127.28, 125.73, 125.34, 118.80, 64.45. **Mass ESI-TOF** (m/z): $[M+Na]^+$ 824.46.

Macrocycle (h)

A solution of 0.60g (0.001 mol) of **f** in 15mL of a 1:1 methanol-dichloromethane mixture and a solution of 0.12g of *o*-phenylenediamine (0.001 mol) in 15mL of the same solvent were added separately and simultaneously by a syringe pump over 4 h to a solution of 0.28g of zinc acetate dihydrate (0.0012 mol) in 600mL of refluxing methanol. The mixture was refluxed for an additional 30' and then 0.28g of sodium carbonate (0.0025 mol) were added. After cooling, the reaction mixture was filtered, slowly concentrated under reduced pressure at room temperature to a volume of about 5 mL, and kept overnight at −18 ◦C. Under these conditions, the product precipitated as a yellow solid that was separated by filtration (0.18 g, yield 24%). **^{1}H-NMR** (200 MHz in DMSO), δ: 8.79 (bs, 2H, CH), 7.74-7.70 (m, 2H, CH), 7.36-7.31 (m, 4H, CH), 7.17-7.13 (m, 2H, CH), 6.63 (d, *J* = 8.7 Hz, 2H, CH), 4.27 (bs, 4H, CH_2), 3.60–3.09 (m, 24H, CH_2). **Mass ESI-TOF** (m/z): $[M+H]^+$ 685.90, $[M+Na]^+$ 707.89.

2-(2-(allyloxy)ethoxy)ethanol (i)

4.8g (0.21 mol) of sodium was dissolved in 50mL (0.53 mol) of diethylene glycol in a 250mL flame-dried flask and kept at 100°C. 18mL (0.21 mol) of allylbromide were added dropwise and the reaction was stirred at the same temperature for 2h, cooled and filtered. The crude product was distilled under vacuum ($T_{dist.}$ = 160°C) to give 14.18g of pure product (yield of 48%). **^{1}H-NMR** (200 MHz in $CDCl_3$), δ: 5.89 (m, 1H, CH), 5.23 (m, 1H, CH), 5.17 (m, 1H, CH), 4.04 (d, 2H, CH_2), 3.75-3.55 (m, 8H, CH_2), 3.45 (bs, 1H, OH).

Heptaethylene glycol bis(allyl ether) (l)

1.53g (0.027 mol) of freshly powdered KOH was added to a stirred solution of 3.95g (0.027 mol) of **i**, 2.71g (0.006 mol) of triethylene glycol bis-tosylate, 0.70g (0.002 mol) of TBAB in 30mL of toluene. The resulting mixture was stirred for 2h at 100°C, then cooled and diluted with 250mL of dichloromethane. The suspension was filtered to remove the precipitate, while the solution was evaporated and the crude product purified by flash column chromatography (silica gel, elution with ethylacetate:acetone = 9:1). 0.69g of the product were obtained with a yield of 29%. **Mass ESI-TOF** (m/z): $[M+Na]^+$ 429.24.

Heptaethylene glycol (m)

0.02g (0.0002 mol) of *p*-toluensulfonic acid and 0.69g of Pd/C 10% were added to a stirred solution of 0.69g (0.002 mol) **l**, in 42mL of MeOH:H_2O = 24:1. The mixture was refluxed under atmosphere of argon for 24h. The pure product was collected by filtration on celite and by evaporation of the solvent, and it was obtained with a yield of 99% (0.55g). **Mass ESI-TOF** (m/z): $[M+Na]^+$ 349.22.

5,5'-(2,5,8,11,14,17,20,23-octaoxatetracosane-1,24-diyl)bis(2-hydroxybenzaldehyde) (n)

Procedure previously reported for product **f**, employing heptaethylene glycol, and after the purification 0.37g of a yellow oil were obtained (yield of 32%). **^{1}H-NMR** (300 MHz in $CDCl_3$), δ: 10.96 (s, 2H, CHO), 9.87 (s, 2H, OH), 7.54-7.46 (m, 4H, CH), 6.95 (d, *J* = 8.4 Hz, 2H, CH), 4.51 (s, 4H, CH_2), 3.65-3.60 (m, 28H, CH_2). **^{13}C-NMR** (300 MHz in $CDCl_3$), δ: 196.33, 136.47, 132.67, 130.00, 120.08, 117.41, 71.87, 70.36, 70.30, 69.26. **Mass ESI-TOF** (m/z): $[M+Na]^+$ 617.27.

5,5'-(2,5,8,11,14,17-hexaoxahenicosane-1,18-diyl)bis(2-hydroxybenzaldehyde) (o)

Procedure previously reported for product **f**, employing pentaethylene glycol, and after the purification 0.47g of a yellow oil were obtained (yield of 20%). **Mass ESI-TOF** (m/z): $[M+Na]^+$ 529.02.

Macrocycle (A)

A solution of 0.48g (0.0009 mol) of **o** in 10mL of methanol and a solution of 0.12g of *o*-phenylenediamine (0.001 mol) in 10mL of solvent were added separately and simultaneously by a syringe pump over 20h to a solution of 0.249g of uranyl acetate dihydrate (0.0012 mol) in 500mL of methanol. The mixture was stirred for an additional 3 days then ethyl acetate was added. The organic phase was washed three times with water and dried. 0.69g of product were obtained after evaporation of the solvent (yield of 92%). **^{1}H-NMR** (200 MHz in DMSO), δ: 9.55 (bs, 2H, CH), 7.49-7.29 (m, 8H, CH), 6.83 (m, 2H, CH), 4.27 (m, 4H, CH_2), 3.63–3.21 (m, 20H, CH_2). **Mass ESI-TOF** (m/z): $[M+Na]^+$ 849.51.

Macrocycle (B)

Procedure previously reported for macrocycle **A**, employing dialdehyde **f**. 0.71g of product were obtained after evaporation of the solvent (yield of 90%). **^{1}H-NMR** (200 MHz in DMSO),

δ: 9.30 (bs, 2H, CH), 7.65 (s, 2H, CH), 7.44 (m, 4H, CH), 6.98 (m, 4H, CH), 4.46 (m, 4H, CH_2), 3.58–3.26 (m, 24H, CH_2). **Mass ESI-TOF** (m/z): $[M+Na]^+$ 912.71.

Macrocycle (C)

Procedure previously reported for macrocycle **A**, employing dialdehyde **n**. 0.14g of product were obtained after evaporation of the solvent (yield of 63%). **^{1}H-NMR** (200 MHz in DMSO), δ: 9.34 (bs, 2H, CH), 7.64-7.14 (bm, 8H, CH), 6.90 (bs, 2H, CH), 4.48 (bs, 4H, CH_2), 3.49–3.15 (m, 28H, CH_2). **Mass ESI-TOF** (m/z): $[M+Na]^+$ 957.02.

Chapter 4

Synthesis and binding studies of new Uranyl-salophen macrocyclic receptors

4.1 Introduction

Cation recognition is a well established branch of supramolecular chemistry and its diffusion is proved by the huge amount of articles concerning this subject. In recent years the importance of anions in biological and environmental systems has been recognised and, as a consequence, the research of compounds capable to bind anions has been highly developed[83].

The majority of the synthesised receptors are designed to selectively recognize cations or anions, but not both of them. However it is quite clear that the counterion plays a fundamental role in modulating the binding strength and selectivity of the receptor. For this reason heteroditopic receptors that can simultaneously interact with cationic and anionic species have attracted great interest.

By the combination of anion and cation receptors, the heteroditopic hosts used for ion-pair recognition often exhibit cooperative and allosteric effects, whereby the association of one ion alters the binding affinity of the counterion through electrostatic and conformational effects.

The design of heteroditopic receptors often implies the separation of the two ions. This brings a coulombic energy penalty, so to avoid this problem, it is desirable to maintain the two components in close contact also after the coordination process. So the host must be designed in order to locate the two binding sites close to each other to amplify the electrostatic interaction. As a consequence ion-pair receptors generally display enhanced affinities for ions when compared to simple ion receptors, and obviously the result is in higher binding constants.

A way to classify ion-pair receptors is based on how they bind the two ions and this happens in three limiting modes. These different ion-pair binding arrangements are

[83] S. K. Kim, J. Sessler, *Chem. Soc. Rev.*, **2010**.

schematically depicted in figure 4.1 and they are defined as: (a) *contact ion pairs*, where the anion and cation are held in direct contact; (b) *solvent-bridged ion pairs,* in which one or more molecules of solvent help link the anion to the cobound cation (c) *host-separated ion pairs*, where anion and cation are bound far from one other.

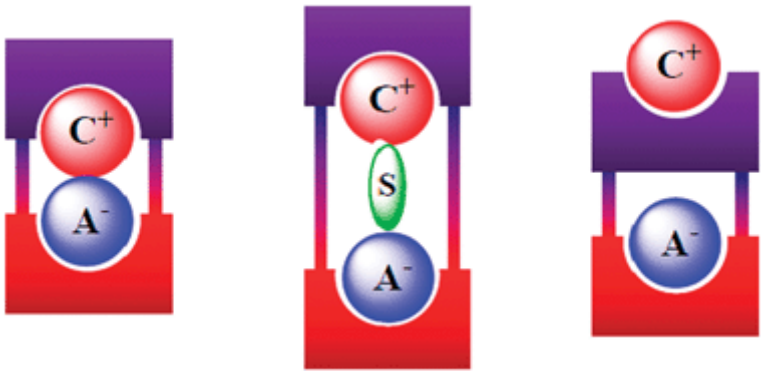

(a) (b) (c)

Figure 4.1 Arrangement of the ion-pair within the receptor (A^- is the anion, C^+ is the cation, S is the solvent).

The synthesis of this class of receptors is really difficult, still many examples are reported in the literature. In the next pages we will give representative examples following the above classification.

a. Contact ion pairs

As already said the realisation of *contact ion pairs* receptors has the big advantage of avoiding the partial destabilisation deriving from charge separation (columbic penalty).

Mahoney et al[84] reported the synthesis of a bicyclic macromolecular ion pair receptor for inorganic salt (figure 4.2 -a-). The host was designed to recognize anions through two amide groups, and cations through a crown ether cycle. X-ray diffraction analysis of the receptor showed how it interacts with solvent molecules in the absence of other guests. Nevertheless the presence of the solvent does not inhibit the complexation of salt. As showed in figure 4.2 -b- when KCl is introduced, it is bound by the receptor as contact ion pair.

[84] J. M. Mahoney, A. M. Beatty, B. D. Smith, *J. Am. Chem. Soc. ,* **2001,** *123,* 5847-5848.

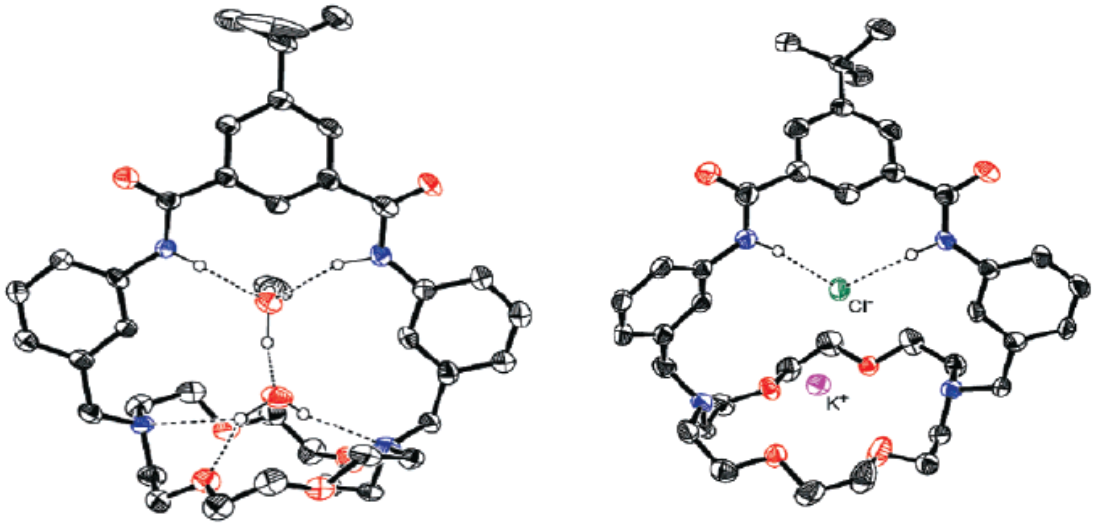

-a- -b-

Figure 4.2 -a- Receptor with a water and a methanol molecules in the cavity. -b- receptor-KCl complex

A different case is that of the family of calyx[6]-cryptamides synthesised by Le Gac[85] (figure 4.3), which represents an example of ion pair receptors for organic salt. These compounds present in close proximity two binding sites for complexation of both a primary ammonium ion and its chloride counterion, which are bound as contact ion pair. With the introduction of neutral guests as pyrrolidin-2-one (PYD), imidazolidin-2-one (IMI) or (±)-4-methylimidazolidin-2-one (MIMI) a substitution takes place and the organic salt leaves the cavity of the calyx[6].

This system is a good example of positive cooperativity, in fact the complexation of the chloride anion can proceed only when an ammonium ion is present in the calixarene cavity and conversely, without Cl^- the receptor is unable to bind the ammonium ion. This effect is related to the structural and electronic changes of the binding sites, which occur when one of the two charged species enters in the cavity. The binding of Cl^- induces the expulsion of the OMe groups from the cavity of the calixarene and brings the oxygen atoms of the ammonium binding site closer, in a perfect geometry to interact with the ammonium hydrogens.

[85] S. Le Gac, I. Jabin, *Chem. Eur. J.*, **2008**, *14*, 548-557.

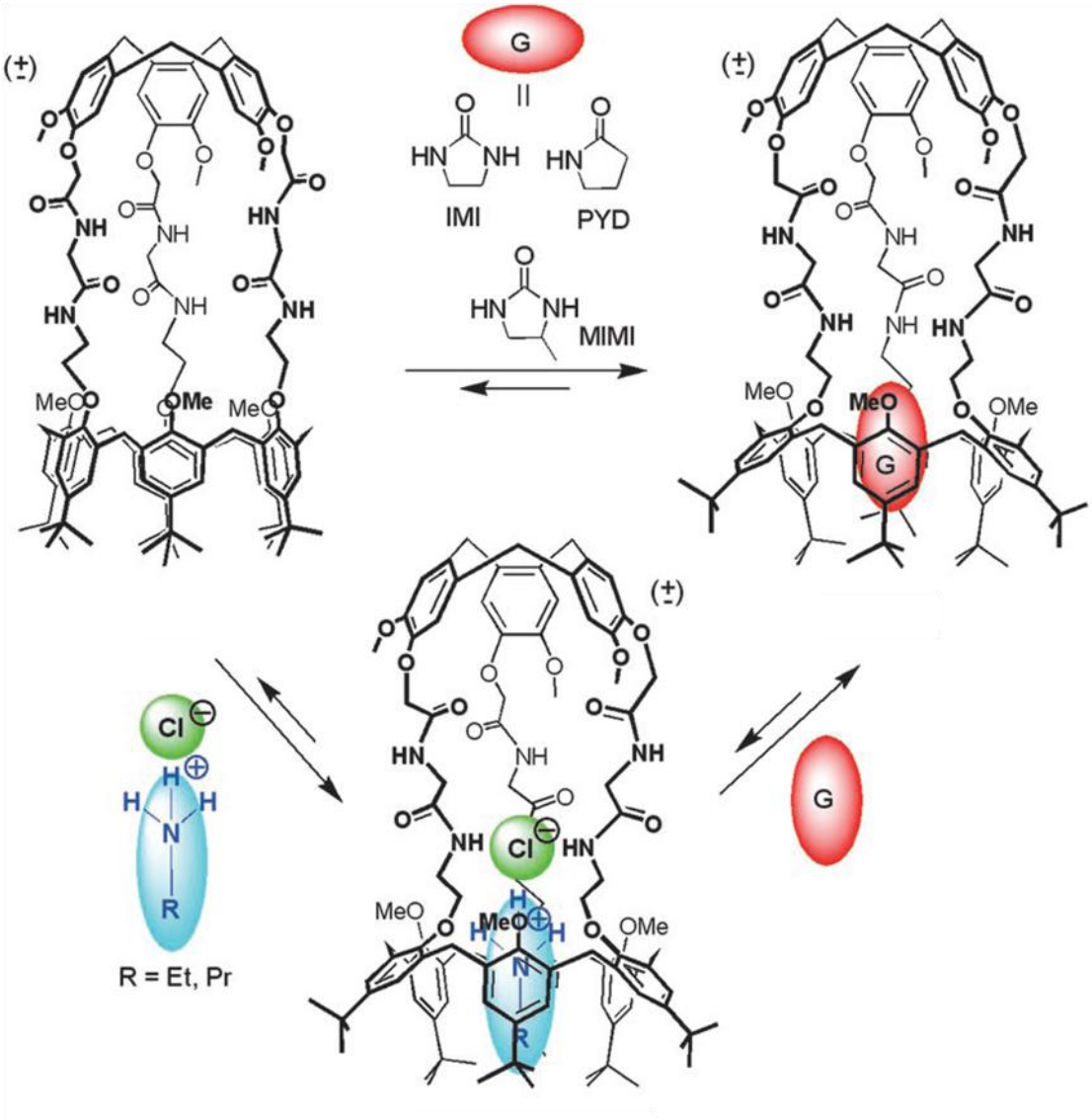

Figure 4.3 Scheme of the equilibrium between the calyx[6]-cryptamide free and its complex with a neutral molecule or with an ammonium salt.

b. Solvent-bridged ion pairs

A receptor that binds salts as separated ions must achieve charge separation and, as a consequence, it requires two strong binding sites to compensate the lattice energy of the salt. This result can be reached involving solvent molecules in the complexation process. In figure 4.4 an example of such systems is showed[86]. This receptor is composed of a dinuclear organotin moiety linked to a crown ether moiety by a methylene group. It is able to bind sodium fluoride. In the complex both the Tin atoms are pentacoordinate and each shows a distorted trigonal bipyramidal configuration.

[86] G. Reeske, M. Schürmann, K. Jurkschat, *Dalton Trans.*, **2008,** 3398-3400.

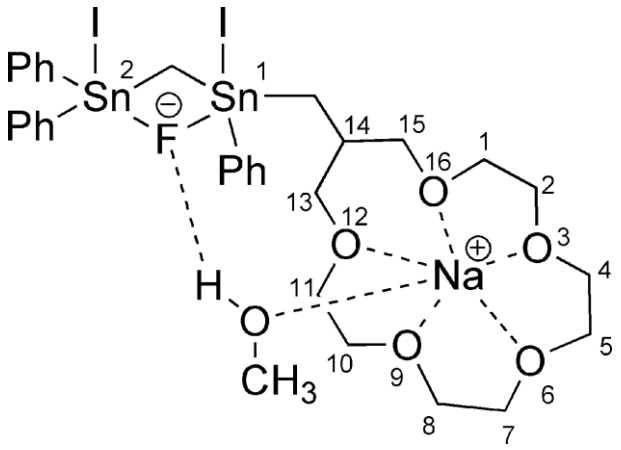

Figure 4.4 Scheme for the crown ether and tin atoms in the complex [receptor·NaF·CH3OH].

The communication between the separated ions of sodium fluoride is provided by an intramolecular O–H· · ·F hydrogen bridge involving a methanol molecule. This is the first example of ditopic complexation of NaF, overcoming its high lattice energy.

c. Host-separated ion pairs

The receptor reported in figure 4.5 has been developed for the solvent extraction of transition metal salt[87]. The ligand framework contains a salen moiety bearing two morpholine groups, and it provides separate dianionic and dicationic binding sites, indeed the phenolic protons have been transferred to the nitrogen atoms of the pendant groups. Concerning this class of receptors a relevant problem may be the different reactivity towards charged species. The reported system represents an example of cooperativity, in which cation binding directly enhances anion binding and thus increasing the system efficiency.

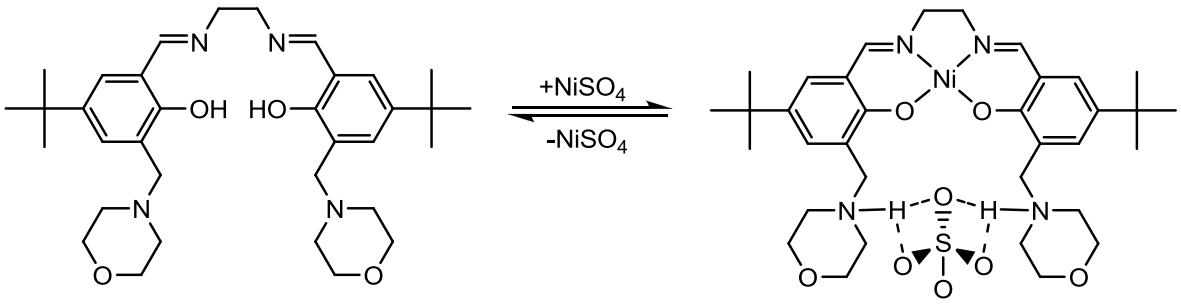

Figure 4.5 Equilibrium between the free-receptor and the $NiSO_4$ complex.

[87] D. J. White, N. Laing, H. Miller, S. Parsons, S. Coles, P. A. Tasker, *Chem. Commun.*, **1999**, 2077-2078.

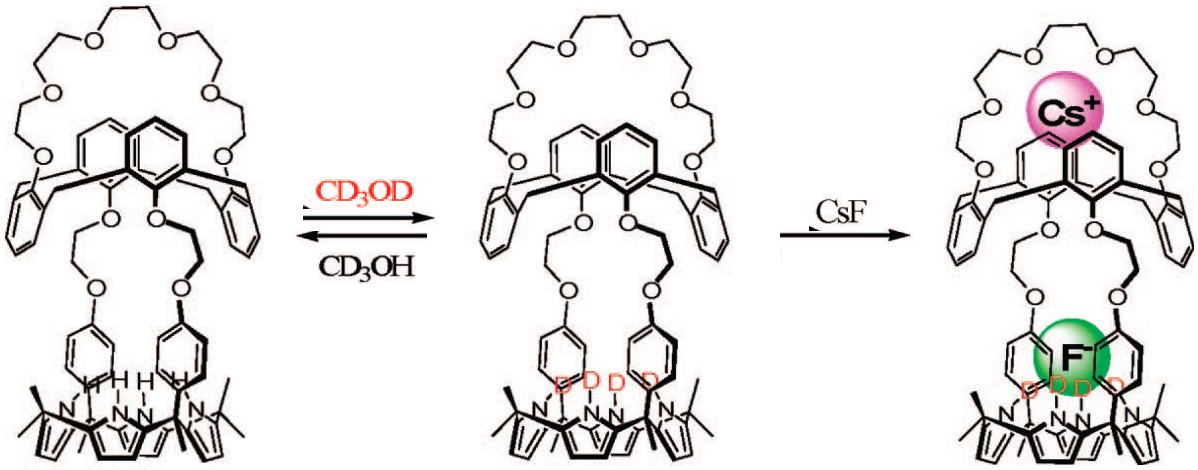

Figure 4.6 Proposed binding interactions involving the crown-6-calix[4]arenecapped calix[4]pyrrole and CsF salt in 10% (v/v) CD3OD in CDCl3.

Another example of separed ion pairs receptor is the crown-6-calix[4]arenecapped calix[4]pyrrole reported in figure 4.6[88]. ^{1}H-NMR and X-ray analysis confirmed that it forms a stable 1:1 complex with CsF and also in this case the complexation is cooperative. This has been demonstrated through experiments conducted in the absence of the cobound cesium cation. In this condition the receptor does not bind neither the fluoride anion, whose bind is then strictly related to previous complexation of the cation.

d. Aim of the research

As already reported in chapter 3, during this PhD thesis, three new Uranyl-salophen macrocycles of different dimension (**A**, **B** and **C**) were synthesized.

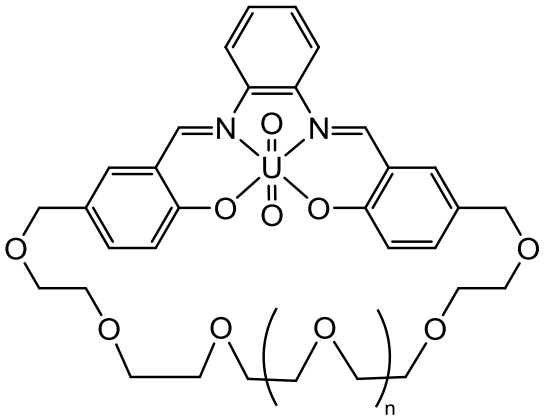

A n = 1
B n = 2
C n = 3

[88] J. L. Sessler, S. K. Kim, D. E. Gross, C.-H. Lee, J. S. Kim, V. M. Lynch, *J. Am. Chem. Soc*., **2008**, 130, 13162-13166.

The introduction of the uranyl-salophen unit and of a polyoxyethylenic (POE) chain in the skeleton was carried out to employ them as ditopic receptors for ion pairs. In this chapter we describe preliminary studies on their behaviour as ditopic receptors. In recent years the uranyl-salophen complexes showed in figure 4.7 have been already studied in my group for their potentiality as ditopic receptors[89]. Since uranyl-salophen complexes are known to bind anions strongly, these derivatives can act as ion-pair receptors thanks to the aromatic side arms, which gives cation-π interactions with the accompanying cation. A preliminary investigation on the behaviour of **A**, **B** and **C** as ditopic receptors for contact ion pairs has been carried out by UV-Vis spectroscopy and ^{1}H-NMR technique.

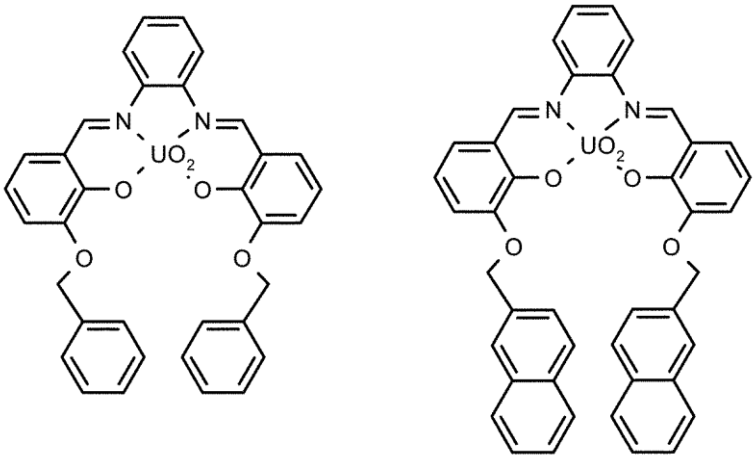

Figure 4.7 Two examples of salophenic ditopic receptors.

e. Spectrophotometric titrations

UV-Vis spectroscopy is often employed to study binding processes in supramolecular chemistry. The advantage of this technique with respect to NMR spectroscopy is the possibility to work at lower host concentration (10^{-5}M) and thus to measure higher binding constants[90]. The addition of increasing amounts of guest to a solution of the host causes variations in the UV-Vis spectra, if interactions take place. Working in a region where guest absorption is negligible, the variations are correlates only with the host-guest association process. The observation of isosbestic points indicates that the stoichiometry of the reaction remains unchanged during the process, and that no secondary reactions occur during the time of the analysis. Then considering this as a 1:1 binding process, the spectrum variations

[89] M. Cametti, M. Nissinen, A. Dalla Cort, L. Mandolini, K. Rissanen, *Chem. Commun.*, **2003**, 2420-2421.
[90] P. Thordarson, *Chem. Soc. Rev.,* **2011**, *40*, 1305-1323.

are related, through the binding isotherm equation 4.1, to the equilibrium constant at a fixed temperature.

$$\Delta A_0 = \frac{\Delta A_\infty K[\mathrm{G}]}{1 + K[\mathrm{G}]} \qquad \textbf{4.1}$$

- $\Delta A_0 = A - A_0$, the difference between the observed absorbance of the system during the titration experiment and the initial absorbance of the receptor;
- $\Delta A_\infty = A_\infty - A_0$, the difference between the absorbance of the saturated system and the initial absorbance of the receptor;
- K = association constant;
- [G] = guest concentration at the equilibrium.

This means that, after each addition, the A variation is a fraction of ΔA_∞ and it depends on K and [G]. Obviously during the titration, increasing the guest concentration, ΔA_0 will equalize ΔA_∞. Equation 4.1 is then used to fit the graphic of absorbance as a function of guest concentration and to calculate the value of the binding constant. Since the real values of [G] are unknown, the analytical guest concentrations will be used in equation 4.1, and the value of K_{bind} will be obtained through an iterative calculation. The alternative is equation 4.2 (where R = receptor).

$$A = A_0 + \Delta A_\infty \frac{[\mathrm{R}]_0 + K^{-1} + [\mathrm{G}] - \sqrt{[R]_0 + K^{-1} + [G]^2 - 4[R]_0[G]}}{2[R]_0} \qquad \textbf{4.2}^{91}$$

- A = experimental absorbance;
- A_0 = initial absorbance of the receptor;
- R_0 = analytical concentration of the receptor;
- [G] = is the total guest concentration in each point, including that fraction bound to the receptor.

[91] K. Hirose, *J. Incl. Phenom. Macrocycl. Chem.*, **2001**, *39*, 193-209.

In the experiment the initial receptor concentration should be chosen in order to have its spectrum absorbance comprised between 0 and 1. On the other hand the expected association constant value determines the concentration range of the guest and that allows to collect as many point as possible in the non-linear part (red zone) of the binding isothermal hyperbola (figure 4.8).

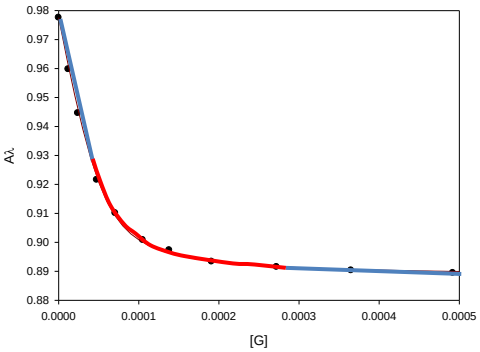

Figure 4.8 Binding isothermal hyperbola

In this region the probability of binding (*p*) is comprised within 0.2-0.8 and it is defined as:

$$p = \frac{[\mathrm{RG}]}{[\mathrm{G}]_0} \qquad \text{when} \qquad [\mathrm{R}]_0 \geq [\mathrm{G}]_0 \qquad \textbf{4.3}$$

$$p = \frac{[\mathrm{RG}]}{[\mathrm{R}]_0} \qquad \text{when} \qquad [\mathrm{R}]_0 < [\mathrm{G}]_0 \qquad \textbf{4.4}$$

After a preliminary titration experiment the meaningful concentration range of the guest should be optimised by a trial-and-error approach.

4.2 Results and discussion

a. UV-Vis titrations

The UV-Vis spectra of the macrocycles **A**, **B** and **C** are reported below. They are characterised by a monotonic increase in light absorption on lowering the wavelength and by a relative maximum around 340nm.

The measurements were performed in the wavelength region comprised within 280-650 nm, using a standard quartz cell (light path = 1 cm) on a double beam Perkin Elmer Lambda 18 Spectrophotometer equipped with a Peltier temperature controller. The UV-Vis light beam interacts only with the aromatic part of the molecule, since the POE chain absorbs at 198nm[92], the same region of the solvents (λ *cut-off* CH_2Cl_2 235nm, λ *cut-off* CH_3CN 210nm).

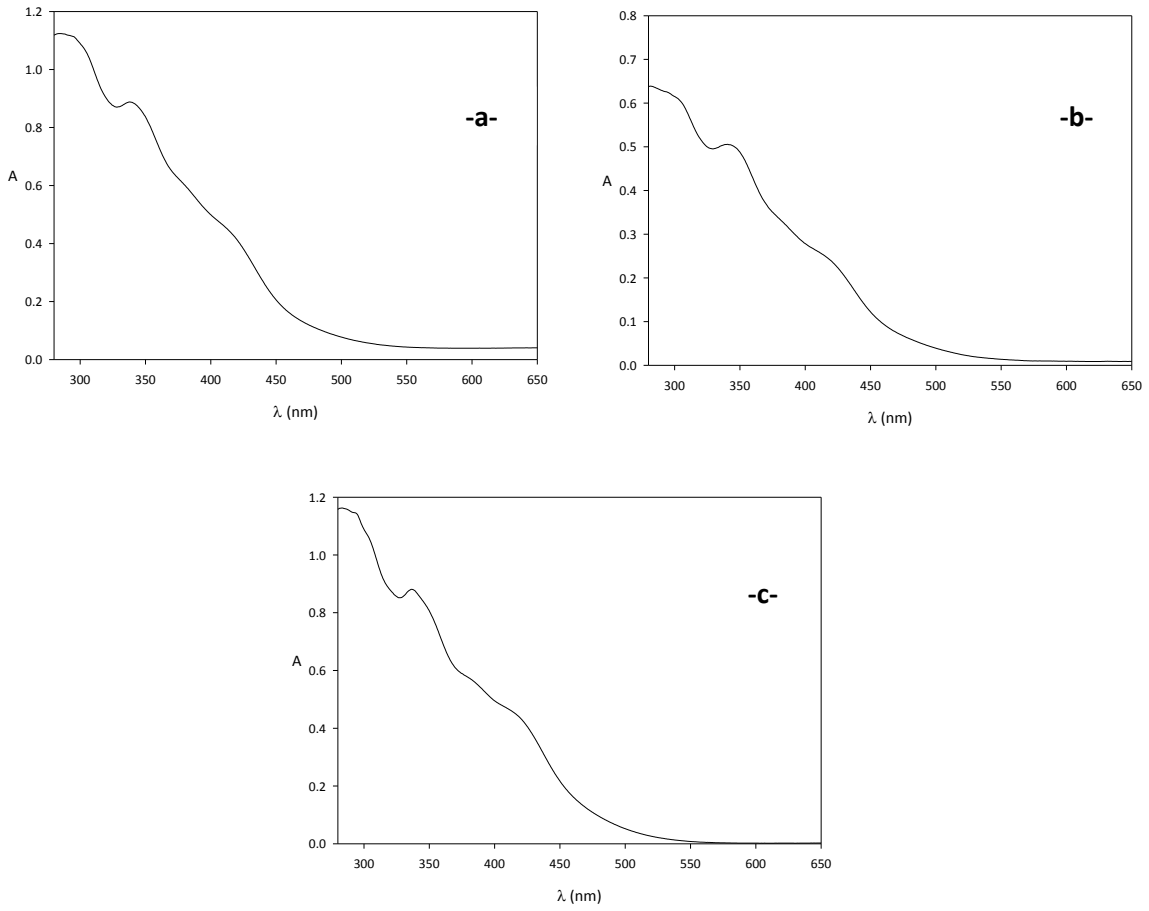

Figure 4.9 Absorption spectrum in CH_2Cl_2:CH_3CN = 1:1 at 25 °C of: complex **A** ($5.02\cdot10^{-5}$ M) **-a-**, **B** ($4.14\cdot10^{-5}$ M) **-b-** and **C** ($5.08\cdot10^{-5}$ M) **-c-**.

[92] H. Xu ,T. Zhu ,R.P. Yu, *Guang Pu Xue Yu Guang Pu Fen Xi*, **2007**, *27,* 1381-1384.

The zero points of UV-Vis titrations were the spectra of the macrocycles solutions. Concentrations around $5 \cdot 10^{-5}$ M provided absorbance values of 0.8-1 at 340nm.

The UV-Vis studies of the macrocycles were performed in mixed solvent (CH_2Cl_2:CH_3CN = 1:1) and the association processes of the three macrocycles with both TMACl and TBACl were analysed. The addition of the guest to the receptor solution caused absorption changes as they are shown in figure 4.10. To fit equation 4.2 we used the absorbance values measured at 340nm, corresponding to the relative maximum present in the spectra.

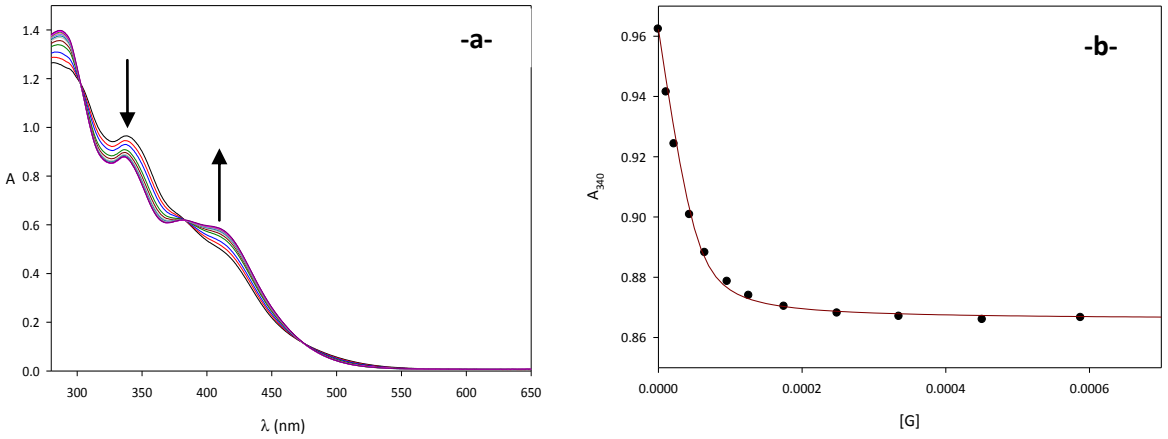

Figure 4.10 -a- UV-Vis titration of macrocycle A with TBACl in CH_2Cl_2:CH_3CN = 1:1 at 25 °C. Three isosbestic points are present in the observed wavelength range. **-b-** Titration curve calculated, points are experimental.

The presence of sharp isosbestic points and the good adherence of the experimental points to the binding isotherm hyperbola confirm the 1:1 stoichiometry of the association process. The K_{ass} obtained for the macrocycles are reported in table 4.1.

Table 4.1 Binding constants (K, M^{-1}) for the complexes formed between macrocycles **A**, **B**, **C** and TMACl and TBACl in CH_2Cl_2:CH_3CN = 1:1 at 25 °C. Errors are in the order of 1-4%.

	TMA^+Cl^-	**TBA^+Cl^-**
A	$1.0 \cdot 10^5$	$1.1 \cdot 10^5$
B	$7.0 \cdot 10^4$	$4.4 \cdot 10^4$
C	$7.6 \cdot 10^4$	$7.4 \cdot 10^4$

To verify that the absorbance changes were due only to the chloride anion interactions, another series of experiments was performed using $TMAPF_6$ as guest (figure 4.11). Indeed PF_6^- is known to be a poor donor and as a consequence it should give no interaction with the metal-salophen moiety. As expected, no variation of absorbance was recorded.

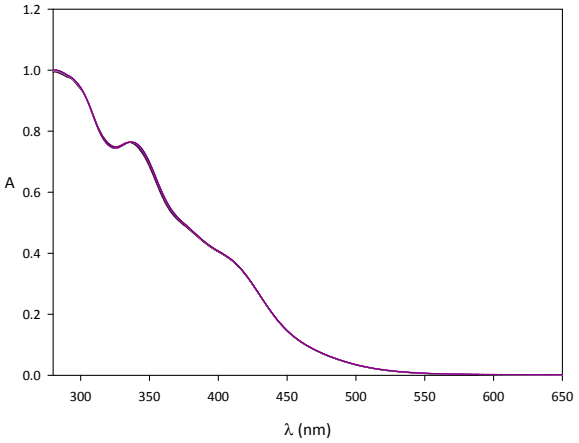

Figure 4.11 UV-Vis titration of macrocycle A with $TBAPF_6$ in CH_2Cl_2:CH_3CN = 1:1 at 25 °C.

b. ^{1}H-NMR titrations on macrocycle A

This technique permits to follow the association process on both the binding sites of the receptor. The NMR experiments consist in subsequent additions of increasing amount of a tetraalkylammonium (TMA or TBA) chloride standard solution to the NMR tube containing the macrocycle solubilised in the same solution of the salt. In this way during the titration the salt concentration remains constant, while the receptor one decreases. The additions caused in all cases upfield shifts of regularly increasing magnitude of the $-CH_3$ signal. In figure 4.12a is reported the $-CH_3$ chemical shift variations of TBA^+ versus the receptor **A** concentration.

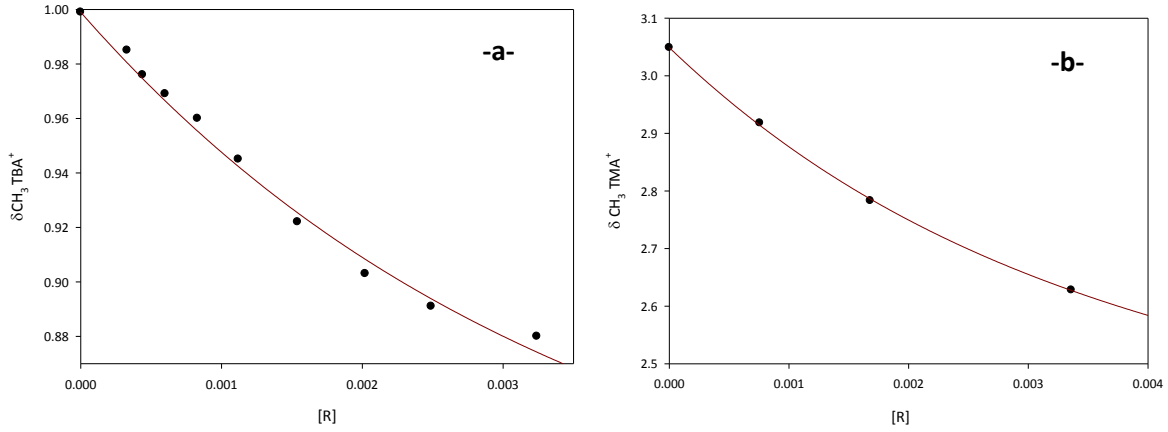

Figure 4.12 Measurements were carried out in a mixed solvent $CDCl_3$:CH_3CN = 4:1 at 25 °C. Titration curves of receptor **A** with TBACl (**-a-**), and with $TBAPF_6$ (**-b-**).

The red line is calculated using equation 4.2 and from its analysis a binding constant of 350±25 M^{-1} was obtained. The titration of the same macrocycle with TMACl gave similar results.

The chemical shift variations observed for the methyl groups of TBA^+ and TMA^+ may be originated by a direct interaction of the cation with the receptor or as a consequence of the anion binding. To gain more information a titration with $TMA^+PF_6^-$ was carried out (figure 4.12b). As previously mentioned, UV-Vis spectra have shown no interaction between the metal center and this anion. Instead in the NMR experiment a significant variation of chemical shift was still observed for the $-CH_3$ protons of TMA^+, comparable to those already observed with TMACl. This result leads us to estimate a binding constant of 350±40 M^{-1}, identical to the one obtained with TMACl.

Finally we synthesised the uranyl-salophen (**R**) to use it as reference compound.

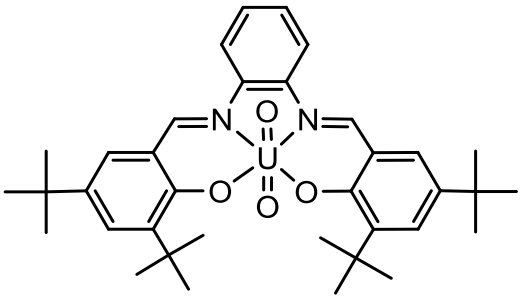

R

The ^{1}H-NMR titration of **R** with $TMAPF_6$ under the same conditions shows no variation of the chemical shifts. This result confirms that the binding constant obtained from the $TMAPF_6$ titration of macrocycle A is an indication of the direct interaction between the cation and the POE chain.

4.3 Conclusions

A series of three new macrocyclic ditopic receptors has been synthesised and their binding properties towards tetraalkylammonium halides have been studied by UV-Vis and ^{1}H-NMR spectroscopy. Strong association constants with TMACl and TBACl were obtained in CH_2Cl_2:CH_3CN = 1:1 mixed solvent by UV-Vis titrations, confirming a strong interaction between the metal center and the *hard* chloride anion. NMR experiments indicate also the presence of an interaction with the cation, whose nature has still to be thoroughly investigated.

Appendix 1

In the frame of a collaboration with the "Università G. d'Annunzio" of Chieti concerning the incorporation of metal-salophen complexes into POPC large unilamellar liposomes (LUV) I synthesised compound **S**. Fluorescence optical microscopy and anisotropy measurements show that the complex is located at the liposomal surface, close to the polar headgroups. The interaction of the POPC phosphate group with Zinc slowly leads to demetallation of the complex. Kinetics studies on this process were performed. The effect of the Zn-salophen complex on the stability of POPC LUV has been also evaluated. It turns out that the inclusion of the complex significantly increases the stability of POPC LUV[93].

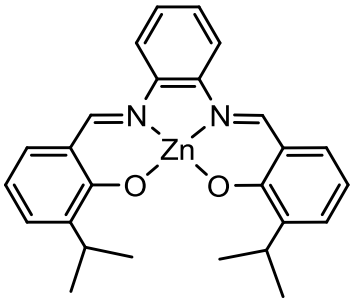

S

Salophen S: A solution of 3-isopropylsalicylaldehyde (0.10g, 0.63 mmol), 1,2-diaminobenzene (0.04g, 0.31 mmol), and zinc acetate dihydrate (0.07 g, 0.31 mmol) in methanol (2.5mL) was refluxed for 1h. The mixture was cooled to room temperature and filtered. The desired product was obtained as a yellow solid in 95% yield. Mp 334–336°C. Elemental analysis: *calc*. for $C_{26}H_{26}N_2O_2Zn$: %C, 67.32; %H, 5.65; %N, 6.04; *found*: C, 7.00; H, 5.82; N, 6.03. **^{1}H-NMR** (300 MHz in CD_3COCD_3): δ: 8.47 (s, 2H, CH); 7.33–7.26 (m, 4H, CH); 7.15–7.12 (dd, 2H, CH); 6.97–6.94 (d, 2H, CH); 6.53–6.47 (t, 2H, CH); 3.48 (m, 2H, CH); 1.11 (s, 12H, CH_3). **^{13}C-NMR** (300 MHz, in CD_3COCD_3): δ: 208.7, 133.0, 131.7, 129.2, 128.9, 126.8, 126.6, 123.1, 121.6, 121.3, 32.6, 23.4. **Mass ESI-TOF** (m/z): $[M+Na]^+$: *calc.* 485.1183; *found* 485.1172.

[93] C. Gasbarri, G. Angelini, A. Fontana, P. De Maria, G. Siani, I. Giannicchi, A. Dalla Cort, *Biochim. Biophys. Acta*, accepted, (doi: 10.1016), in press.